

A HYDROCHEMICAL SURVEY OF GROUNDWATER FLOW IN THE ROCHESTER METROPOLITAN AREA, MINNESOTA

Tipping, Robert G.

Minnesota Geological Survey, 2642 University Avenue W. St. Paul, MN, 55114, USA

Minnesota Geological Survey Open File Report 14-05

June, 2014



UNIVERSITY OF MINNESOTA



Funded through the Environment and Natural Resource Trust Fund as recommended by the Legislative and Citizen's Commission on Minnesota Resources (LCCMR).

Contents

Executive summary.....	1
Introduction.....	3
Background and data sources.....	4
Geologic Setting.....	5
Hydrogeology	8
Bedrock hydrostratigraphy.....	8
Unconsolidated aquifers and aquitards	11
Hydraulic head gradients	11
Previous groundwater chemistry investigations	14
Methods.....	16
Results.....	17
Discussion.....	22
Regional cross sections	22
Regional water chemistry summary.....	25
Above the Cummingsville-Glenwood aquitard	25
Above the lower Prairie du Chien Group	25
Below the lower Prairie du Chien Group.....	27
Conclusions.....	28
Suggested use.....	31
Recommendations for further work	32
Acknowledgements.....	32
List of Figures	33
References cited.....	81
Appendices (GIS data included in supplementary files).....	86

Executive summary

Historical chemical and isotopic data for Olmsted County were used to distinguish groundwater types based on similar chemical and isotopic composition. The extent of recent waters, identified by detectible tritium or chloride concentrations above background levels, was mapped in three dimensions. The distribution of these waters was compared to permeability of unconsolidated sediments, the hydrostratigraphy of Paleozoic bedrock, and potential vertical hydraulic gradients within the Rochester Central Metropolitan Area (RCMA) based on reported pumping levels from high-capacity municipal wells.

The spatial distribution of recent waters – waters with chloride concentrations above a maximum natural background level of two milligrams per liter (mg/L) and/or detectible tritium content – can be explained, in part by permeability differences and thickness of unconsolidated sediments overlying bedrock. Consistent presence of recent waters at lower elevations in bedrock aquifers over the period of record (1990-2010) in the eastern RCMA and along Bear Creek valley may be attributable, in part, to shallow-to-bedrock conditions, combined with higher sand content in unconsolidated sediments in that area. Conversely, deep-to-bedrock conditions in the western RCMA with higher clay content delayed the advance of recent waters to lower elevations in bedrock aquifers during the 1990's and early 2000's; but by 2010, recent waters were also present at these lower elevations.

Chemical differences are also attributable, in part, to bedrock hydrostratigraphy. North and northeast of the RCMA, recent waters are largely limited to the upper portion of the Prairie du Chien Group (Shakopee Formation). Jordan water samples from the same area have significantly lower chloride levels. Elevated nitrate levels within the Shakopee Formation also support the lack of hydraulic connection between the Shakopee Formation and Jordan Sandstone

in this area. In addition to large differences in hydraulic head from underlying aquifers, groundwater in the Upper Carbonate Plateau typically has significantly higher calcium to magnesium ratios than waters from the underlying St. Peter Sandstone, Prairie du Chien Group and Jordan Sandstone. These differences in chemical composition help delineate source waters for groundwater moving laterally and vertically into the Prairie du Chien Group and Jordan Sandstone within the RCMA.

The spatial distribution of groundwater chemical types is also a function of changes in vertical hydraulic gradients with time. Within the last 20 years, the extent of recent waters within the RCMA has expanded both horizontally and vertically. Groundwater calcium to magnesium ratios in the Prairie du Chien Group (Shakopee aquifer) and the Jordan Sandstone (Jordan aquifer) within the RCMA have also increased and show greater variability through time, indicating a greater percentage of recharge to these aquifers moving vertically within the RCMA and from the Decorah edge than before high-capacity pumping began.

At local and regional scales, project deliverables improve groundwater model calibration by helping to refine conceptual models of groundwater flow. Residence time data, reflected in the distribution of vertical recharge to upper bedrock aquifers, can be used to guide interpretation of calibration results as an alternative to calibration strictly by hydraulic head values alone. These steps can result in a more realistic distribution of hydraulic conductivity parameters in numeric models.

Introduction

This report summarizes work performed by the Minnesota Geological Survey (MGS) in partial fulfillment of work as described under Legislative and Citizens Commission on Minnesota Resources grant M.L. 2010, Chap. 362, Sec.2, subdivision 3a, MGS County Atlas and Related Hydrogeologic Research. The goal of this investigation was to provide information useful to understanding recharge to bedrock aquifers in the Rochester metropolitan area, such that the resource can be managed effectively (Figure 1).

Resource managers make decisions which hinge on questions related to groundwater such as *What is the groundwater quality in my area? Is the groundwater getting worse or better? If we increase our use of the groundwater, what are the consequences?* Effective management of groundwater resources and the land-use activities above them requires better information on how these aquifers recharge, and how long the water contained in them has been underground.

While groundwater pathways into bedrock aquifers can be complex, two fundamental components of this flow system can be addressed: 1.) what is the composition, spatial distribution and hydraulic characteristics of geologic materials overlying the aquifer of interest, and 2.) what is the spatial distribution of vertical hydraulic gradient that drives groundwater downward into these aquifers? These two components of groundwater flow are addressed in part by groundwater flow models, which typically evaluate vertical flow in aquitards only, and by aquifer sensitivity mapping by the Minnesota Department of Natural Resources, which evaluates travel times base on permeability estimates and tritium content only, and not on hydraulic head gradients. This investigation looks at the chemical composition of groundwater primarily in the Prairie du Chien Group and the Jordan Sandstone, and interprets the distribution of groundwater chemical types in context of the composition, spatial distribution, and water-bearing

characteristics of overlying geologic materials, along with the distribution of vertical hydraulic gradients from the water table to these bedrock units.

Background and data sources

The late 1980's and early 1990's were a period of extensive water chemistry sampling and residence time analysis and classification based on the isotopic composition of groundwater in southeastern Minnesota. (e.g. Almendinger and Mitton, 1995; Smith and Nemetz, 1996; MPCA 1992-1993 GWMAP Data, summarized in Tipping, 1994; Wall and Regan, 1991, MPCA, 1999). This work coincided with groundwater flow investigations in the Rochester area (Delin, 1991; Delin and Almendinger, 1993). These investigations provided a baseline of chemical and groundwater flux data that has been built upon since that time both with additional sampling and analysis (Decorah Edge Recharge Area Monitoring – Rochester-Olmsted Planning Department, 2012; Lindgren, 2001; Mubarak, 2003; Crawford, 2012).

The chemical and isotopic data used in this report are from groundwater samples, the majority of which were taken between 1988 and 2012. Most data are from Olmsted County Environmental Resources (Terry Lee, written communication) that include data sampled as part of the Decorah Edge Recharge Area Monitoring – herein referred to as Clean Water Partnership (CWP) data, and other data analyzed by the Olmsted County Lab. The CWP data represent three sampling periods: 1989-1991, when many of the wells were sampled quarterly; 2001; and 2011-2012. Other historic water chemistry data come from the United States Geological Survey (USGS) (USGS, 2013), a 1994 baseline investigation – Southeast Minnesota Water Resources Board (Tipping, 1994), and Minnesota Pollution Control Agency Environmental Data Access (MPCA, 2013). Along with data collected as part of an ongoing groundwater monitoring

program in Dakota County (Dakota County, 2006), the Rochester-Olmsted County data are one of the few datasets in Minnesota that have repeated chemical analyses from the same well, over time frames from seasons to decades.

An additional subset of regional nitrate data (Runkel et al, 2013) which overlaps to some extent with results used in this investigation, were also analyzed to look at spatial and temporal distributions of nitrate below the Decorah Shale. The subset, herein referred to as MPCA_nitrate data, contains nitrate samples taken from 1988 through 2010. In addition to nitrate data contained in this report, this dataset includes data from Minnesota Department of Health (MDH) public water supply database, nitrate data from newly constructed wells, and regional voluntary nitrate program.

As with groundwater level measurements, groundwater chemical data are best understood by grouping data according to aquifer, position relative to aquitards, and hydraulic gradient. Additional information has been collected on bedrock hydrostratigraphy of southeastern Minnesota (Runkel et al., 2003; Runkel et al., 2006; Tipping et al., 2006, Anderson et al., 2011) that has markedly improved our understanding of bedrock controls on groundwater flow. This investigation looks at the spatial and temporal distribution of groundwater chemical types within the context of this revised hydrogeologic framework.

Geologic Setting

The regional geologic setting of southeastern Minnesota is characterized by relatively flat-lying, eroded Paleozoic bedrock, overlain by unconsolidated deposits mostly related to glacial processes, ranging in thickness from a few to several hundred feet thick. The western edge of Olmsted County borders the “drift dominated landscape” of southeastern Minnesota,

consisting of a relatively continuous blanket of unconsolidated sediment greater than 50 feet thick (Runkel et al., 2013). To the east, the majority of the county is part of the “bedrock dominated landscape” of southeastern Minnesota, where unconsolidated sediment greater than 50 feet thick is present only in patches, and the land surface topography is similar to the underlying bedrock topography (Runkel et al., 2013). The resultant geomorphology of this area is characterized by broad plateaus and mesas underlain by resistant limestone and dolostone, separated by escarpments and cut by narrow valleys. Within Olmsted County, two broad plateaus dominate the landscape: the Upper Carbonate Plateau, composed of the upper part of the Galena Group (Prosser, Stewartville and Dubuque Formation where present) with patches of overlying Maquoketa and Wapsipinicon Group in the highlands to the west, south and east of the Rochester Central Metropolitan Area (RCMA); and the Prairie du Chien Plateau, within and to the north and northeast of the RCMA (Figure 1). Separating the two plateaus is the eroded edge of the Upper Carbonate Plateau composed of, from bottom to top, the St. Peter Sandstone, Glenwood and Platteville Formations, Decorah Shale, and Cummingsville Formation (Figure 2a).

The eroded edge of the Upper Carbonate Plateau has been recognized from early groundwater modeling as an area of preferential recharge to underlying bedrock aquifers (Delin, 1991; Delin and Almendinger, 1993) (Figure 2b), and has been the subject of continued hydrogeologic investigations (e.g. Lindgren, 2001) and hydrochemical sampling and analysis (Olmsted County Environmental Resources (OCER) Clean Water Partnership (CWP) program , 2014; Mubarak, 2003), because concerns over recharge groundwater quality to Rochester’s water supply (e.g. Lindgren, 2001;). Groundwater chemical data from wells finished in the St. Peter

Sandstone, Prairie du Chien Group and Jordan Sandstone are analyzed based on their position relative to the Decorah Edge (this investigation) (Figure 2c).

The bedrock is composed of fine -to coarse-grained, quartz-rich sandstones; carbonate rock (limestone and dolostone); and very fine-grained sandstone, siltstone and shale. Individual formations are typically 50 to 200 feet thick (Figure 3). Olmsted County sits on the eastern limb of a regional structural depression known as the Hollandale Embayment. As a consequence, bedrock layers within the county dip slightly (less than 2 degrees) to the southwest.

Covering the bedrock surface are unconsolidated deposits typically less than 50 feet thick, with greater thicknesses to the west where they fill bedrock valleys. These deposits can generally be divided into coarse-grained sand- and gravel-dominated material deposited mostly in rivers, and finer-grained material that includes significant silt and clay deposited in lakes, flood plains, as till accumulating from melting glaciers, and as loess (windblown) deposits. In the uplands east and south of the Rochester metropolitan area, unconsolidated deposits are composed of loess, patchy till and sand and gravel deposits less than 50 feet thick (Hobbs, 1988). Textures range from silt (loess) to patches of loam to sandy loam. Bedrock valleys are filled with terrace deposits and alluvium, with textures ranging from silty and fine sand, to coarse sand and gravel. To the west, thicker, more continuous deposits of till are present, particularly in bedrock valleys, where thicknesses can exceed 200 feet. Textures range from loam to clay loam. Patches of weathered bedrock residuum are present over much of the bedrock surface where carbonates are uppermost bedrock.

Hydrogeology

Bedrock hydrostratigraphy

Our understanding of groundwater movement within the bedrock of southeastern Minnesota, particularly with regard to contaminant transport, has greatly improved since implementation of a hydrostratigraphic approach to hydrogeologic characterization (Runkel et al., 2003). In this approach, hydraulic data are interpreted and hydraulic conductivities are calculated in the context of measured and/or observed three-dimensional distributions of porosity and permeability, rather than assigning bulk hydraulic conductivity based on lithostratigraphic boundaries.

Results of this approach demonstrate that groundwater movement within southeastern Minnesota bedrock is consistent with the concept of “triple porosity” systems (e.g. Worthington, 2003). In this system, porosity and permeability are categorized into three groups: 1.) a three-dimensional matrix element with relatively low porosity and permeability, where large volumes of groundwater are stored; 2.) a two-dimensional planar element such as bedding planes and vertical fractures; and 3.) a one-dimensional integrated channel element where most groundwater moves. Channels are typically found along bedding planes and vertical joints. Where turbulent flow occurs they are referred to as conduits; in the case of carbonate rock, these channels can enlarge to cave passages. The two-dimensional planar elements move water stored in the matrix to the channels.

The predictable (mappable) distribution of triple porosity elements within these rocks, known as their hydrostratigraphic attributes, are a function of the matrix composition of the rock – either shale, siltstone, carbonate or sandstone – and its depositional, structural and erosional history. In addition to structural deformation resulting in fractures, it is recognized that long periods of time are missing from the rock record, when these rocks were exposed to weathering

and karstification. An important outcome of research on Paleozoic bedrock hydrostratigraphy over the last 15 years is documentation that these porosity features occur at specific stratigraphic positions (e.g. Runkel, et al., 2003, Runkel et al., 2006, Tipping, et al., 2006, Alexander et al., 2013). For example, bedding parallel fracture networks are densely clustered along specific stratigraphic intervals. Conversely, other stratigraphic intervals have been shown to be resistant to the through-going development of vertical fractures (e.g. Meyer et al., 2008, Anderson et al., 2011, Meyer et al., 2014), and these can limit groundwater flow in the vertical direction – acting as an important component in defining regional aquitards in southeastern Minnesota (Runkel et al., 2013).

Collectively these investigations represent a significant departure from the traditional hydrostratigraphic model for the Rochester area. Previous groundwater flow models have treated the St. Peter Sandstone, Prairie du Chien Group, and Jordan Sandstone as a single aquifer unit (Delin and Woodward, 1984; Delin and Almendinger, 1993). Specific changes to the conceptual model are the separation of these rocks into a Shakopee aquifer, a lower Oneota aquitard and a Jordan aquifer. Where not breached by vertical fractures or multi aquifer wells, the lower Oneota Dolomite and Coon Valley member of the Prairie du Chien Group provides hydraulic separation between the Shakopee Formation and the Jordan Sandstone, as seen in measureable flow between the two units in open boreholes and water level measurements, particularly evident when the Jordan is under stressed (pumping) conditions (Runkel et al., 2003; Tipping et al., 2006). In addition, local variability in the thickness of the Coon Valley member of the Prairie du Chien Group has a marked effect on selected Rochester Public Utility municipal well yields (Runkel, 1996). Runkel found that lower productivity in several municipal wells was

associated with unusually thick, low permeability Coon Valley section and subsequent thinner, more permeable quartzose Jordan facies in the open-hole intervals.

Additional changes to the traditional hydrostratigraphic conceptual model applicable to the Rochester metropolitan area is the separation of the lower Cummingsville Formation of the Galena Group from the overlying rocks, collectively referred to herein as the Galena aquifer. The lower Cummingsville Formation is composed of alternating beds of carbonate and shale that have both low matrix permeability and form discrete units that terminate vertical fractures, making it an effective aquitard (Runkel et al., 2006; Runkel et al., 2013).

Also relevant to the hydrostratigraphy of the Rochester area is the basal St. Peter Sandstone. Within the Twin Cities artesian basin, fine-clastic interbeds of siltstone and shale are present in the lower 50 to 70 feet of the St. Peter Sandstone (Olsen, 1976; Mossler, 2008), and have been shown to have low vertical hydraulic conductivity (Woodward, 1986; Runkel et al., 2003; Runkel et al., 2007). Within the RCMA, data related to this phenomena is limited. Lindgren, 2001 found vertical hydraulic head differences across the basal St. Peter nested observation wells located near the Decorah Formation edge in Rochester, although this difference may reflect groundwater mounding due to enhanced vertical groundwater flow in this setting. It is assumed in this investigation that permeability in the basal St. Peter Sandstone relative to the Cummingsville-Glenwood and lower Prairie du Chien does not significantly restrict vertical groundwater movement.

The revised hydrostratigraphic framework is summarized in Figure 3. ESRI multipatch versions of digital elevation models for the top elevations of these revised hydrostratigraphic constructed for Rochester Public Utilities (Tipping and Runkel, 2008) have been included as deliverables as part of this investigation for improved three-dimensional display.

Unconsolidated aquifers and aquitards

The vertical distribution of textures in unconsolidated deposits is an important factor in estimating vertical recharge to underlying bedrock aquifers. County-wide stratigraphy of unconsolidated deposits has not been mapped. In the absence of subsurface mapping, the vertical distribution of textures were estimated using statistical interpolation methods, given an adequate distribution of drillers records (Tipping, 2012). Results provide an approximate distribution of textures with depth, at regularly spaced intervals in horizontal and vertical dimensions. The distribution of material predominantly referred to as clay in driller's logs is distinctly different from the distribution of sandy materials for the Rochester metropolitan area (Figure 4). Although values intermingle by elevation where both textures are in the same area, some clear patterns emerge; thick deposits of relatively low permeability, predominantly fine-grained clayey material are present to the west, both in the uplands and bedrock valleys. To the southeast, bedrock valleys – Bear Creek Valley in particular – is filled relatively high permeability, coarse-grained sandy material; otherwise, unconsolidated materials on top of bedrock are thin to absent.

Hydraulic head gradients

Hydraulic head data come from a number of different sources, and vary temporally. The most useful data come from frequent measurements in areas with nested wells completed at different elevations. Across the Decorah Shale, Platteville Limestone and Glenwood Formations, nested water level measurements are available from USGS investigations on the hydrogeology of the Decorah Edge (Lindgren, 2001). Within the St. Peter Sandstone and Prairie du Chien Group, and between the upper Prairie du Chien and Jordan Sandstone, data are

available from the USGS (Lindgren, 2001), Rochester Public Utilities (RPU) and DNR observation wells (RPU, 2013; MnDNR, 2014), and RPU municipal supervisory and control data acquisition (SCADA) (RPU, 2013). Within the Upper Carbonate Plateau, these types of data are not available in Olmsted County, but have been collected at the BP Spring Valley Terminal in Fillmore County (see Runkel et al., 2013).

The distribution of vertical hydraulic head gradients within bedrock and unconsolidated deposits identify both major geologic controls and the impact of high capacity pumping on groundwater flow. The highest hydraulic heads occur within the Upper Carbonate Plateau. There, a regional aquifer system sits above the Cummingsville-Glenwood aquitard, with hydraulic head levels over 200 feet above the hydraulic head levels of the combined Prairie du Chien and Jordan aquifers (Figure 5). Under natural (non-pumping) conditions, the lowest hydraulic head occurs at the elevations of the major rivers leaving the county: 858 feet along the Zumbro River, downstream of the Shady Lake Dam; and 805 to 810 feet on the North Fork and Middle Branch of the Whitewater River at the Olmsted-Winona County border, herein referred to as regional discharge elevations.

Within the Rochester metropolitan area, hydraulic heads are often at lower elevations than these regional discharge elevations due to high capacity pumping. In the absence of synoptic, metro-wide measurements of seasonal changes in hydraulic head within the Prairie du Chien and Jordan aquifers, potential vertical gradients have been inferred by comparing maximum and minimum hydraulic heads in RPU wells completed in the Prairie du Chien and/or the Jordan Sandstone (RPU, 2013). Results show a potential departure from regional discharge elevations in the central and northwestern metropolitan area (Figure 5).

The distribution of wells pumping more than 10,000 gallons per day as permitted by and reported to the DNR show the spatial distribution of potential high capacity pumping impact on vertical hydraulic head gradients (Figure 6). Data from 2008 show that high capacity pumping is concentrated in the RCMA, with other wells distributed regionally primarily around local population centers. (Minnesota Department of Natural Resources, 2011).

The effect of pumping in the central metropolitan area compared to the rest of the county can be seen by comparing static water levels in observation wells to precipitation levels over time. Figure 7 shows precipitation data from the Rochester Airport, along with static water levels from observation wells completed in the St. Peter Sandstone, the Prairie du Chien Group and the Jordan Sandstone. The wells are located approximately west to east from the central metropolitan area, past the Decorah edge, and underneath the Cummingsville-Glenwood confining unit. Changes with time within the Prairie du Chien Group – identified as locations 1,2 and 3 in the figure – are dependent on location; well 1 is in the central metropolitan area and shows markedly lower elevation and greater variability due to high-capacity pumping; wells 2 and 3 are near or at the Decorah edge respectively, and show a seasonal rise due to focused spring recharge. Static water levels within a Jordan well (location 4) – also at the Decorah edge, and a St. Peter well (location 5) – located below the Cummingsville-Glenwood aquitard, show little seasonal change. The higher elevation and lack of variability in the Jordan well compared to Prairie du Chien pumping center observation well at location 1 shows that it is beyond the extent of vertical drawdown due to pumping, and is representative of aquifer conditions with the Jordan underneath the Cummingsville-Glenwood aquitard.

Regional contours of potentiometric surfaces above and below the Cummingsville-Glenwood aquitard show distinct differences in groundwater flow directions that are relevant to

groundwater quantity and quality in the Rochester area (Figure 8). Blue contours show the generalized potentiometric surface for groundwater in bedrock below the Cummingsville-Glenwood aquitard. Blue arrows show direction of groundwater flow within these rocks; red contours show the generalized potentiometric surface for groundwater in bedrock above the Cummingsville-Glenwood aquitard. Red arrows show direction of groundwater flow within these rocks. Note direction of groundwater flow below the aquitard is incongruent to the flow above it, particularly in the area southwest of Elgin-northeast of Rochester. The approximate location of a regional groundwater divide for aquifers beneath the aquitard is shown as a black dashed line. The groundwater divide marks the contributing area – groundwater-shed boundary for the Rochester metropolitan area and moves in response to changes in pumping levels and regional aquifer recharge (Delin and Almendinger, 1993; Lindgren, 2001).

Previous groundwater chemistry investigations

Several investigations of groundwater chemical data in Olmsted County have been completed or underway that are relevant to this investigation. Nemetz, 1993, and Smith and Nemetz, 1996 interpreted data along flowpaths east of the central metropolitan area as hydrochemical systems that operate independently of geologic constraints; Mubarak, 2003 in a chloride-nitrate investigation, identified primary sources of chloride in Olmsted County groundwaters as road salt, septic systems, and KCl fertilizer. He incorporated bedrock hydrostratigraphy into his analysis by ranking samples based on number of overlying bedrock units; Wilson and Crawford, 2006 completed a chloride budget for the county, working on the hypothesis that chloride concentrations in groundwater could be accounted for by an inventory of chloride sources. They noted that although chloride concentrations in streams leaving the county accounted for chloride amounts from land-use inventories within the uncertainty of the data,

chloride levels in groundwater were rising, and that some unaccounted for fraction of the inventoried load was being lost to groundwater.

Crawford, 2012 reviewed Clean Water Partnership (CWP) data over the period of the program's three sample periods: 1989-1991, 2001, and 2011. CWP wells were originally selected based on their construction and were limited to those completed and cased into the St Peter Sandstone, Prairie du Chien Group or Jordan Sandstone (Crawford, 2012). Many of the 1989-1991 wells were sampled quarterly. In order to investigate trends, Crawford 2012 compared means plus or minus 2 standard deviations for major cations and anions from sampled wells against single measurements that were taken from the same wells in 2001 and 2011. In addition, Crawford compared major cation and anion concentrations, along with cation concentration ratios – calcium to magnesium in particular - to factors related to physical setting, including aquifer, well depth, residence time (based on tritium), first encountered bedrock, and presence of the Decorah Shale. Crawford found that wells with the Galena Group as first encountered bedrock had lower dissolved oxygen than others. Wells with Platteville Formation as first encountered bedrock had higher specific conductance, total milli-equivalents, chloride, sodium and sulfate. Wells with Platteville Formation as first bedrock are located near the edge of the Decorah Formation, and are interpreted as receiving recharge waters with higher concentrations of anthropogenic components that are “focused” to this location by lateral flow through the Cummingsville Formation and the top of the Decorah Formation. Calcium to magnesium ratios were found to be a potential tracer for groundwater movement, with higher ratios associated with groundwater originating within the Galena Group, where a lower dolostone component in these rocks results in lower groundwater magnesium concentrations.

Methods

Chemical data used in this investigation fall into two broad categories – groundwater samples with complete analyses of major cations and anions, and groundwater samples with selected anions, such as chloride, sulfate and nitrate. In addition, several samples from both groups include tritium analyses which were also used to distinguish hydrochemical types.

Data with complete analyses of major cations and anions were further subdivided into data whose charge balance error – sum of cation milliequivalents minus anion milliequivalents, divided by total milliequivalents – was less than 5 percent. This subset was used to identify dominant cations and anions, and to investigate the spatial distribution and variability of calcium to magnesium molar ratios. Molar ratios were calculated based on activities of calcium and magnesium. It should be noted that anion ratios, chloride to bromide in particular, are useful for distinguishing chloride sources as natural or anthropogenic. Bromide analyses were, for the most part, not available in this dataset, so this type of anthropogenic “fingerprinting” of chloride was not possible.

It is possible, however, to use tritium data to establish background levels of anions, such as chloride, by comparing concentrations for samples having detectible tritium with samples that do not. Once background levels are established, the second category of data – those samples with limited anion analyses only, can be used to map the distribution of waters with anion concentrations above natural background levels. The elevations of these waters were mapped by interpolating the bottom-of-casing (top of open-hole) elevations for wells from where the samples were taken. These data were used to compare spatial distribution of chloride in post-1999 compared with 1990 data. Given that there are far more data in the second category, the Rochester-Olmsted County dataset is ideally suited for this type of analysis.

Chloride, nitrate, sulfate and calcium-magnesium molar ratios from all St. Peter, Prairie du Chien and Jordan data were compared spatially with respect to the edge of the Decorah Formation by separating results into three sample sets: zone 1, underneath and greater than 500 meters from the Decorah Edge; zone 2, within 500 meters of the Decorah Edge; and zone 3, not underneath and greater than 500 meters from the Decorah Edge. Changes in these data over time were also analyzed by dividing zone data into three date groups based on CWP sample periods: date group 1, from 1989 – 1991; date group 2, from 2001-2002 and date group 3, from 2009-2012. Date group 3 was modified to include all post-2008 data in order to increase sample size.

Data were analyzed using non-parametric methods, using either a two-sided Kruskal-Wallis test for comparing more than two sample populations, or a two-sided rank-sum test when only two sample populations were compared (Helsel and Hirsch, 2002). Sample concentrations listed in the dataset as “0” were assigned a value of 0.0999 for statistical analysis; values listed as below detection were assigned their detection limit. Results were interpreted in the context of our revised bedrock hydrostratigraphic framework, textural composition and thickness of unconsolidated deposits, and hydraulic gradients.

Results

In a system where chemical composition of groundwater is controlled solely by the dissolution of dolomite, bicarbonate molar concentrations would be expected to be twice the molar concentration of calcium plus magnesium:



This ratio is shown as a straight line in Figure 9. Waters with no detectable tritium, shown in blue, generally plot close to the line, whereas recent waters, shown in red, plot above it. A comparison of major cations with residence times provides a clear distinction in water types. Vintage waters are, for the most part, calcium-magnesium-bicarbonate waters, whose chemistry is controlled by dissolution of calcite and dolomite. Recent waters are characterized by the presence of other anions besides bicarbonate; ion exchange, in part involving sodium chloride and potassium chloride recharging waters produce calcium and magnesium chloride waters, resulting in points that plot above the dolomite dissolution line.

Piper plots from repeated samples in both MPCA ambient data and Clean Water Partnership data show changes in the composition of major cations and anions with time. Samples from 1992 for wells in the Jordan, Galena and Prairie Chien Group are water of calcium-magnesium-bicarbonate waters, with slightly less magnesium relative to calcium in Galena Group waters (Figure 10a). MPCA ambient data from three wells with both 1992 and 1997 data – points show changes in Prairie du Chien, St. Peter, and Galena Group water chemistry in those wells over the period of 5 years; changes are primarily seen in anion composition, with an increase in chloride and sulfate content (Figure 10b).

Clean Water Partnership (CWP) data from Jordan wells sampled in 1989-1991 plot in a tight cluster as calcium-magnesium-bicarbonate waters – indicative of natural background conditions; data from 2011 for the same wells show an increase in calcium relative to magnesium, and an increase in chloride and sulfate content (Figure 11a). CWP data from Prairie du Chien wells sampled in 1989-1991 also are calcium-magnesium-bicarbonate waters, but show a greater variability in chemical composition relative to Jordan wells from the same time period;

the pattern is repeated in 2011 samples, with a greater percentage of well water chemistry changing to primarily to higher chloride content (Figure 11b).

Relative to the Decorah edge for all sample dates, calcium-magnesium ratio medians are similar for St. Peter zone 1 and zone 2 data (p-value 0.1), not similar for Prairie du Chien zones 1, 2 and 3 data with zone 2 having the highest median value (p-value 0.003) and similar for Jordan zones 1, 2 and 3 data (p-value 0.1) (Figure 12). When ratios are compared through time, St. Peter data show an increase in zone 1 (p-value = 0.05) and zone 2 (p-value 0.04) (Figure 13); Prairie du Chien data show similar median values for zones 1, 2 and 3 (Figure 14); and Jordan data show similar median values for zone 1 but with a small sample set, similar median values for zone 3 (p-value 0.5) and an increase in median and range of values for zone 2 (p-value 0.004) (Figure 15).

Natural background levels of chloride in southeastern Minnesota groundwater have been identified as less than 2 mg/L (Tipping, 1994) and below detection (less than ~0.4 mg/L) in CWP wells (Crawford, 2012). Low natural background levels for chloride in data (this study) are best seen in scatterplot and summary statistics for chloride concentrations in groundwater samples with and without detectable tritium (Figure 16). Box plots show median, upper and lower quartile and outlier values for chloride concentrations versus tritium detection. Median chloride concentrations for samples with detectible tritium are significantly higher than from samples without detectable tritium at $\alpha = 0.05$. The spread of chloride values from samples with detectable tritium is greater and reflected in a higher mean value for this data group.

Chloride data show differences in spatial distribution based on hydrogeologic setting (hydrostratigraphy and hydraulic gradient), and how those patterns have changed over time.

Within the central metropolitan area, there are significant differences in chloride content between wells completed in the upper Prairie du Chien Group (Shakopee aquifer) and the Jordan Sandstone. This can be seen in boxplots of chloride concentrations in Prairie du Chien and Jordan samples, grouped by northwestern, northeastern, southwestern, southeastern portions of the central metropolitan area (Figure 17). In all cases, median values and spread are greater in Prairie du Chien samples than in Jordan samples. Jordan samples show the greatest spread in the southeastern and southwestern regions; Prairie du Chien samples show the greatest spread in the northeastern and northwestern regions.

Chloride concentrations in groundwater within the central metropolitan area have increased since the 1980s. A southwestern metropolitan area Prairie du Chien well sampled repeatedly by Olmsted County Lab, shows steadily increasing chloride with time for the period of 1989 through 2009 (Figure 18). Comparison of 1981 to 2011 data from RPU Prairie du Chien and Jordan wells show that chloride concentrations above a background level of 2 mg/L below at elevations below 870 feet have spread considerably in the horizontal direction and slightly deeper (Figure 19).

Relative to the Decorah edge for all sample dates, chloride median values increase from zone 1 to zone 2 for St. Peter data (p-value < 0.0005), dissimilar for Prairie du Chien and Jordan zones 1,2 and 3, with zones 2 and 3 having higher medians and more variability (p-value < 0.0005, and p-value = 0.003 respectively) (Figure 20). When chloride concentrations are compared through time, St. Peter data show an similar median values for zones 1 and 2 (p-value = 0.4 and 0.8 respectively) (Figure 21); Prairie du Chien data show similar median values for zones 1 and 3 (p-value 0.2 and 0.9 respectively, and dissimilar medians for zone 2 (p-value 0.003) with values increasing and becoming more variable with time (Figure 22); and Jordan

data show dissimilar median values for zone 1 (p-value 0.02) with increasing variability in post-2008 data, and similar median values for zones 2 and 3 (p-value 0.55 and 0.08 respectively), also with increasing variability in post-2008 data (Figure 23).

Relative to the Decorah edge for all sample dates, nitrate median values are similar to chloride results, with an increase from zone 1 to zone 2 for St. Peter data (p-value < 0.002), dissimilar values for Prairie du Chien and Jordan zones 1,2 and 3, with zones 2 and 3 having higher medians and more variability (p-value < 0.0005, and p-value = 0.0001 respectively) (Figure 24). When nitrate concentrations are compared through time, St. Peter data show similar median values for zones 1 and 2, (p-value < 0.005 and 0.75 respectively), although all median values are below the highest detection limit (Figure 25). Within the Prairie du Chien Group, nitrate concentrations are statistically different from one another for zones 1 and 2 (p-value < 0.005, 0.001 respectively) for periods 1989-1992, 2001-2002 post 2008, although as with the St. Peter samples, all median concentrations are below the highest detection limit in the dataset (0.02 mg/L NO₃-N). For zone 3, there is no statistical difference in median concentrations between periods 1989-1992 and 2001-2002, (p-value 0.31) (Figure 26). For Jordan samples, time groups 1989-1992, 2001-2002 and post 2008 are statistically different from one another for zones 1, 2 and 3 (p-value 0.14; < 0.005 and < 0.005 respectively, although medians for all sample sets are below the highest detection limit in the dataset (0.02 mg/L NO₃-N). For both zone 2 and zone 3, the largest spread in nitrate concentrations occurs in the 1989-1991 sample set (Figure 27).

Relative to the Decorah edge for all sample dates, sulfate median values are similar for St. Peter zones 1 and 2 (p-value = 0.55), but different from one another for both Prairie du Chien and Jordan data, with highest Prairie du Chien median value occurring in zone 2, and increasing

median values from zone 1 to zone 3 for Jordan data (p-value < 0.0005 and < 0.0005 respectively) (Figure 28). When sulfate concentrations are compared through time, St. Peter data show similar median values for zones 1 and 2 (p-value = 0.2 and 0.7 respectively) (Figure 29); Prairie du Chien data show similar median values for zones 1 and 3 (p-value 0.4 and 0.2 respectively), and dissimilar medians for zone 2 (p-value 0.005) with values increasing with time (Figure 30). Jordan data show dissimilar median values for zones 1 and 2 (p-value 0.001 and < 0.0005 respectively) with increasing variability in post-2008 data, and similar median values for zone 3 (p-value 0.06), slightly increasing variability in post-2008 data (Figure 31).

Discussion

Regional cross sections

Physical setting, hydraulic gradient and chemical data are summarized by cross section in Figures A through E. A key for cross section symbols is included in Figure 32; cross section locations are shown on Figure 1. Regional cross sections A-A' through E-E' (Figures 33-37) show variation in chemical types both with depth and through time along the general direction of groundwater flow towards the central Rochester metropolitan area.

In the region west of Byron to the RCMA, thick unconsolidated deposits are present on top of bedrock, composed largely of fine grained “clayey” material based on the interpolated texture model (Figure 33). Unconsolidated sediments in this area are thicker than elsewhere in the greater metropolitan area. In the bedrock, the Cummingsville-Glenwood confining layer is present to the far west and has limited extent. The potential vertical hydraulic gradient, based on the range of drawdowns reported for RPU wells, is most pronounced in areas where overlying

unconsolidated deposits are thin. 1989-1992 chemical data show vintage to mixed waters to the west underneath the thick till cap, and recent waters to the east.

From Oronoco to the RCMA, unconsolidated deposits are thin to absent, with not enough data to characterize grain size in the texture model (Figure 34). The Cummingsville-Glenwood confining layer is absent, with the Shakopee Formation of the Prairie du Chien Group uppermost bedrock over most of the region. The potential vertical hydraulic gradient is present to the south, with a greater change in hydraulic head in the vicinity of RPU 28. 1987-1991 data show recent water present predominantly in the Shakopee Formation of the Prairie du Chien Group. Data from the same time period show vintage to mixed waters within the Jordan throughout the cross section. By 2000, the distribution of recent waters is at the top of the Jordan Sandstone.

From northwest of Eyota to the RCMA, unconsolidated deposits are thin to absent over much of the cross section, with thicker deposits to the west composed in part of sandy material based on the interpolated texture model (Figure 35). The Cummingsville-Glenwood confining layer is present, with the incised Stewartville Formation as upper-most bedrock. Hydraulic head differences across the Cummingsville-Glenwood confining layer are greater than 100 feet; within the central metropolitan area, the potential vertical hydraulic head is greater than 100 feet to the west. 1990-1991 data show recent to mixed waters within the Shakopee Formation in where the Cummingsville-Glenwood confining layer is absent, and vintage to mixed waters in the Jordan Sandstone. Post-1999 data show recent waters within the Shakopee Formation extending underneath the Cummingsville-Glenwood confining layer.

From southwest of Eyota to the RCMA, thick unconsolidated deposits present in the Bear Creek Valley consist largely of sandy material based on the surficial geologic map and the

interpolated texture model (Figure 36). The Shakopee Formation of the Prairie du Chien Group is uppermost bedrock within the valley, and over most of the cross section. The Cummingsville-Glenwood confining layer is present to the southwest. Vertical gradients across the Cummingsville-Glenwood confining layer are greater than 100 feet, and the potential vertical gradient is greater than 100 feet in the central metropolitan area. 1987-1990 data show recent waters to mixed waters both within the Shakopee Formation and the Jordan Sandstone. Post-1999 data show recent waters reaching the top of the Jordan over portions of the cross section and extending back underneath the Cummingsville-Glenwood confining layer.

South of the RCMA, unconsolidated deposits are largely thin over much of the cross section, with patches of thicker deposits on the Upper Carbonate Plateau (Figure 37). Within the central metropolitan area, thicker deposits are present, composed of sand and gravel based on the interpolated texture model. Head differences across the Cummingsville-Glenwood confining layer are greater than 100 feet; the potential vertical changes due to high capacity pumping in the Prairie du Chien and Jordan aquifers extend underneath the Cummingsville-Glenwood confining layer. 1986-1990 data show recent to mixed waters within the Shakopee Formation in areas where the Cummingsville-Glenwood confining layer is not present and recent water from one well open to Prosser and Cummingsville Formations on the Upper Carbonate Plateau. A groundwater divide for aquifers below the Cummingsville-Glenwood confining layer is present in the middle of the cross section. 1990 data show vintage water, dated at 1400 years old, within the St. Peter Sandstone south of the groundwater divide and mixed to recent waters in the Jordan Sandstone within the central metropolitan area. Post-1999 data show presence of recent water extending underneath the Cummingsville-Glenwood confining layer, and to greater depths within the Shakopee Formation.

Regional water chemistry summary

Above the Cummingsville-Glenwood aquitard

Within Olmsted County, groundwater flow systems and chemical data can be broken into three major bedrock divisions based on the presence of regional aquitards (Figure 38).

Above the Cummingsville-Glenwood aquitard, groundwaters consist of recent waters, characterized by calcium to magnesium molar ratios of greater than 2.2, detectible NO₃-N, and elevated chloride. Historic groundwater chemistry data from the Upper Carbonate Plateau within Olmsted County is limited. Available analyses for major cations and anions indicate that the water has slightly higher calcium to magnesium ratios than the underlying Prairie du Chien and Jordan waters, (Figure 10a and 10b) due to greater calcite than dolomite content of the bedrock within the Galena Group (Mossler, 2008; Crawford, 2013). This conclusion is supported by regional historic data from the Galena aquifer within southeastern Minnesota (Tipping, 1994).

The presence of elevated nitrate within the Galena aquifer in Olmsted County is documented in data largely from domestic wells, analyzed by Olmsted County lab, site specific studies by the USGS at the Decorah edge, regional sampling as part of MCPA's ambient groundwater monitoring program (GWMAP), and from spring data collected in the late 1980's for the Olmsted County Atlas (Maki, 1989). Regional mean nitrate concentrations in upper-most bedrock for the bedrock dominated landscape of southeastern Minnesota range from 5 to 15 mg/L NO₃-N (Runkel et al., 2013).

Above the lower Prairie du Chien Group

Data from this bedrock division come from wells completed in the St. Peter Sandstone and Shakopee Formation of the Prairie du Chien Group. Below the Cummingsville-Glenwood aquitard and away from its edge (zone 1), groundwaters are characterized by calcium to

magnesium molar ratios of less than 2.2, low or limited NO₃-N, chlorides less than 2 mg/L. Groundwaters from near the confining layer edge (zone 2) have elevated chloride, elevated sulfate, and more variable calcium to magnesium molar ratios, typically greater than 2.2. Away from the edge in the area where the Cummingsville-Glenward aquifer has been eroded away (zone 3) waters (primarily Prairie du Chien samples) have elevated and more variable chloride and nitrate concentrations. Calcium to magnesium molar ratios are less variable than in zone 2, and have lower median values.

Distinct chemical composition within this bedrock division identifies areas of recent recharge and recharge source water. Calcium-magnesium ratios in Shakopee samples have higher median values in zone 2 compared with zones 1 and 3, indicative of focused recharge from above the Cummingsville-Glenwood confining unit. Chloride data also support the model of focused recharge from above the Cummingsville-Glenwood confining unit: median chloride concentrations from St. Peter samples are higher in zone 2 compared to zone 1; Shakopee samples have higher median chloride values in zones 2 and 3 compared to zone 1.

Focused recharge within zone 2 is also reflected in sulfate data for this bedrock division. Median sulfate values are slightly higher in zone 2 Shakopee samples compared with zones 1 and 3. Sources of elevated sulfate are considered to be from two sources: anthropogenic – primarily from atmospheric deposition; and from pyrite oxidation. Crawford 2012 identifies an atmospheric source for sulfate, with differences in surface water (OCER, 2012) (decreasing trend) and groundwater (increasing trend) attributable to residence time differences – quicker response of surface waters to atmospheric decline in surface waters than groundwaters. Emission controls related to the Clean Air Act have resulted in decreases in wet deposition rates of sulfate and hydrogen ion (Lehmann and Gay, 2011). Pyrite oxidation may also be a source of

sulfate in groundwaters. Oxidation of disseminated pyrite within the Platteville and Glenwood Formations produce sulfate that would produce elevated concentrations in zone 2 Shakopee wells.

Below the lower Prairie du Chien Group

Data from this bedrock division come from wells completed in the Jordan Sandstone. As with data St. Peter and Shakopee wells, distinct chemical composition and chemical variability within the Jordan identifies areas of recent recharge and recharge source water. Over the last twenty years, Jordan aquifer chemical composition in the central metropolitan area has changed in small, but significant ways. Within zone 1, groundwaters within the Jordan Sandstone have lower chloride and sulfate concentrations relative to groundwater above it, and have consistent calcium-magnesium molar ratios of less than 2.2. Although the water remains a calcium-magnesium-bicarbonate type, calcium magnesium ratios in zones 2 and 3 have increased slightly, and are more variable. Furthermore, chloride concentrations have steadily increased, and are more variable with time in zones 1, 2 and 3. Higher calcium to magnesium ratios and rising chloride concentrations at lower elevations indicate that the Jordan is receiving more vertical recharge in the central metropolitan area than it was in 1980s. Water supplying Jordan municipal water wells in the 1980s was likely water that had moved laterally from the south and southeast, with calcium to magnesium ratios similar to overlying/recharging Prairie du Chien waters. Since that time, a greater portion of recharge has come from and near Decorah edge settings, where waters from the Galena aquifer with higher calcium to magnesium ratios move downward into the Shakopee and underlying Jordan. Rising chloride levels in the Shakopee aquifer reflect possible increases in chloride loading during this time period, and/or slow replacement of older, low-chloride waters within the Shakopee aquifer.

Variability in water chemistry within all bedrock divisions also identifies areas of recent recharge. Both chloride and nitrate results from St. Peter, Shakopee and Jordan samples are more variable in zone 2, and in zone 3 for Shakopee and Jordan samples. For all wells sampled more than 4 times since 1999, greatest variability measured by highest standard deviations occurs in near surface samples and in zone 2 wells with top-of-open-hole elevations less than 800 feet (Figure 39), below the natural regional discharge elevation of 858 feet downstream of the Shady Lake Dam. The cause of this variability could be a combination of seasonal loading, shorter residence times, and larger vertical hydraulic gradients. In addition, variable flow paths under different hydrologic conditions due to secondary porosity and permeability in these rocks would result in variable water chemistry – particularly in conservative chemical components such as chloride.

Conclusions

The spatial distribution of recent waters – waters with chloride concentrations above a maximum natural background level of two milligrams per liter and/or detectible tritium content, calcium to magnesium ratios greater than 2.2, nitrate as nitrogen concentrations greater than 2 mg/L and sulfate concentrations greater than 22 mg/L – can be explained, in part by permeability differences and thickness of unconsolidated sediments overlying bedrock. Consistent presence of recent waters at lower elevations in bedrock aquifers over the period of record (1990-2010) in the eastern RCMA and along Bear Creek valley may be attributable, in part, to shallow-to-bedrock conditions, combined with higher sand content in unconsolidated sediments in that area. Conversely, deep-to-bedrock conditions in the western RCMA with higher clay content limited the advance of recent waters to lower elevations in bedrock aquifers during the 1990's and early

2000's; by 2010, recent waters were also present at these lower elevations. These changes with time may reflect an increase in vertical hydraulic gradient with time.

Chemical differences are also attributable, in part, to bedrock hydrostratigraphy. North and northeast of the RCMA, recent waters are largely limited to the upper portion of the Prairie du Chien Group (Shakopee Formation). Jordan water samples from the period of record from the same area have significantly lower chloride levels. Elevated nitrate levels within the Shakopee Formation compared to the Jordan aquifer also support the lack of hydraulic connection between the Shakopee Formation and Jordan Sandstone in this area. In addition to large differences in hydraulic head from underlying aquifers, groundwater in the Upper Carbonate Plateau typically has significantly higher calcium to magnesium ratios than waters from the underlying St. Peter Sandstone, Prairie du Chien Group and Jordan Sandstone. These differences in chemical composition help delineate source waters for groundwater moving laterally and vertically into the Prairie du Chien Group and Jordan Sandstone within the RCMA.

Recent waters based on elevated calcium to magnesium ratios and chloride, nitrate and sulfate concentrations extend underneath the Decorah edge primarily in the east and southeast metropolitan area (Figure 40). The presence of these waters underneath the edge support the hydrostratigraphic model that vertical fractures provide pathways through the Cummingsville-Glenwood confining unit near its edge.

The spatial distribution of groundwater chemical types is also a function of changes in vertical hydraulic gradients with time. Within the last 20 years, the extent of recent waters within the RCMA has expanded both horizontally and vertically. Groundwater calcium to magnesium ratios in the Prairie du Chien Group (Shakopee aquifer) and the Jordan Sandstone (Jordan aquifer) within the RCMA have also increased and show greater variability through time,

indicating a greater percentage of recharge to these aquifers moving vertically within the RCMA and from the Decorah edge than before high-capacity pumping began.

Much effort has been dedicated over the past decade to characterize water bearing characteristics of aquifers and aquitards in the Paleozoic rocks found in the Twin Cities area and elsewhere (Bradbury and Runkel, 2011). While advances have been made in our understanding of horizontal fractures, we are just beginning to understand and document the role of vertical fractures in these systems (e.g. Meyer et al., 2008; Anderson et al., 2011; Runkel et. al, 2013, Meyer et al., 2014). Elevations of detectable tritium and elevated chloride in the RCMA are lower than regional discharge elevations, showing the influence of high capacity pumping on groundwater flowpaths. More water moves in a vertical direction within the central RCMA than before high-capacity pumping began. In the Twin Cities metropolitan area, flow log and borehole video data provide evidence for rapid downward flow in multi-aquifer test wells located near municipal well fields (Tipping, 2012). It is likely that similar conditions are present in the Rochester metropolitan area. Less well documented, but likely just as important is downward flow through vertical fractures (Hart, 2006). In both cases of multi-aquifer wells and vertical fractures, increased gradients caused by hi-capacity pumping create conditions for rapid migration of water in the vertical direction. The implications of enhanced vertical recharge to the municipal recharge municipal well fields are two-fold. Wells that are receiving enhanced vertical recharge can be expected to be good suppliers of water in the future because the aquifer recharges rapidly compared to wells that are primarily receiving lateral recharge. However these same wells are more susceptible to surface contamination within wellhead protection areas, at rates likely faster than those predicted by conventional groundwater modeling.

Suggested use

Project deliverables were designed to provide water planners with both regional and site specific data for understanding groundwater flow in a geographic information systems (GIS) environment. Distribution of subsurface textures in unconsolidated deposits and hydrochemical facies mapping provide information on vertical permeability to bedrock aquifers. Digital elevation modeling of post-1999 recent water distribution show how flowpaths in RCMA groundwaters have changed with time. Multipatch models of bedrock surfaces provide a valuable tool to groundwater educators and decision makers for describing subsurface conditions to the general public.

At local and regional scales, project deliverables improve groundwater model calibration by helping to refine conceptual models of groundwater flow. Residence time data, reflected in the distribution of vertical recharge to upper bedrock aquifers, can be used to guide interpretation of calibration results as an alternative to calibration strictly by head values alone. Regional finite difference modeling can give reasonable predictions with regard to aquifer yield and drawdown, and refining aquifer and confining unit thicknesses in the model based on our revised hydrstratigraphic framework can improve model results.

In contrast, the distribution of chemical types (hydrochemical facies), elevated chloride concentrations in particular, are the result of water movement through secondary porosity and permeability, features not typically represented in regional groundwater flow models. As such, they often provide evidence of hydraulic connections over time and distances not consistent with calculated travel times from regional groundwater flow models. Predicting changes to spatial and temporal changes to water quality within the RCMA will require evaluating model results in

the context of continued hydrochemical facies mapping. These steps can result in a more realistic distribution of hydraulic conductivity parameters in numeric models.

Recommendations for further work

- Continue repeated sampling of either the same wells and over a greater geographic area through time. This type of data is not common in Minnesota, and provides a valuable means to identify changes in groundwater flowpaths through time. This type of information is not available from water level measurements alone.
- Expand network of nested observation wells with continuous logging of head levels within the RCMA, near the Decorah Edge and below the Upper Carbonate Plateau. This type of information with in necessary for accurate calibration of groundwater flow models, particularly with regard to estimates of vertical recharge to bedrock aquifers.

Acknowledgements

The author gratefully acknowledges funding from the Environment and Natural Resource Trust Fund as recommended by the Legislative and Citizen's Commission on Minnesota Resources (LCCMR) for their support of this investigation. Meetings and informal discussions with Kimm Crawford, along with Caitlin Meyer, Terry Lee and Phil Wheeler at Olmsted County Environmental Resources helped guide the content of this report and the format of the associated databases.

List of Figures

Figure 1. Investigation covers the extended Olmsted County, Minnesota. Datasets used are from Olmsted County Clean Water Partnership, sampling; 1994 baseline investigation: Southeast Minnesota Water Resources Board – Minnesota Pollution Control Agency; Minnesota Pollution Control Agency Environmental Data Access; United States Geological Survey National Water Inventory System (NWIS) data. Locations of cross sections (Figures 33 through 37) are shown.

Figure 2. **A.)** Generalized depiction of the Upper Carbonate Plateau escarpment, characteristic of the landscape setting surrounding the western, southern and eastern sides of the Rochester Central Metropolitan Area. The Upper Carbonate Plateau is underlain by carbonate rock with solution-enhanced porosity reflected by karst features such as sinkholes and disappearing streams. (Modified from Mossler and Hobbs, 1995; Runkel et al., 2013). **B.)** Focused recharge near the edge of the Decorah Formation – see text for discussion. **C.)** Subdivision of the St. Peter Sandstone, Prairie du Chien Group and Jordan Sandstone into zones based on their position relative to the edge of the Decorah Formation: zone 1 covers portions of these bedrock units that are underneath the Cummingsville-Glenwood aquitard and greater than 500 meters from the Decorah edge; zone 2 covers portions of these bedrock units that are within 500 meters of the Decorah edge; and zone 3 covers portions of these bedrock units not underneath the Cummingsville-Glenwood confining unit and greater than 500 meters from the Decorah Edge. Zones are used to analyze chemical results from these bedrock units relative to the Decorah edge.

Figure 3. Geologic and hydrogeologic columns for southeastern Minnesota. **A.)** Lithostratigraphic units - Bedrock of southeastern Minnesota is composed of coarse clastic, fine clastic or carbonate rock; stratigraphic names are typically associated with a dominant rock type, but that several units, such as the Jordan, are composed of an admixture of coarse and fine clastic rocks. **B.)** Hydrogeologic units. Bedrock of southeastern Minnesota classified on the basis of their hydraulic attributes. These attributes reflect both the distribution of matrix porosity and permeability, and secondary porosity and permeability (macropores). Unshaded portion of columns refers to section discussed in this investigation (Modified from Mossler, 2008).

Figure 4. Regional map showing distribution of subsurface relatively coarse-grained (red) and fine grained (blue) sediments, based on interpolation from CWI. Color indicates occurrence at any depth from the land surface to bedrock, having a minimum thickness of 10 feet. See text for reference to interpolation methods.

Figure 5. Regional area map showing vertical difference in hydraulic head relevant to groundwater quantity and quality in the Rochester area. Shown in blue are contours of vertical hydraulic head differences between aquifers within the upper carbonate group compared to

aquifers below the Glenwood Formation and overlying rocks. Large vertical differences greater than 200 feet are present across the combined Cummingsville, Decorah, Platteville, and Glenwood Formations; shown in red are differences in between minimum and maximum values for RPU wells open to the Prairie du Chien Group and/or the Jordan sandstone (RPU, 2013). Large vertical hydraulic head gradients within the Rochester metropolitan area result in enhanced vertical recharge (see text for discussion).

Figure 6. Regional area map showing the distribution of wells pumping more than 10,000 gallons a day in 2008, as permitted by and reported to the DNR. Symbol size shows relative reported pumping levels. High capacity pumping is concentrated in the central metropolitan area, with other wells distributed regionally primarily around local population centers. (Minnesota Department of Natural Resources, 2011).

Figure 7. Static water levels in selected observation wells compared to precipitation levels over time. Changes with time within the Prairie du Chien Group – identified as locations 1,2 and 4 in the figure – are dependent on location; well 1 is in the central metropolitan area and shows markedly lower elevation and greater variability due to high-capacity pumping; wells 2 and 4 are near or at the Decorah edge respectively, and show a seasonal rise due to focused spring recharge. Static water levels within a Jordan well – also at the Decorah edge, and a St. Peter well – located below the Decorah, show little seasonal change. The higher elevation and lack of variability in the Jordan well compared to Prairie du Chien pumping center observation well at location 1 shows that it is beyond the extent of vertical drawdown due to pumping, and is representative of aquifer conditions with the Jordan underneath the Cummingsville-Glenwood confining unit.

Figure 8. Regional area map showing horizontal differences in hydraulic head relevant to groundwater quantity and quality in the Rochester area. Blue contours show the generalized potentiometric surface for groundwater in bedrock below the Cummingsville-Glenwood confining unit. Approximate location of a regional groundwater divide is shown as a black dashed line. Blue arrows show direction and relative magnitude of groundwater flow within these rocks; red contours show the generalized potentiometric surface for groundwater in bedrock above the Cummingsville-Glenwood confining unit. Red arrows show direction of groundwater flow within these rocks. Note direction of groundwater flow below the confining unit is oblique to the flow above it, particularly in the area southwest of Elgin-northeast of Rochester. (see text for discussion).

Figure 9. Scatterplot of calcium plus magnesium compared to bicarbonate concentration in millimoles per liter for all water well samples with charge balance errors less than 5 percent. Age classification based on the presence of detectable tritium. Location map shows distribution of points. Box plots show median, upper and lower quartile and outlier values for distance from point to the dolomite dissolution line for recent, mixed and vintage waters.

Figure 10. Piper plots of data from MPCA ambient groundwater monitoring program showing regional background and changes groundwater chemical composition through time: **a.)** 1992 data for wells in the Jordan, Galena and Prairie Chien group – points show all water of calcium-magnesium-bicarbonate type, with slightly less magnesium relative to calcium in Galena Group waters; **b.)** data from 3 wells with both 1992 and 1997 data – points show changes in Prairie du Chien, St. Peter, and Galena Group water chemistry over time. Changes are primarily seen in anion composition, with an increase in chloride and sulfate content over a five year period.

Figure 11. Piper plots of data from Clean Water Partnership program for the greater metropolitan area from Prairie du Chien and Jordan wells sampled both in 1989-1991 and 2011. **a.)** Jordan wells from 1989-1991 plot in a tight cluster as calcium-magnesium-bicarbonate waters – indicative of natural background conditions; 2011 points show an increase in calcium relative to magnesium, and an increase in chloride and sulfate content. **b.)** Prairie du Chien wells from 1989-1991 also are calcium-magnesium-bicarbonate waters, but show a greater variability in chemical composition relative to Jordan wells from the same time period; pattern is repeated in 2011 samples, with a greater percentage of well chemistry changing to primarily to higher chloride content.

Figure 12. Ca-Mg molar ratios in the St. Peter Sandstone, Prairie du Chien Group and Jordan Sandstone compared by well location relative the Decorah Edge. Ca-Mg ratio results were separated into three zones: zone 1, underneath and greater than 500 meters from the Decorah Edge; zone 2, within 500 meters of the Decorah Edge; and zone 3, not underneath and greater than 500 meters from the Decorah Edge. Results for the Prairie du Chien Group show median values are not similar (p-value 0.003) with highest median value in zone 2. Median values for the St. Peter and Jordan are similar within zones.

Figure 13. Ca-Mg molar ratios in the St. Peter Sandstone relative to the Decorah Edge through time. For zones 1 and 2, rank-sum test show median ratios are not similar (p-values 0.005 and 0.04 respectively). Zone 2 samples are limited to only 4 results from the western RCMA only.

Figure 14. Ca-Mg molar ratios in the Prairie du Chien Group relative to the Decorah Edge through time. Rank-sum show ratios in zones 1 and 2 are not statistically different from one another when comparing time periods 1989-1991 against post 2009 data (p-values 0.49 and 0.80 respectively).

Figure 15. Ca-Mg molar ratios in the Jordan Sandstone relative to the Decorah Edge through time. Rank-sum test shows zone 2 median values are different from one another (p-value 0.0004, with higher median value in post-2009 samples).

Figure 16. Scatterplot and summary statistics for chloride concentrations in wells with and without detectable tritium. Location map shows distribution of points. Box plots show median, upper and lower quartile and outlier values for chloride concentrations versus tritium detection. Median chloride concentrations for samples with detectable tritium are significantly higher than

from samples without detectable tritium at $\alpha = 0.05$. The spread of chloride values from samples with detectable tritium is greater and reflected in a higher mean value for this data group.

Figure 17. Boxplots of chloride concentrations in Prairie du Chien and Jordan samples, grouped by northwestern, northeastern, southwestern, southeastern metro regions. In all cases, median values and spread are greater in Prairie du Chien samples than in Jordan samples. Jordan samples show the greatest spread in the southeastern and southwestern regions; Prairie du Chien samples show the greatest spread in the northeastern and northwestern regions.

Figure 18. Chloride trend with time for Prairie du Chien well 139135, southwestern metropolitan area. Well sampled repeatedly by Olmsted County lab, shows steadily increasing chloride with time for the period of 1989 through 2009.

Figure 19a. Metro area map showing the 1981 horizontal and vertical distribution of recent waters in RPU wells below an elevation of 870 feet. Raster created from contours of open hole top (casing bottom) elevation for wells with chloride concentrations greater than 2 mg/L.

Figure 19b. Metro area map showing the 2011 horizontal and vertical distribution of recent waters in RPU wells below an elevation of 870 feet. Raster created from contours of open-hole top (casing bottom) elevation for wells with chloride concentrations greater than 2 mg/L. Compared to the 1981 distribution shown in Figure 15a, recent waters below an elevation of 870 feet have spread considerably in the horizontal direction, and slightly more in the vertical direction.

Figure 20. Chloride concentrations in the St. Peter Sandstone, Prairie du Chien Group and Jordan Sandstone compared by well location relative the Decorah Edge. Chloride results were separated into three zones: zone 1, underneath and greater than 500 meters from the Decorah Edge; zone 2, within 500 meters of the Decorah Edge; and zone 3, not underneath and greater than 500 meters from the Decorah Edge. Results for the Prairie du Chien Group and Jordan Sandstone show highest median values and greatest concentration spread in zones 2 and 3 compared with zone 1; The St. Peter Sandstone results showed higher median value and greater concentration spread in zone 2 compared with zone 1.

Figure 21. Chloride concentrations in the St. Peter Sandstone relative to the Decorah Edge through time. For zones 1 and 2, Kruskal-Wallis test show concentrations over time are not statistically different from one another for either zone (p-values 0.4 and 0.8 respectively). Zone 1 median concentrations are below regional background concentrations (2 mg/L chloride).

Figure 22. Chloride concentrations in the Prairie du Chien Group relative to the Decorah Edge through time. For zone 1 and 3, Kruskal-Wallis test show concentrations are statistically similar (p-value = 0.2, 0.9 respectively) for periods 1989-1992, 2001-2002 post 2008 although

median concentrations for zone 3 are trending towards higher values and greater overall spread. For zone 2, median values are statistically different between periods 1989-1992 and 2001-2002 (p-value 0.003), and are trending towards higher values and greater overall spread.

Figure 23. Chloride concentrations in the Jordan Sandstone relative to the Decorah Edge through time. Kruskal-Wallis tests show time groups 1989-1992, 2001-2002 and post 2008 statistically different from one another for zone 1 (p-value 0.02), although zone 1 medians for all sample sets are below regional background concentrations (2 mg/L chloride). Both zone 2 and zone 3 sample sets are not statistically different from one another. Largest spreads occur in post-2008 sample sets for all three zones.

Figure 24. Nitrate concentrations in the St. Peter Sandstone, Prairie du Chein Group and Jordan Sandstone compared by well location relative the Decorah Edge. Nitrate results were separated into three zones: zone 1, underneath and greater than 500 meters from the Decorah Edge; zone 2, within 500 meters of the Decorah Edge; and zone 3, not underneath and greater than 500 meters from the Decorah Edge. Results for the Prairie du Chien Group and Jordan Sandstone show highest median values and greatest spread of concentrations in zone 3 followed by zone 2 and zone 1; The St. Peter Sandstone results showed higher median values in zone 2 than in zone 1.

Figure 25. Nitrate concentrations in the St. Peter Sandstone relative to the Decorah Edge through time. For zone 1, Kruskal-Wallis test show concentrations are statistically different from one another (p-value < 0.005), although all median concentrations are below the highest detection limit in the dataset (0.02 mg/L NO₃-N); for zone 2, there is a greater spread in 2001-2002 values than 1989-1992 group – rank-sum test shows no statistical difference in median concentrations, without a high level of confidence (p-value 0.75).

Figure 26. Nitrate concentrations in the Prairie du Chien Group relative to the Decorah Edge through time. For zone 1 and 2, Kruskal-Wallis test show concentrations are statistically different from one another (p-value < 0.005, 0.001 respectively) for periods 1989-1992, 2001-2002 post 2008, although all median concentrations are below the highest detection limit in the dataset (0.02 mg/L NO₃-N); for zone 3, rank-sum test shows no statical difference in median concentrations between periods 1989-1992 and 2001-2002, without a high level of confidence (p-value 0.31) .

Figure 27. Nitrate concentrations in the Jordan Sandstone relative to the Decorah Edge through time. Kruskal-Wallis tests show time groups 1989-1992, 2001-2002 and post 2008 statistically different from one another for zones 1, 2 and 3 (p-value 0.14; < 0.005 and < 0.005 respectively, although medians for all sample sets are below the highest detection limit in the dataset (0.02 mg/L NO₃-N). For both zone 2 and zone 3, the largest spread in nitrate concentrations occurs in the 1989-1991 sample set.

Figure 28. Sulfate concentrations in the St. Peter Sandstone, Prairie du Chien Group and Jordan Sandstone compared by well location relative the Decorah Edge. Sulfate results were separated into three zones: zone 1, underneath and greater than 500 meters from the Decorah Edge; zone 2, within 500 meters of the Decorah Edge; and zone 3, not underneath and greater than 500 meters from the Decorah Edge. St. Peter sample sets are statistically similar to one another (p-value 0.55) and Prairie du Chien sample sets are not statistically similar to one another, with the highest median value occurring in zone 2. The Jordan sample set medians are statistically different from one another (p-value < 0.0005), with an increase in median values from zone 1 to zone 3.

Figure 29. Sulfate concentrations in the St. Peter Sandstone relative to the Decorah Edge through time. For zones 1 and 2, Kruskal-Wallis test show concentrations are not statistically different from one another (p-value = 0.2 and 0.7 respectively).

Figure 30. Sulfate concentrations in the Prairie du Chien Group relative to the Decorah Edge through time. For zone 1 and 3, Kruskal-Wallis test show concentrations are not statistically different from one another (p-value = 0.4 and 0.2 respectively) for periods 1989-1992, 2001-2002 post 2008; for zone 2, Kruskal-Wallis test shows medians are not similar, median values increasing over the three time periods.

Figure 31. Sulfate concentrations in the Jordan Sandstone relative to the Decorah Edge through time. Kruskal-Wallis tests show time groups 1989-1992, 2001-2002 and post 2008 statistically different from one another for zones 1 and 2 and 3 (p-values 0.001 and < 0.0005 respectively), with highest median values in post 2008 samples. Zone 3 medians for all three time periods were statistically similar to one another (p-value 0.06).

Figure 32. Cross section key for Figures 33 through 37. The line depicting bottom of post-1999 waters is generalized and does not capture all top-of-open hole recent water elevations shown on cross sections.

Figure 33. Regional cross section A-A', West of Byron to central metropolitan area. Thick (greater than 100 feet) unconsolidated deposits are present in the western and central parts of the cross section, composed mostly of fine-grained "clayey" sediment; thinner unconsolidated deposits, consisting of coarser-grained "sandy" sediment to the east. Potential downward gradient due to municipal well pumping shown in eastern part of the cross section. Wells sampled prior to 1991 show mostly vintage to mixed waters below thicker, low permeability sediments to the west, and recent and mixed waters to the east. Locations and open-hole intervals of RPU wells shown for reference.

Figure 34. Regional cross section B-B', Oronoco to central metropolitan area. Less than 50 feet of unconsolidated deposits are present over most of the cross section. Eroded remnants of St. Peter Sandstone, along with an isolated mesa of Platteville Formation are present in the central and northern parts of the cross section; otherwise most of the cross section shows Prairie du

Chien Group as upper-most bedrock. Wells sampled prior to 1992 show recent waters in the Shakopee Formation of the Prairie du Chien Group, and vintage to mixed waters in the Jordan Sandstone. Potential downward gradient due to municipal well pumping shown in eastern part of the cross section. Post-1999 chloride concentrations from Olmsted County lab samples show recent waters present at elevations at or below the top of the Jordan Sandstone. Locations and open-hole intervals of RPU wells shown for reference.

Figure 35. Regional cross section C-C', Northwest of Eyota to central metropolitan area. Less than 50 feet of unconsolidated deposits are present over most of the cross section; Galena Plateau present in eastern two-thirds of the cross section. Potential downward gradient due to municipal well pumping shown to the west. Wells sampled prior to 1991 show recent to mixed waters within the Shakopee Formation to the west, vintage to mixed waters within the Shakopee Formation underneath the Cummingsville-Glenwood confining unit, and vintage to mixed waters in the Jordan Sandstone. Post-1999 chloride concentrations from Olmsted County lab samples show recent waters extending to elevations at the top of the Jordan Sandstone in the central metropolitan area to the west, and into the Shakopee Formation to the east, underneath the Cummingsville-Glenwood confining unit.

Figure 36. Regional cross section D-D', Southwest of Eyota, along the Bear Creek valley to central metropolitan area. Fifty feet or greater of unconsolidated deposits consisting mostly of coarser-grained "sandy" material present over mostly the Prairie du Chien Group, along with some remnants of St. Peter Sandstone and small mesas of Platteville Formation. Potential downward gradient due to municipal pumping is present to the north east; excess hydraulic head within the Galena Group diminishes east of the Galena plateau edge. Wells sampled prior to 1992 show predominantly recent waters within the Shakopee Formation in the central and northeastern parts of the cross section, and mixed waters in the Jordan Sandstone within the same area. Post-1999 chloride concentrations from Olmsted County lab samples show recent waters at similar elevations to pre-1991 sampling, and extending into the Shakopee Formation underneath the Galena plateau.

Figure 37. Regional cross section E-E', Northwest of Stewartville to central metropolitan area. Less than 50 feet of unconsolidated sediment present over most of the cross section, with thicker deposits in the central metropolitan area characterized as mostly coarse-grained "sandy" sediment. Galena plateau is present in the southern two-thirds of the cross section. Potential downward gradient due to municipal pumping is present to the north and extends back underneath a portion of the Cummingsville-Glenwood confining unit; excess hydraulic head within the Galena Group diminishes south of the Galena plateau edge. A groundwater divide within the St. Peter, Prairie du Chien Group and Jordan Sandstone is shown. Wells sampled prior to 1991 show vintage waters within the St. Peter south of the groundwater divide, with a carbon-14 date for one well of 1,400 years. Recent water is present in the one well sampled within the Galena Group, and waters within the Shakopee Formation and Jordan Sandstone are vintage to mixed below and near the Galena Plateau edge and recent within the

central metropolitan area. Post-1999 chloride concentrations from Olmsted County lab samples show recent waters present within the Shakopee Formation underneath the Cummingsville-Glenwood confining unit, and at the top of the Jordan Sandstone within the central metropolitan area.

Figure 38. Oblique view from the north of bedrock surfaces, separated into three categories based on the presence of regional aquitards: **A.)** bedrock units above the St. Peter Sandstone. Groundwaters in the upper carbonate plateau (above the Cummingsville-Glenwood confining unit) consist of recent waters, characterized by calcium to magnesium molar ratios greater than 2.2, detectible NO₃-N, elevated chloride. **B.)** St. Peter Sandstone and upper Prairie du Chien Group. Groundwaters in these bedrock units fall into two categories: vintage waters below the Decorah, Platteville and Glenwood Formations, characterized by calcium to magnesium molar ratios of less than 2.2, low or limited NO₃-N, chlorides less than 2 mg/L; recent waters where the St. Peter Sandstone or Prairie du Chien group are first bedrock, characterized by elevated chloride, elevated sulfate, and more variable calcium to magnesium molar ratios, typically greater than 2.2. These waters are also found underneath the Glenwood Formation and overlying rocks in areas where the horizontal hydraulic gradient within the Prairie du Chien Group is oblique the horizontal hydraulic gradient in the upper carbonate group (see Figure 8); **C.)** Jordan Sandstone, lower chloride and sulfate concentrations relative to category “B” waters, consistent calcium to magnesium molar ratios of less than 2.2 below the Glenwood Formation, and more variable where the Glenwood and bedrock units above it are not present.

Figure 39. Comparison of chloride concentration standard deviations to top-of-open-hole elevations for all wells sampled more than 4 times since 1999. Greatest variability measured by highest standard deviations occurs in near surface samples and in zone 2 wells with open hole elevations less than 800 feet.

Figure 40. Chemical indicators of recent waters within the St. Peter Sandstone, Prairie du Chien Group and Jordan Sandstone: **A.)** mapped extent of calcium to magnesium ratios greater than 2.2; **B.)** chloride concentrations greater than 2 mg/L; **C.)** nitrate as nitrogen concentrations greater than 2 mg/L; **D.)** sulfate concentrations greater than 22 mg/L. Images produced from rasters “camg_p99_comb”, “cl_p99_comb”, “no3n_p99_comb” and “so4_p99_comb” respectively.

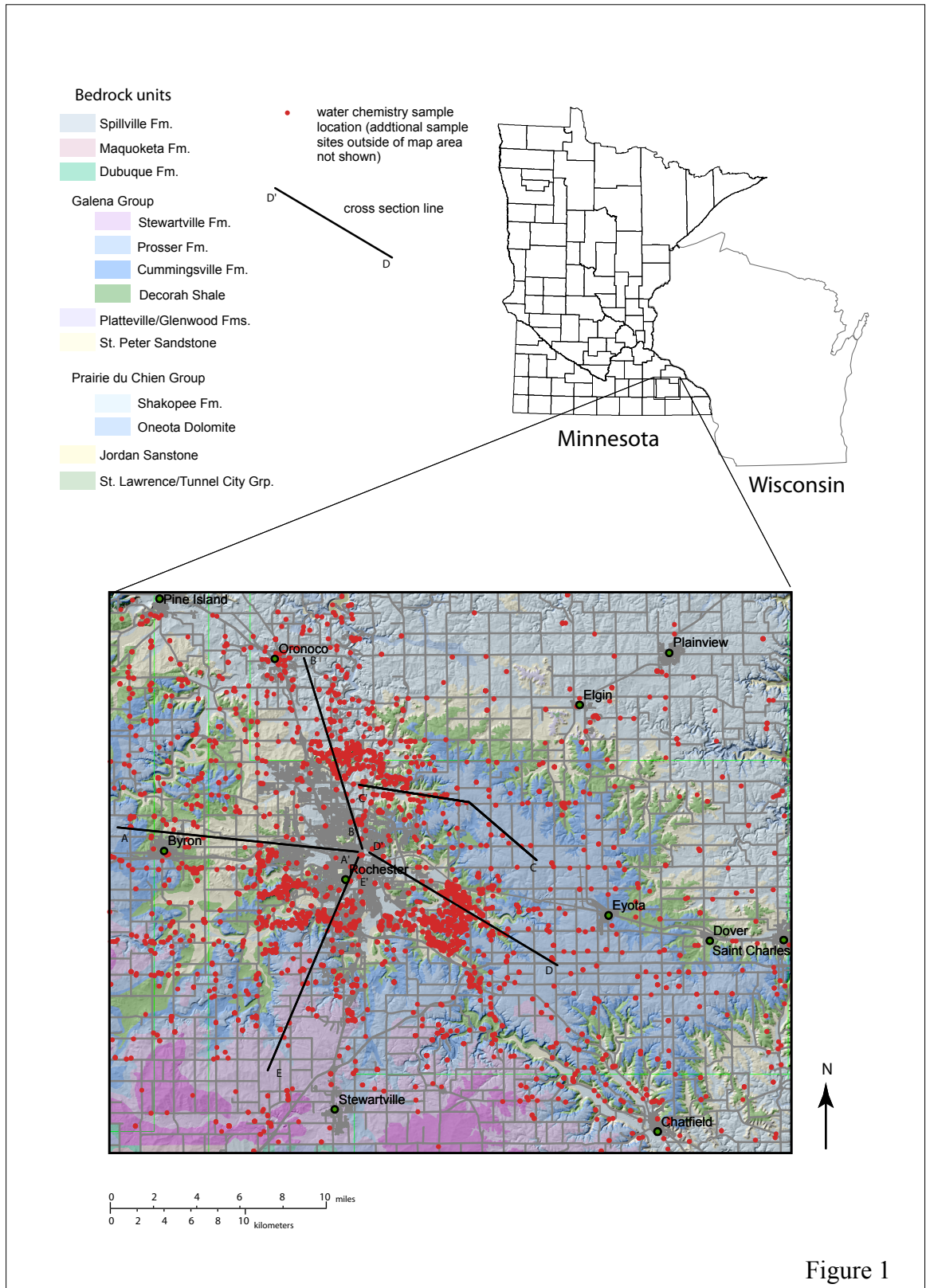
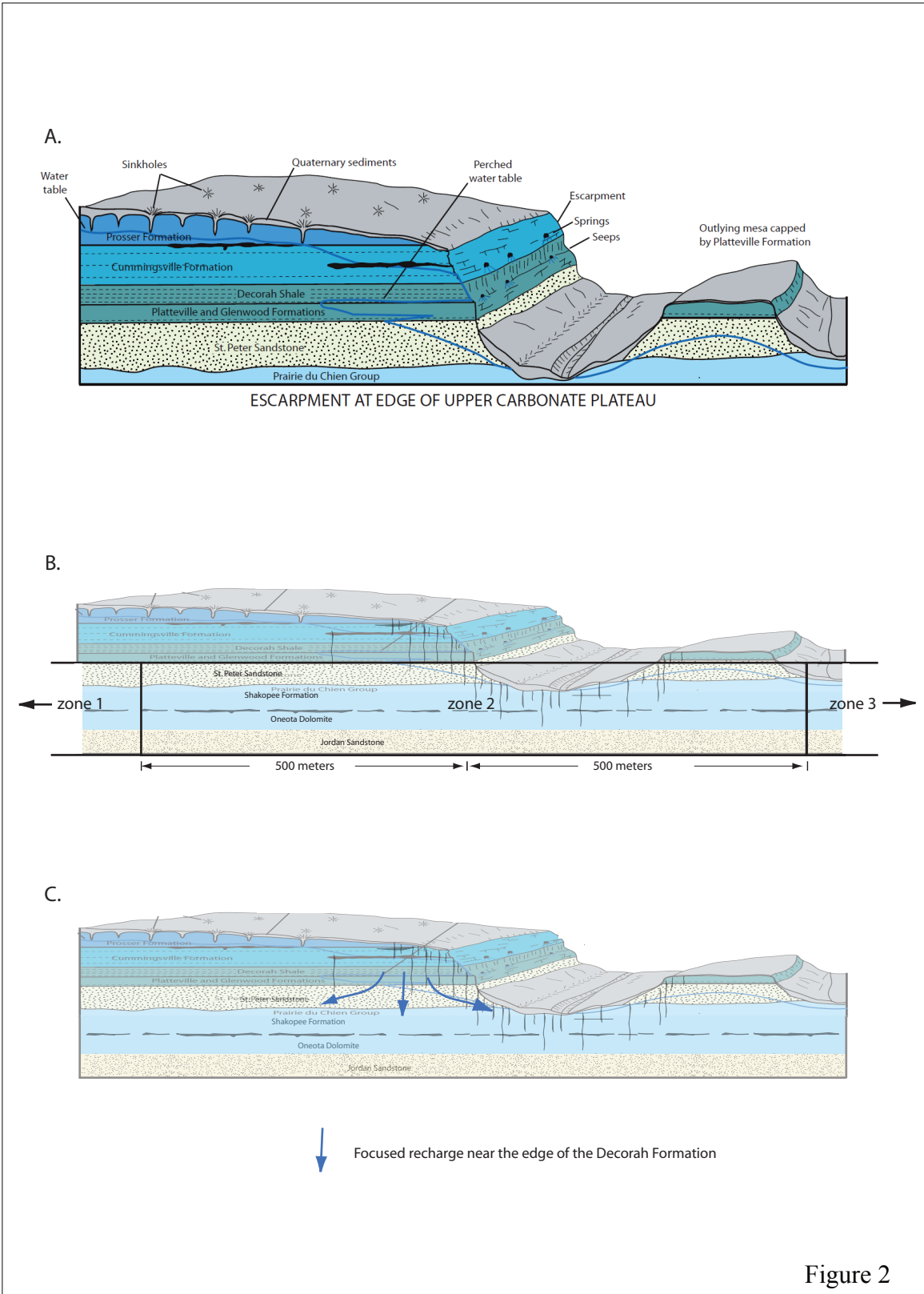
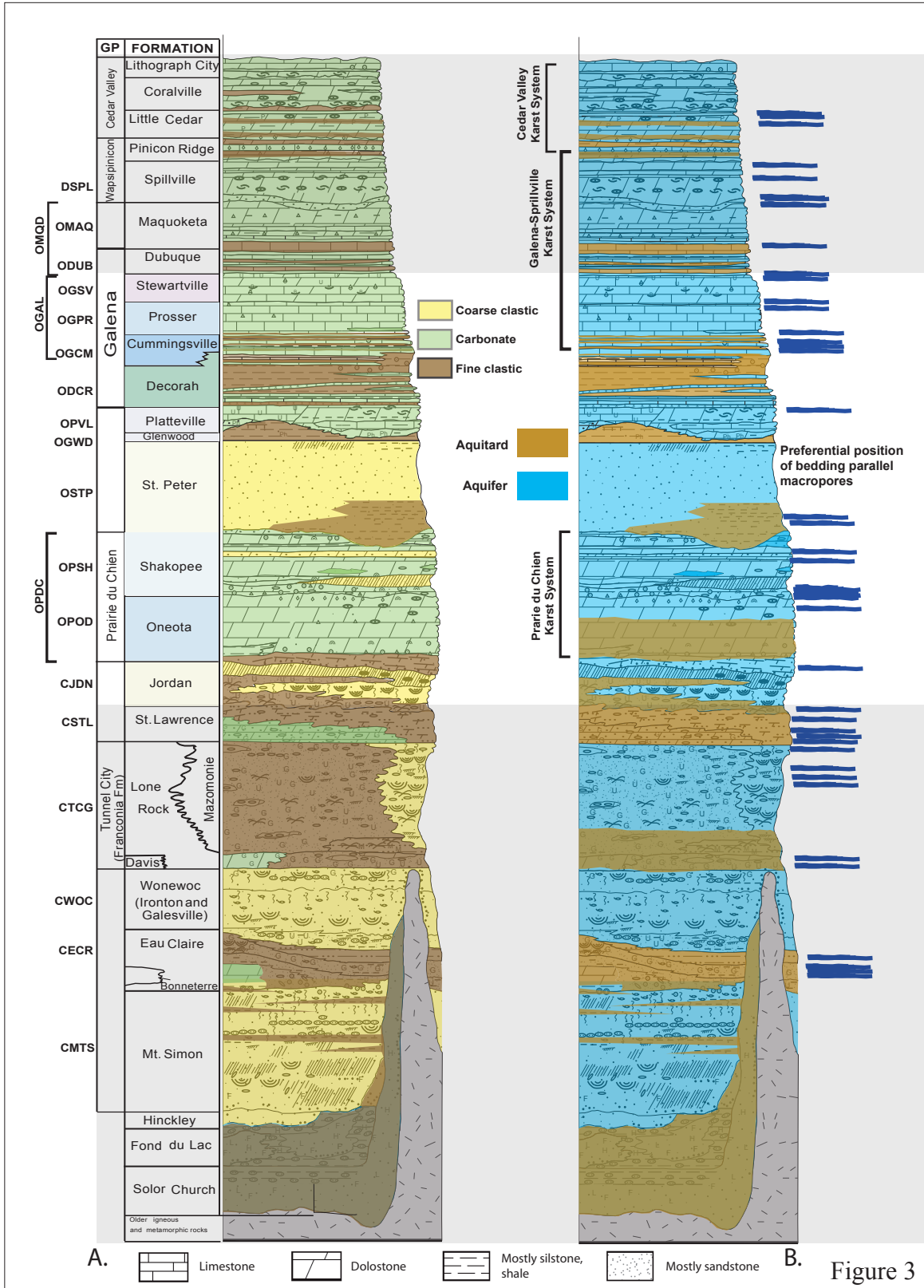
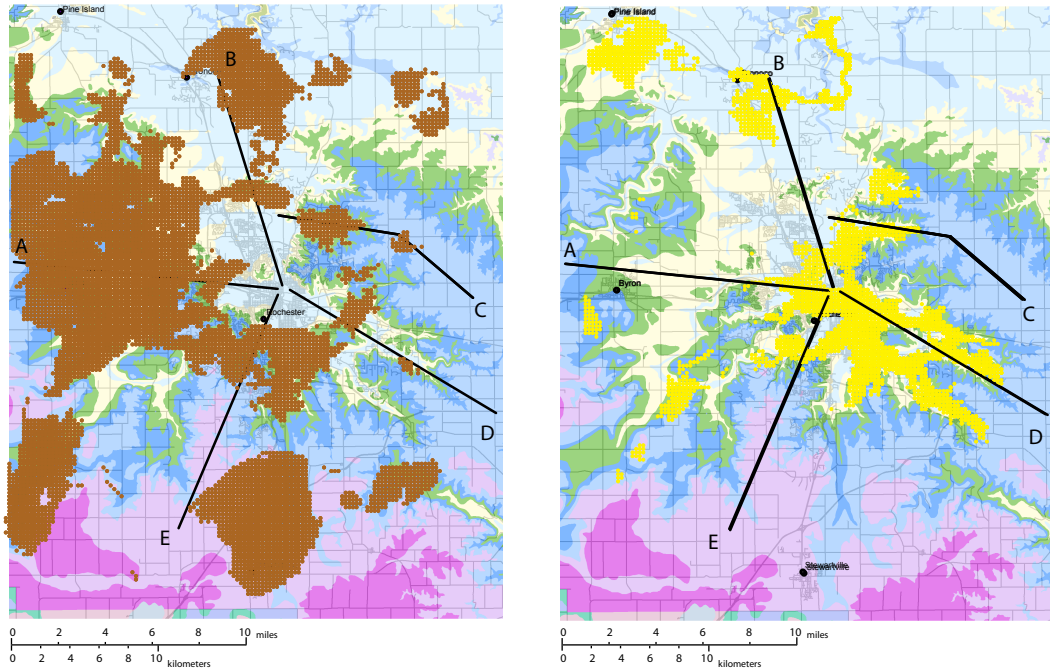


Figure 1



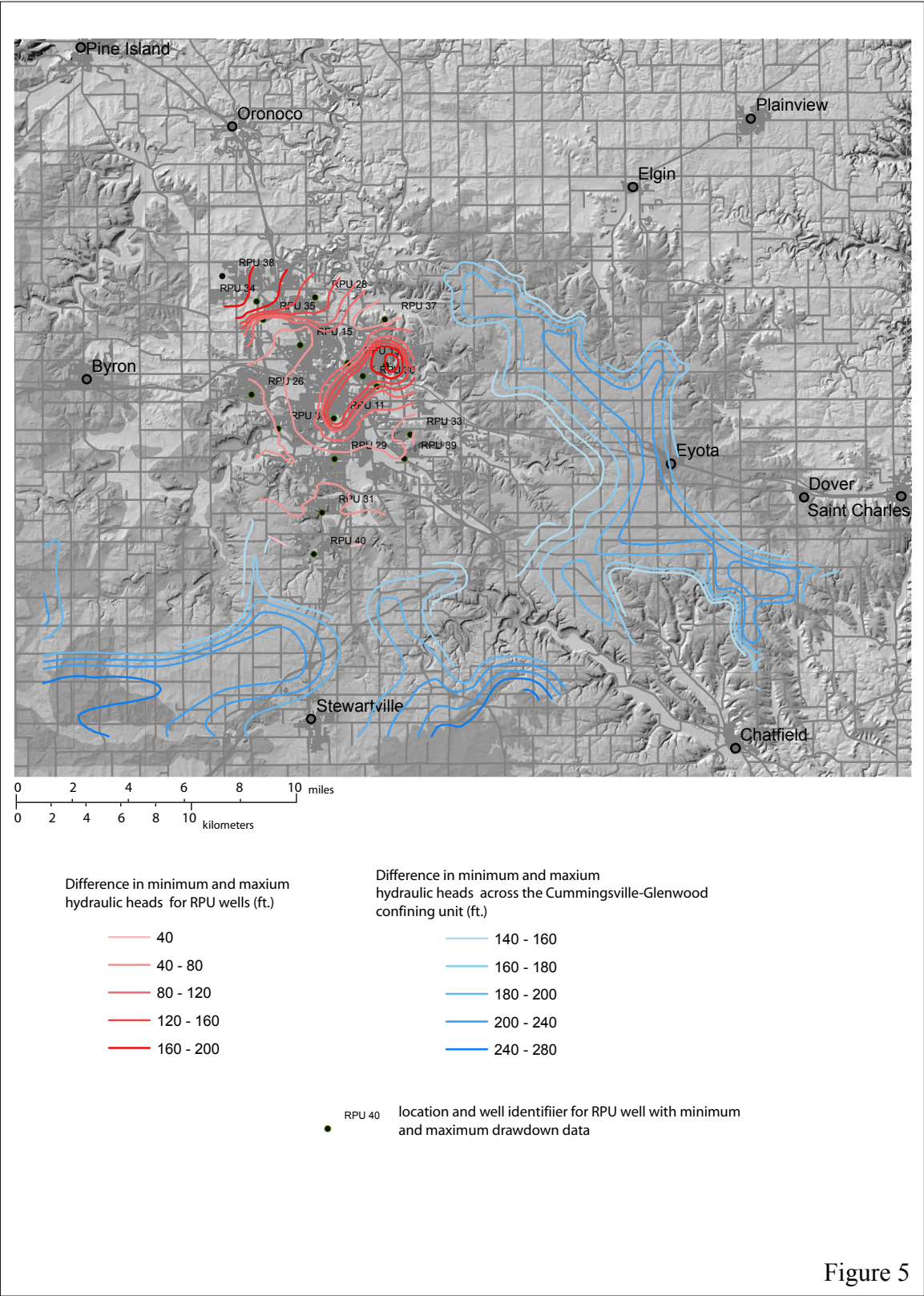




- mapview of three-dimensional likelihood of fine-grained "clayey" unconsolidated deposits, interpolated from County Well Index (CWI) stratigraphic records

- mapview of three-dimensional likelihood of coarse-grained "sandy" unconsolidated deposits, interpolated from County Well Index (CWI) stratigraphic records

Figure 4



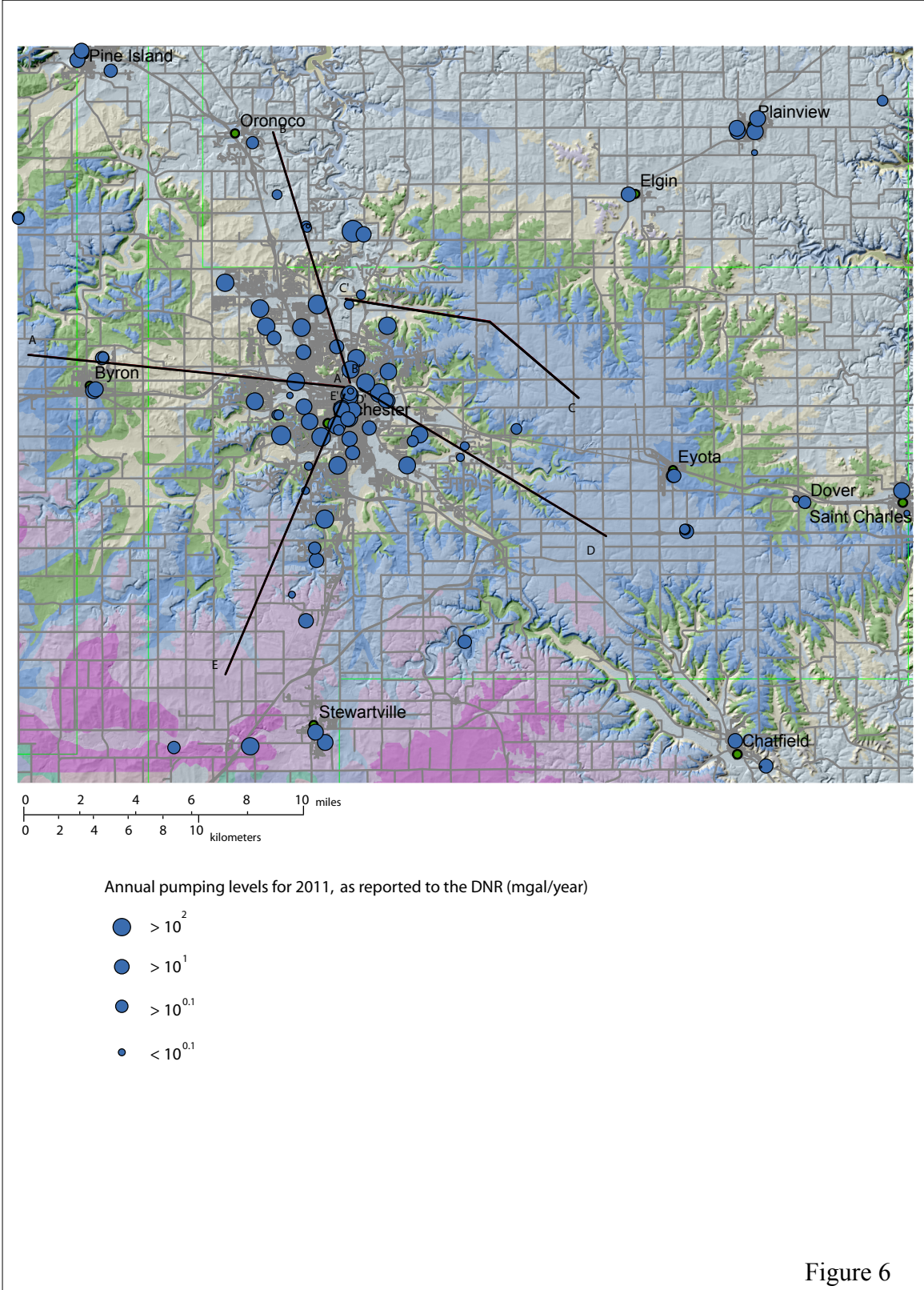
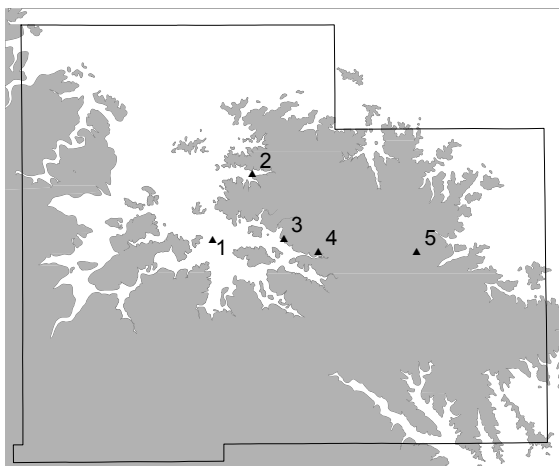
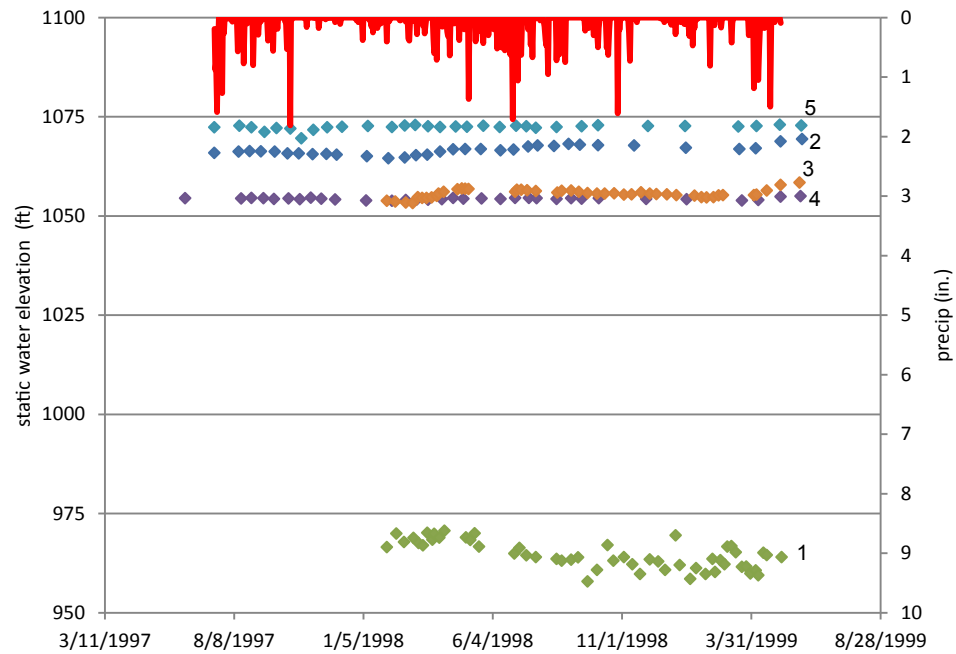


Figure 6

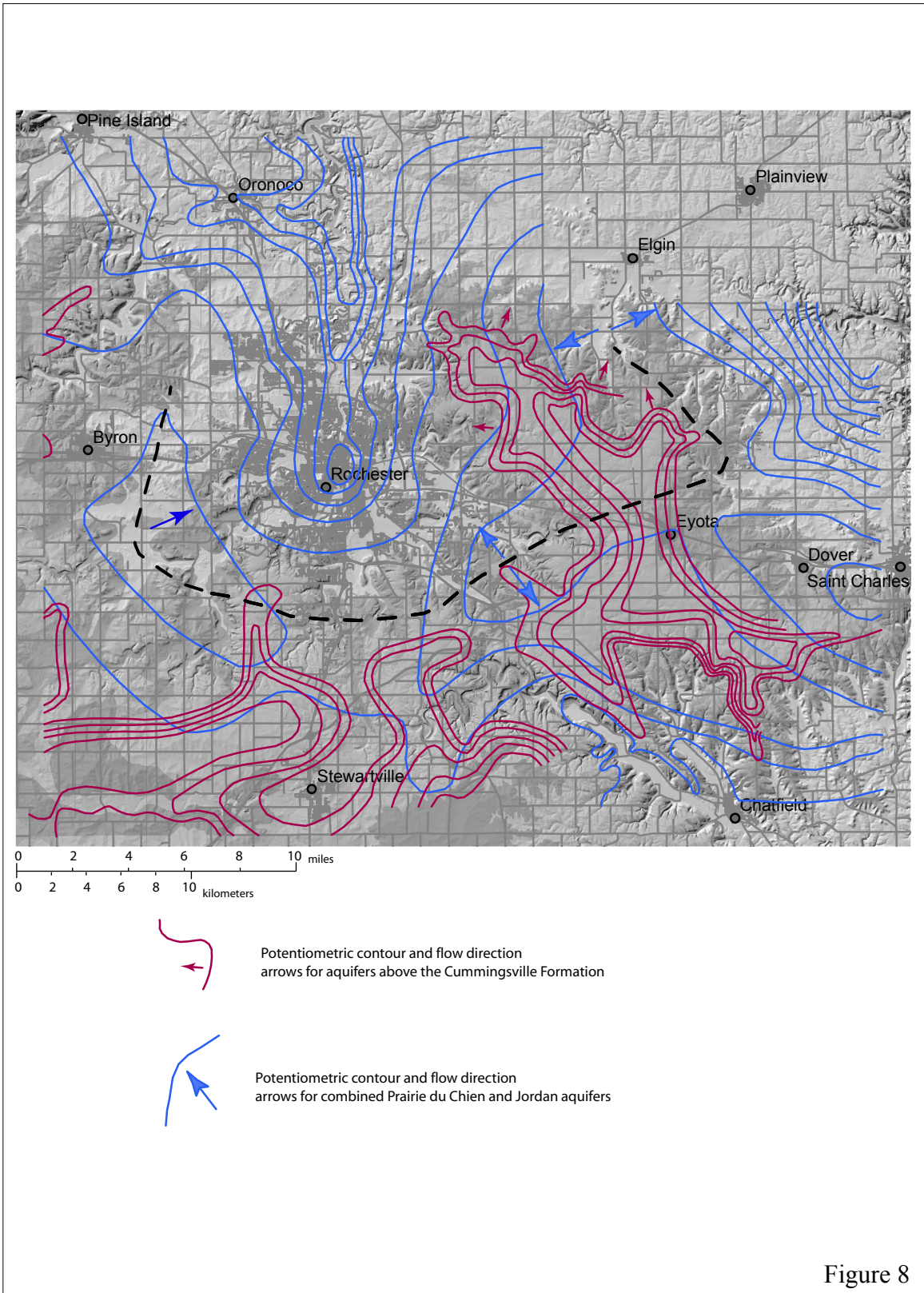
USGS observation well static water elevations and Rochester Airport precipitation data



Decorah Formation extent shown in gray.

	unique no.	aquifer	setting
▲ 1	601283	Prairie du Chein	pumping center
▲ 2	220772	Prairie du Chein	just beyond odcr edge
▲ 3	591905	Prairie du Chein	odcr edge
▲ 4	446667	Jordan	odcr edge
▲ 5	148301	St. Peter	below odcr

Figure 7



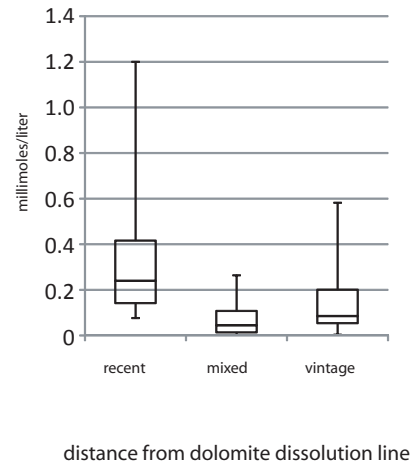
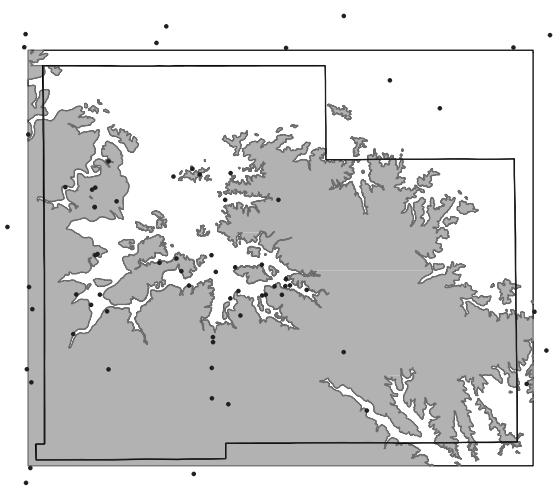
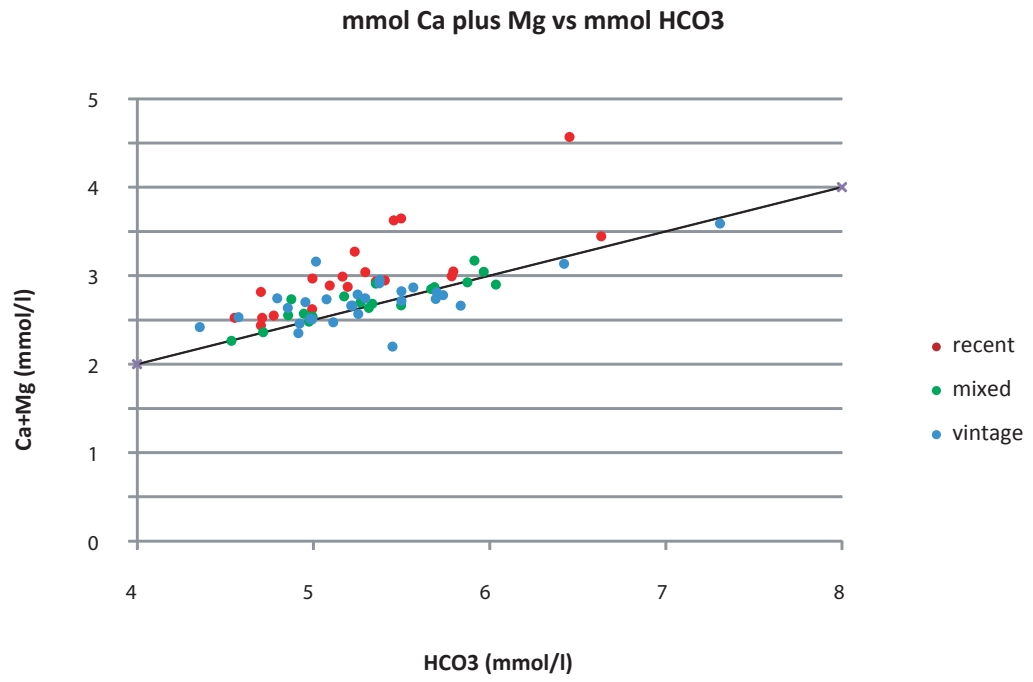


Figure 9

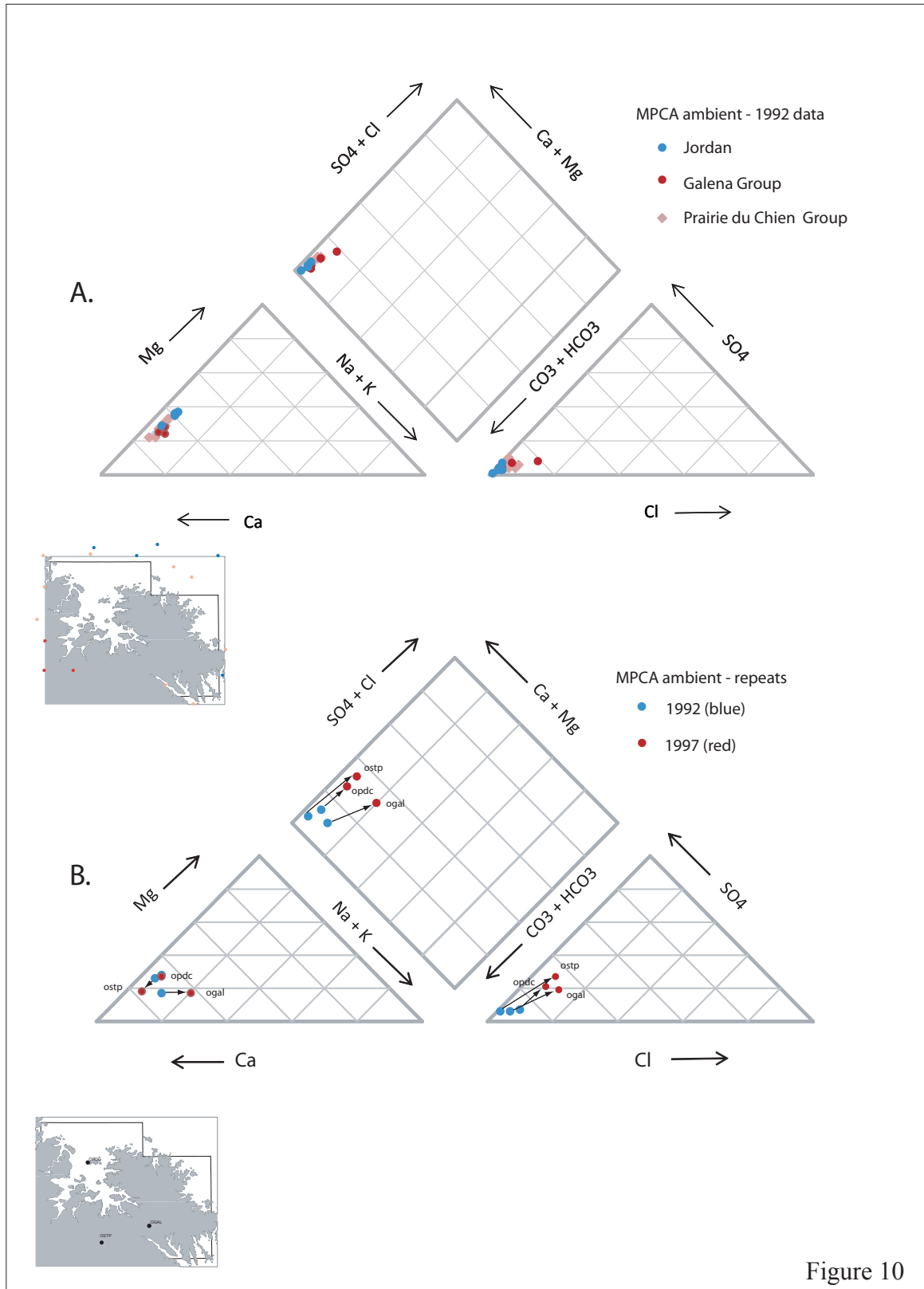
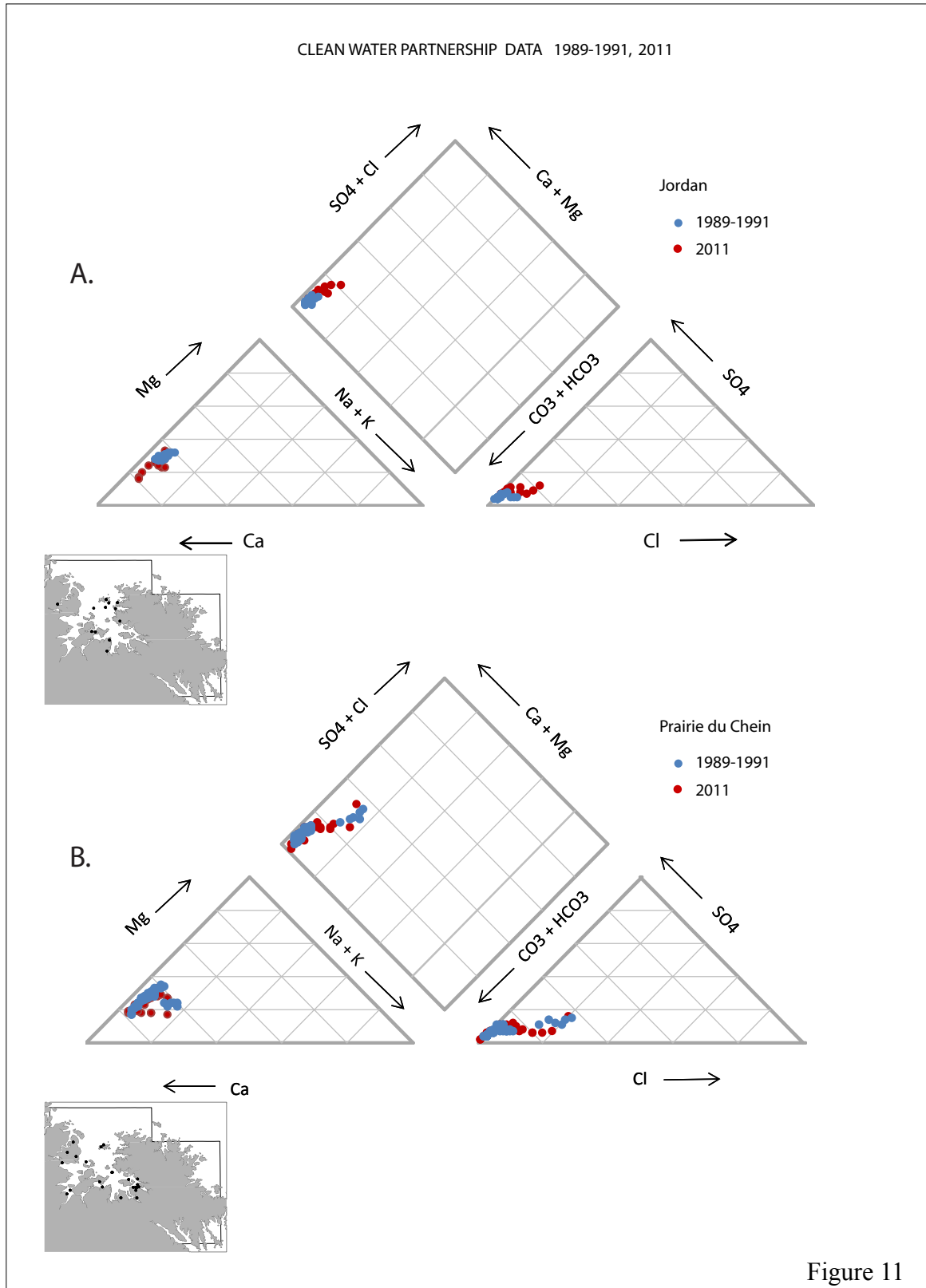


Figure 10



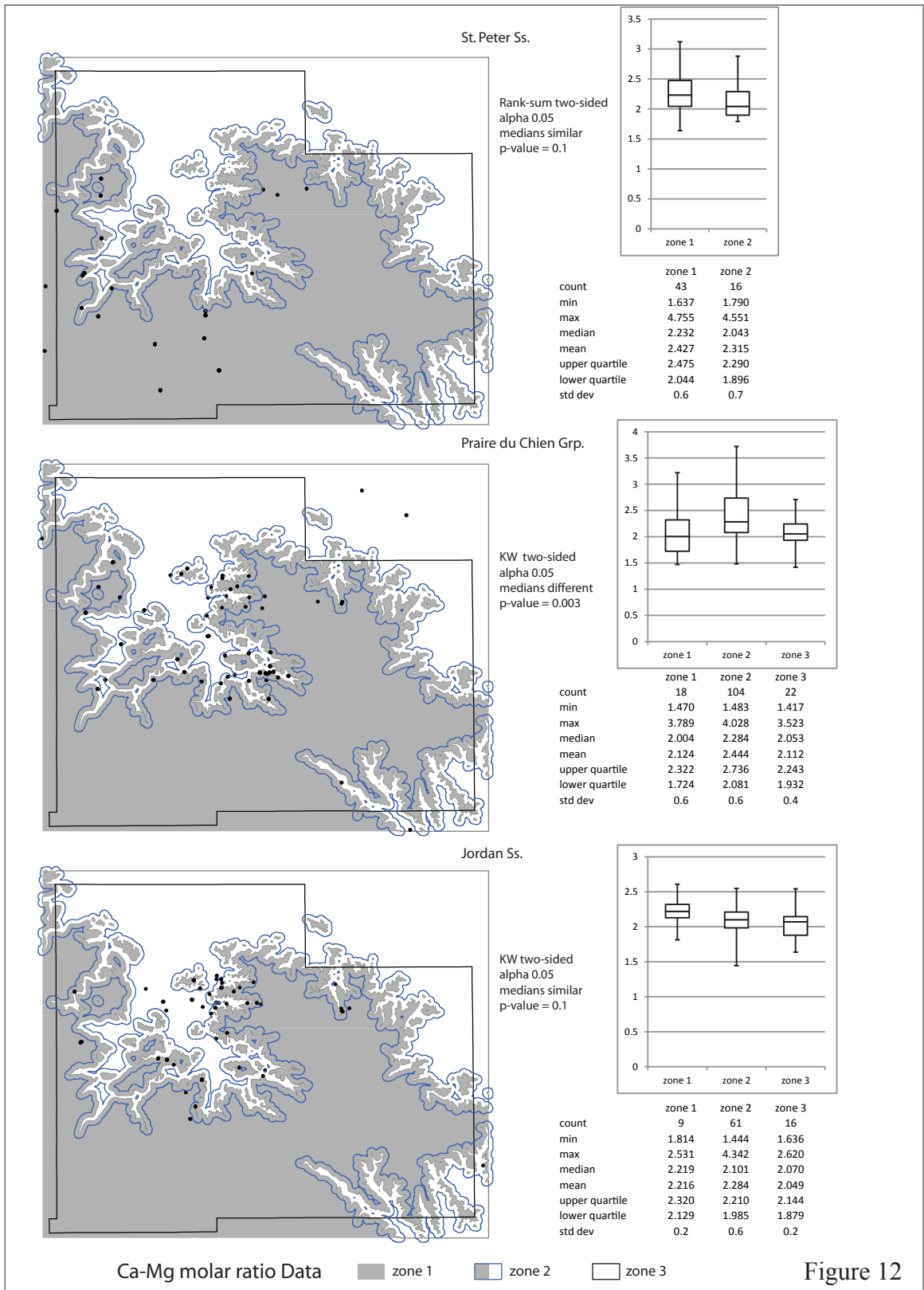


Figure 12

Ca-Mg molar ratios over time - St. Peter Sandstone

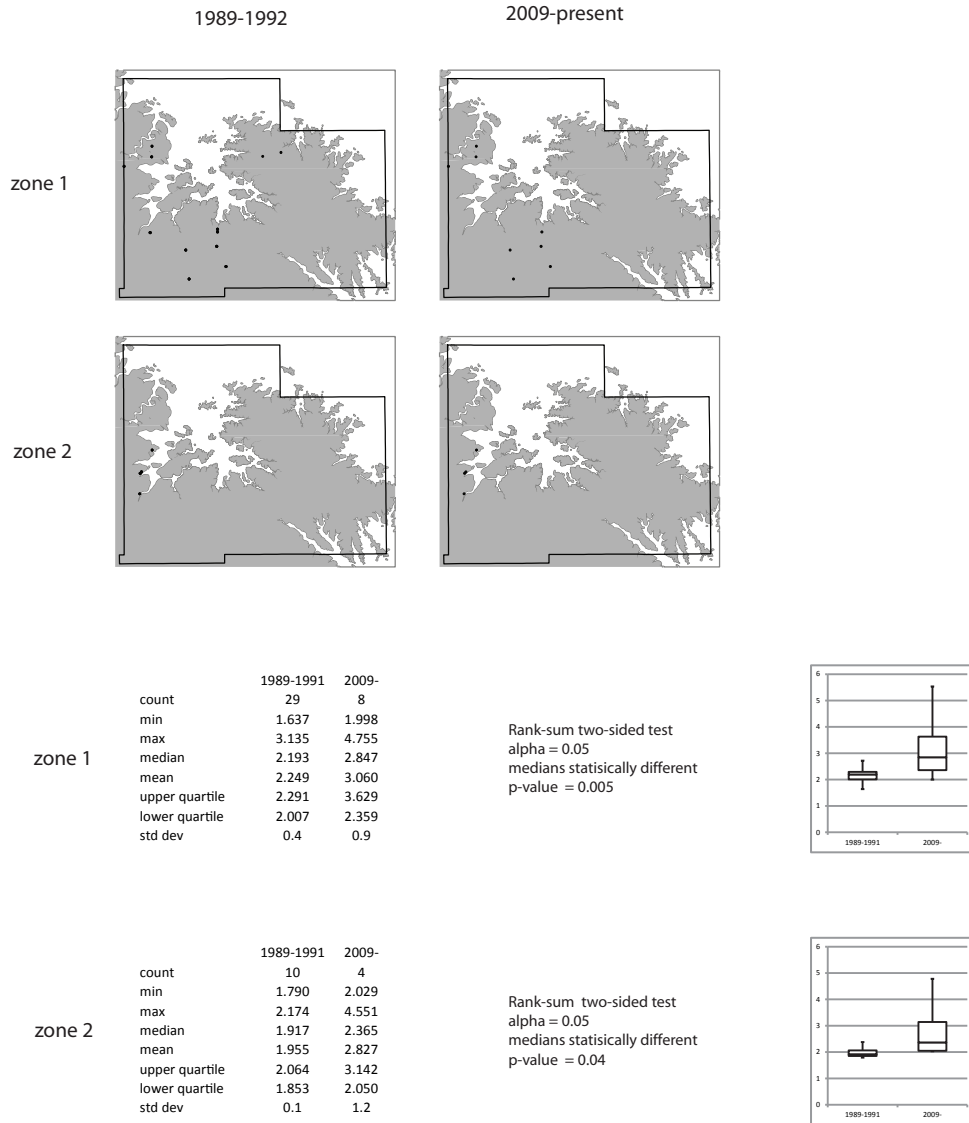
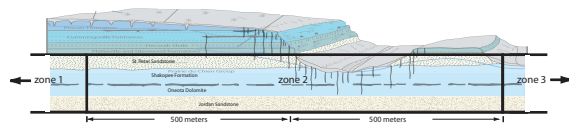


Figure 13

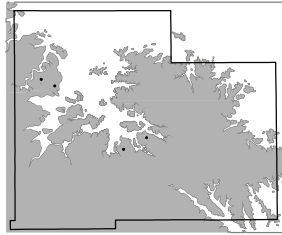
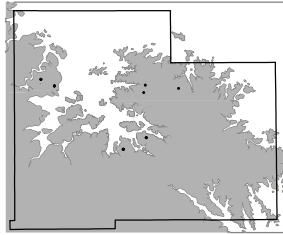


Ca-Mg molar ratios over time - Prairie du Chien Group

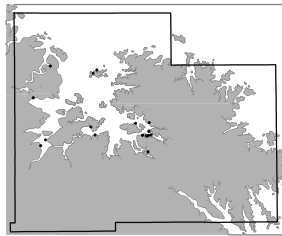
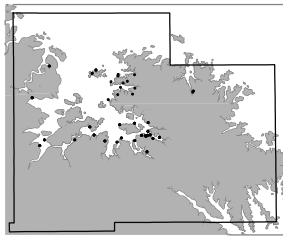
1989-1992

2009-present

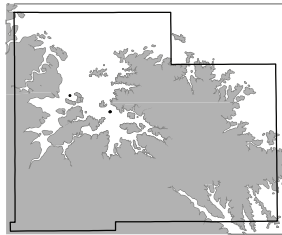
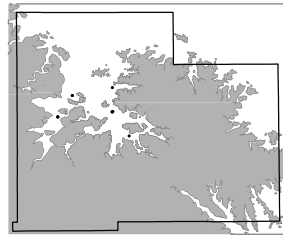
zone 1



zone 2

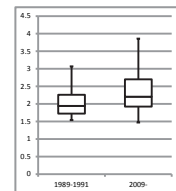


zone 3



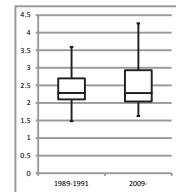
	1989-1991	2009-
count	14	4
min	1.538	1.470
max	2.732	3.789
median	1.943	2.207
mean	2.040	2.418
upper quartile	2.262	2.699
lower quartile	1.724	1.925
std dev	0.4	1.0

Rank-sum two-sided test
alpha = 0.05
medians not statistically different
p-value = 0.49



	1989-1991	2009-
count	83	17
min	1.483	1.625
max	4.028	3.724
median	2.285	2.282
mean	2.415	2.539
upper quartile	2.700	2.934
lower quartile	2.101	2.043
std dev	0.5	0.7

Rank-sum two-sided test
alpha = 0.05
medians not statistically different
p-value = 0.80



	1989-1991	2009-
count	14	3
min	1.716	1.931
max	3.523	2.348
median	2.128	2.027
mean	2.239	2.102
upper quartile	2.369	2.188
lower quartile	1.975	1.979
std dev	0.5	0.2

n/a

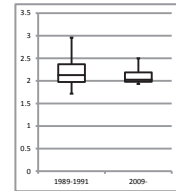
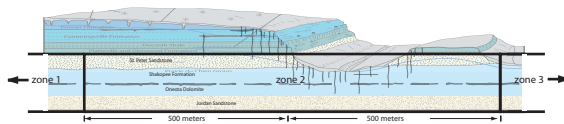


Figure 14

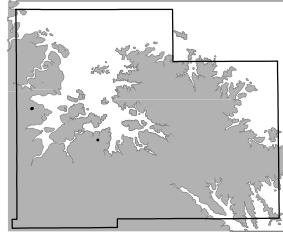
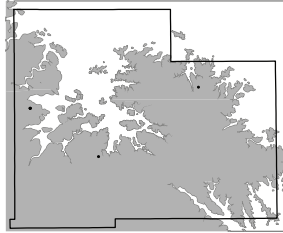


Ca-Mg molar ratios over time - Jordan Sandstone

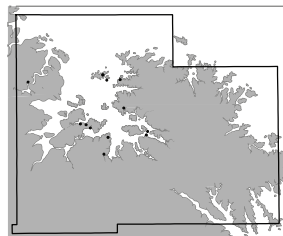
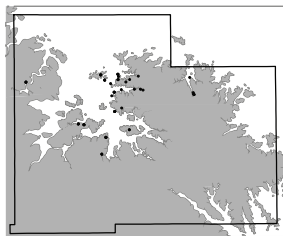
1989-1992

2009-present

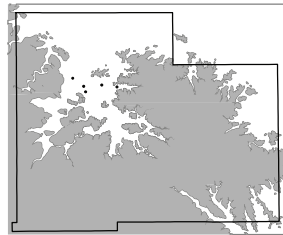
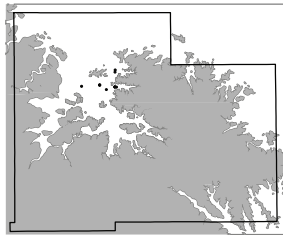
zone 1



zone 2



zone 3



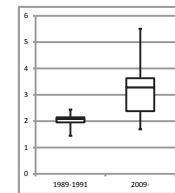
	1989-1991	2009-
count	5	3
min	2.047	1.814
max	2.531	2.423
median	2.195	2.320
mean	2.224	2.186
upper quartile	2.219	2.372
lower quartile	2.129	2.067
std dev	0.2	n/a

n/a

n/a

	1989-1991	2009-
count	46	13
min	1.444	1.688
max	2.898	4.342
median	2.080	3.285
mean	2.073	3.065
upper quartile	2.148	3.631
lower quartile	1.952	2.379
std dev	0.3	0.9

Rank-sum two-sided test
alpha = 0.05
medians statistically different
p-value = 0.0004



	1989-1991	2009-
count	11	5
min	1.787	1.636
max	2.164	2.620
median	2.058	2.082
mean	1.999	2.159
upper quartile	2.130	2.436
lower quartile	1.861	2.021
std dev	0.1	0.4

Rank-sum two-sided test
alpha = 0.05
medians not statistically different
p-value = 0.50

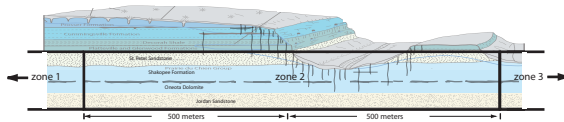
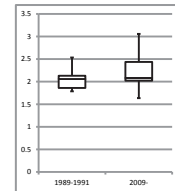
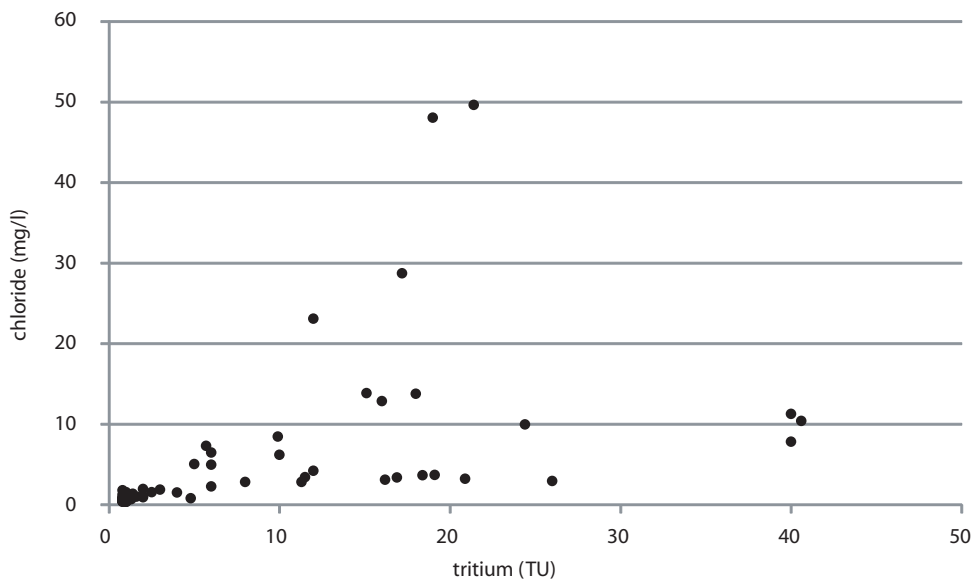
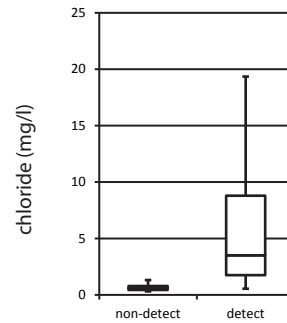


Figure 15



	chloride (ppm)	
	tritium non-detect	tritium detect
min	0.31	0.55
max	1.76	49.59
median	0.58	3.51
mean	0.68	7.90
upper quartile	0.79	8.79
lower quartile	0.44	1.75
std dev	0.37	11.26
	n = 29	n = 40



median values different at 0.05 significance level ($p < 0.00001$ two sided test)

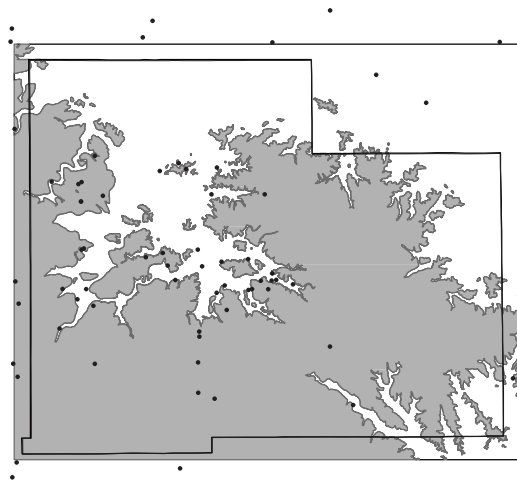
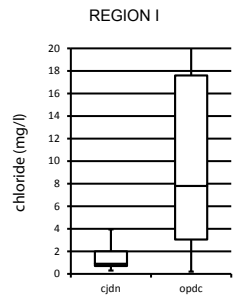
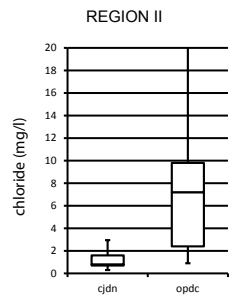


Figure 16



chloride (ppm)

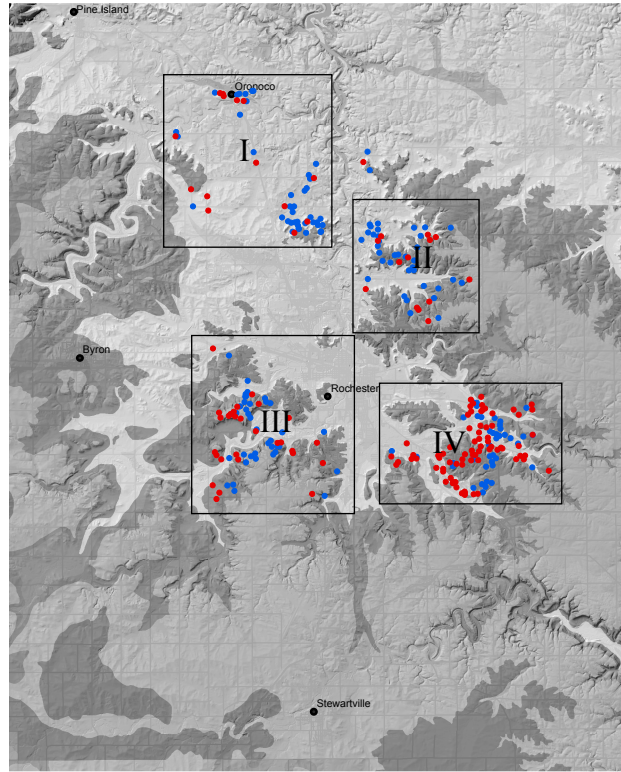
	Jordan	Prairie du Chien
min	0.3	0.2
max	152.25	143
median	0.9	7.8
mean	7.70	22.62
upper quartile	2	17.6
lower quartile	0.7	3.05
std dev	24.5	38.9
n = 41		n = 14



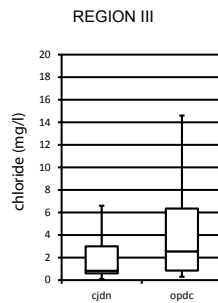
chloride (ppm)

	Jordan	Prairie du Chien
min	0.3	0.9
max	17.7	57.4
median	0.8	7.2
mean	2.14	10.5
upper quartile	1.6	9.8
lower quartile	0.7	2.4
std dev	3.76	14.87
n = 35		n = 13

maximums shown as 1.5 * interquartile range

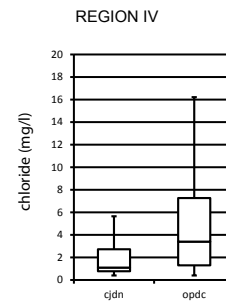


• Jordan well • Prairie du Chien well



chloride (ppm)

	Jordan	Prairie du Chien
min	0.1	0.3
max	42.4	71.2
median	0.83	2.55
mean	4.9	7.5
upper quartile	3	6.3
lower quartile	0.6	0.85
std dev	9.82	14.00
n = 37		n = 28



chloride (ppm)

	Jordan	Prairie du Chien
min	0.4	0.4
max	26.2	30.9
median	1.1	3.4
mean	3.4	5.5
upper quartile	2.7	7.3
lower quartile	0.8	1.3
std dev	5.18	5.90
n = 40		n = 75

Figure 17

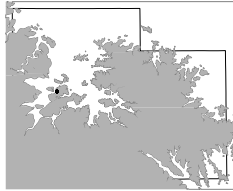
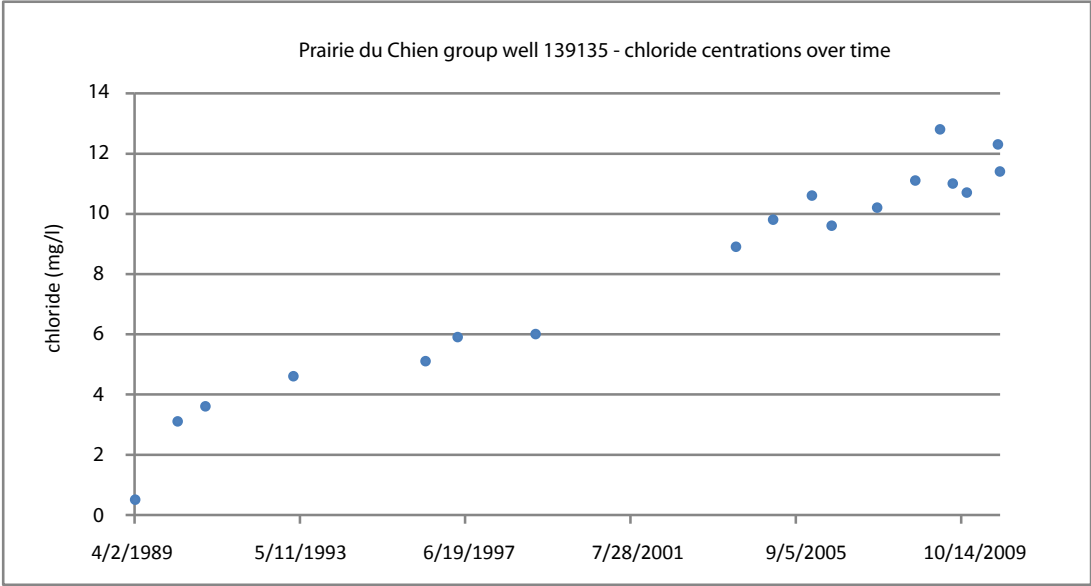


Figure 18

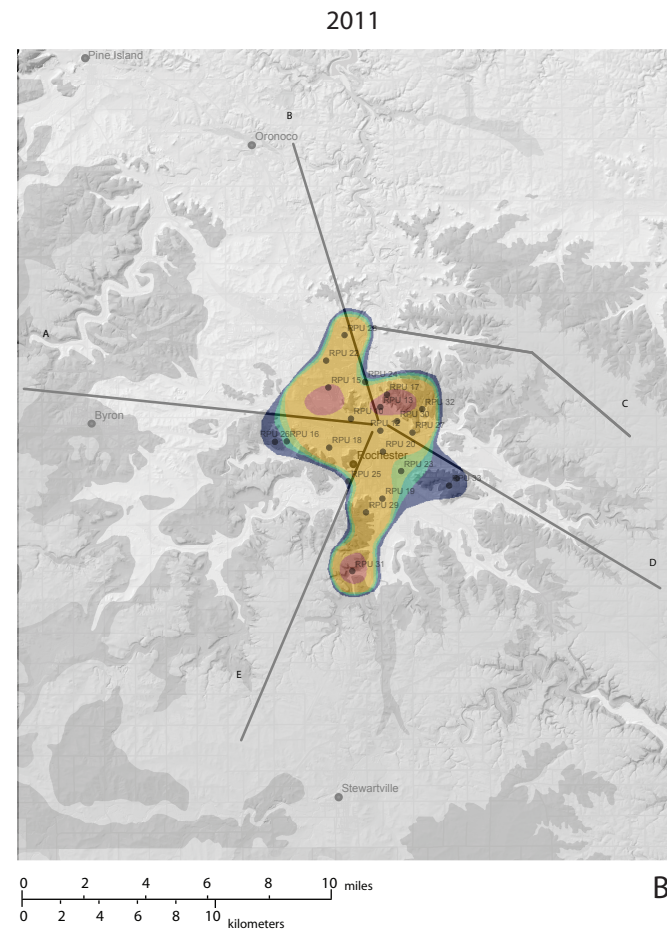
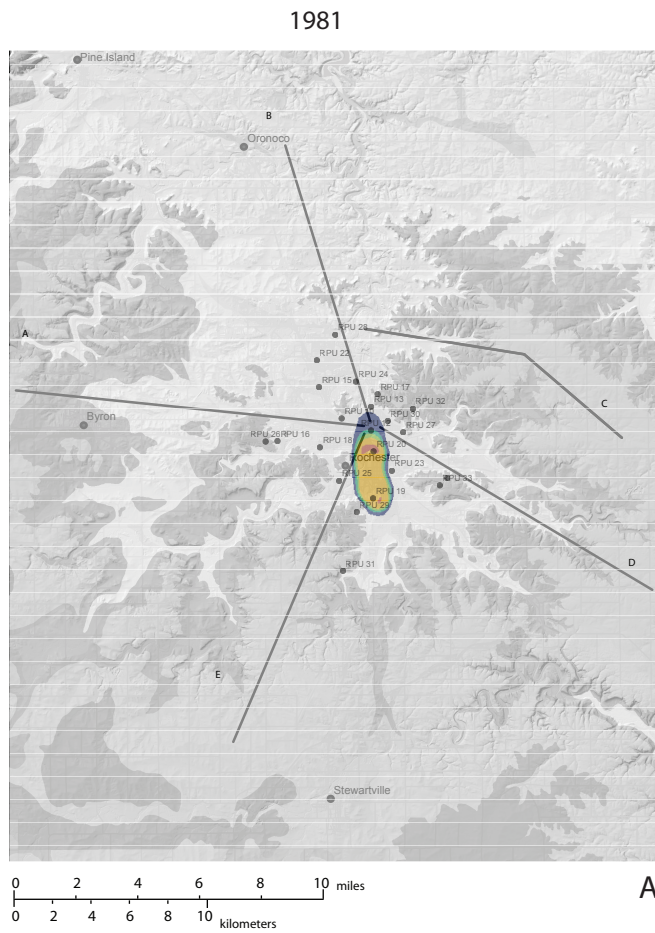


Figure 19

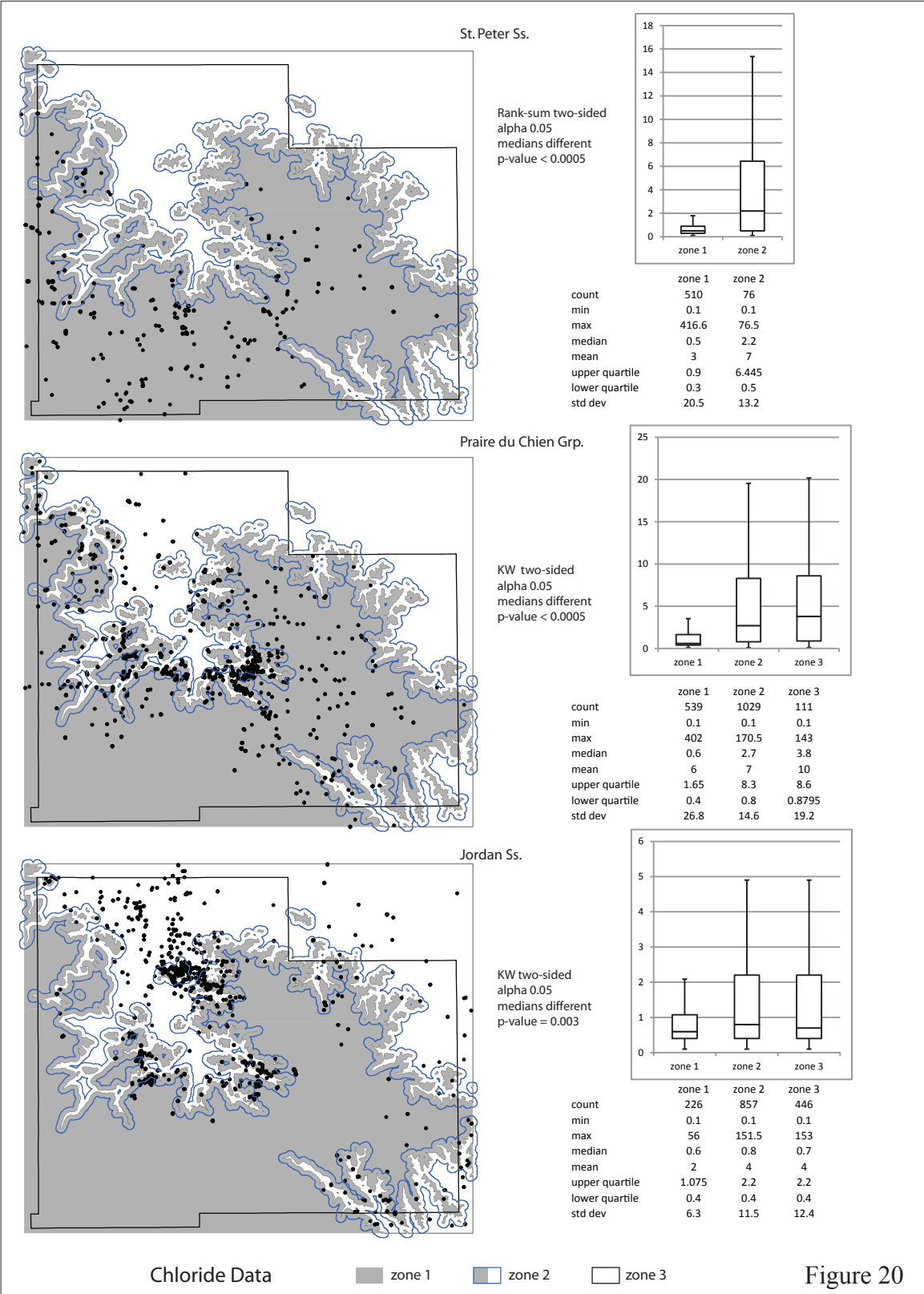
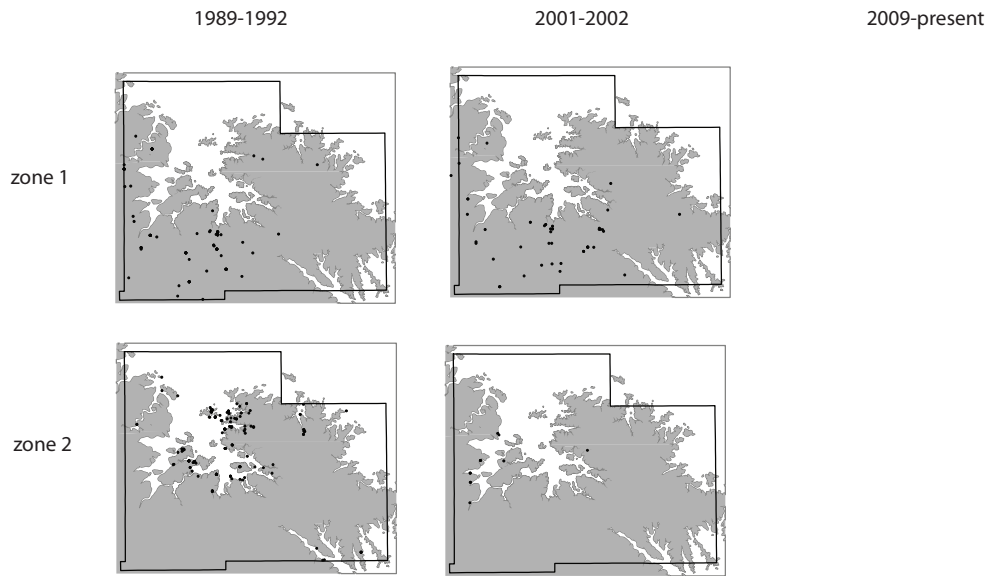


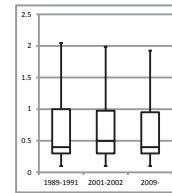
Figure 20

Chloride concentrations over time - St. Peter Sandstone



	1989-1991	2001-2002	2009-
count	101	50	63
min	0.1	0.1	0.1
max	106.3	13.5	24.9
median	0.4	0.5	0.4
mean	1.93	1.42	1.43
upper quartile	0.999	0.975	0.95
lower quartile	0.3	0.3	0.3
std dev	10.7	2.5	3.4

Kruskal-Wallis two-sided test
alpha = 0.05
medians not statistically different
p-value = 0.4



	1989-1991	2001-2002	2009-
count	23	11	6
min	0.1	0.2	0.2
max	48.9	23.6	6
median	1.4	2.3	2.3
mean	5	5	2
upper quartile	3.1825	4.2	2.8
lower quartile	0.45	0.6	0.825
std dev	10.4	6.8	2.1

Kruskal-Wallis two-sided test
alpha = 0.05
medians not statistically different
p-value = 0.8

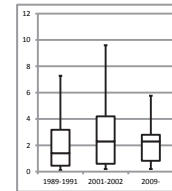
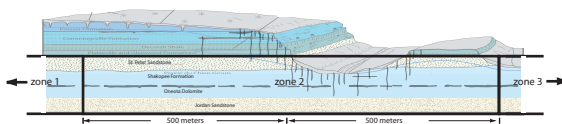


Figure 21



Chloride concentrations over time - Prairie du Chien Group

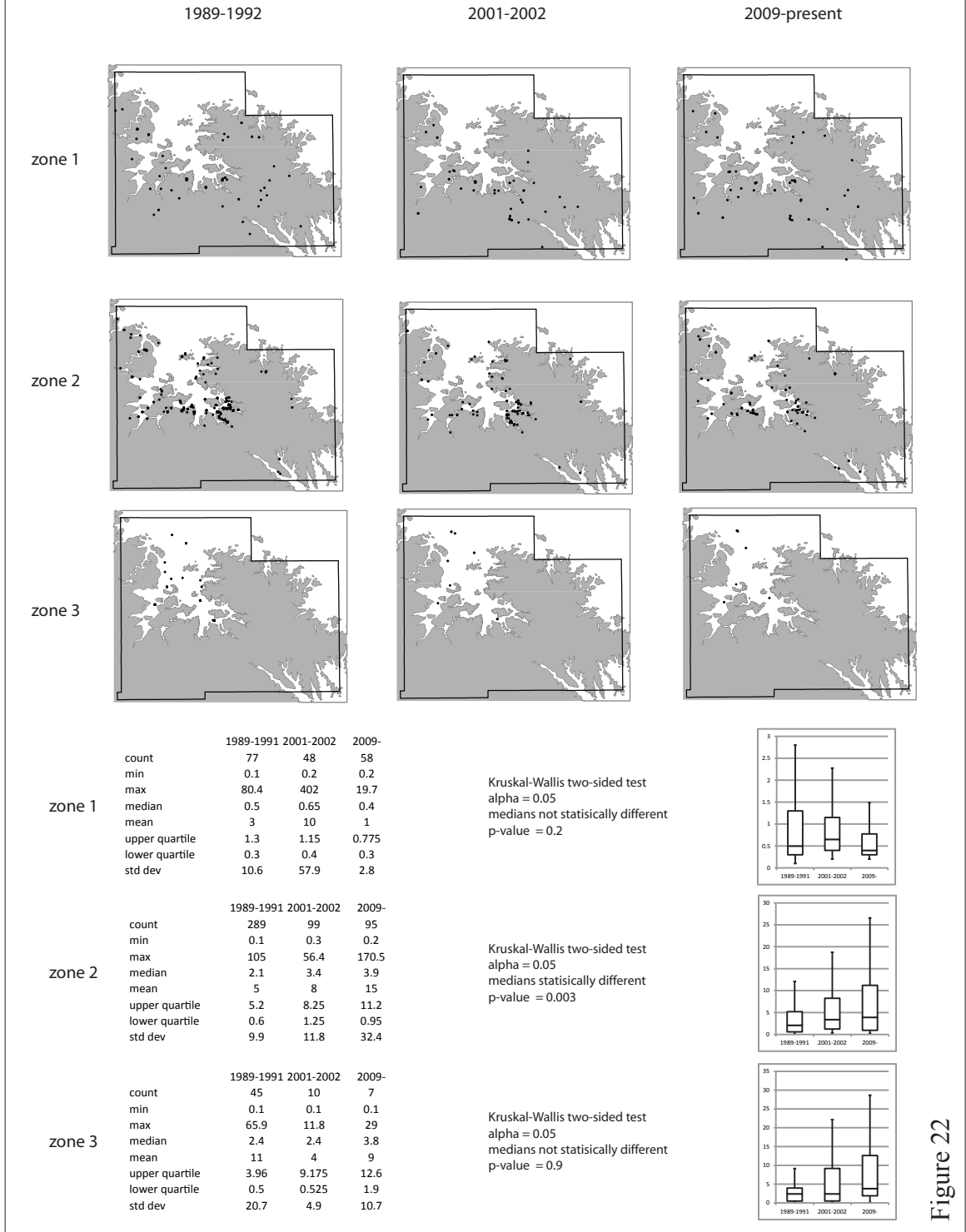
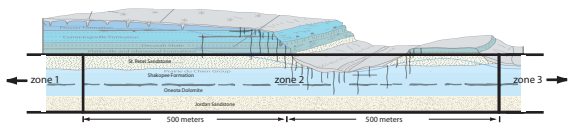
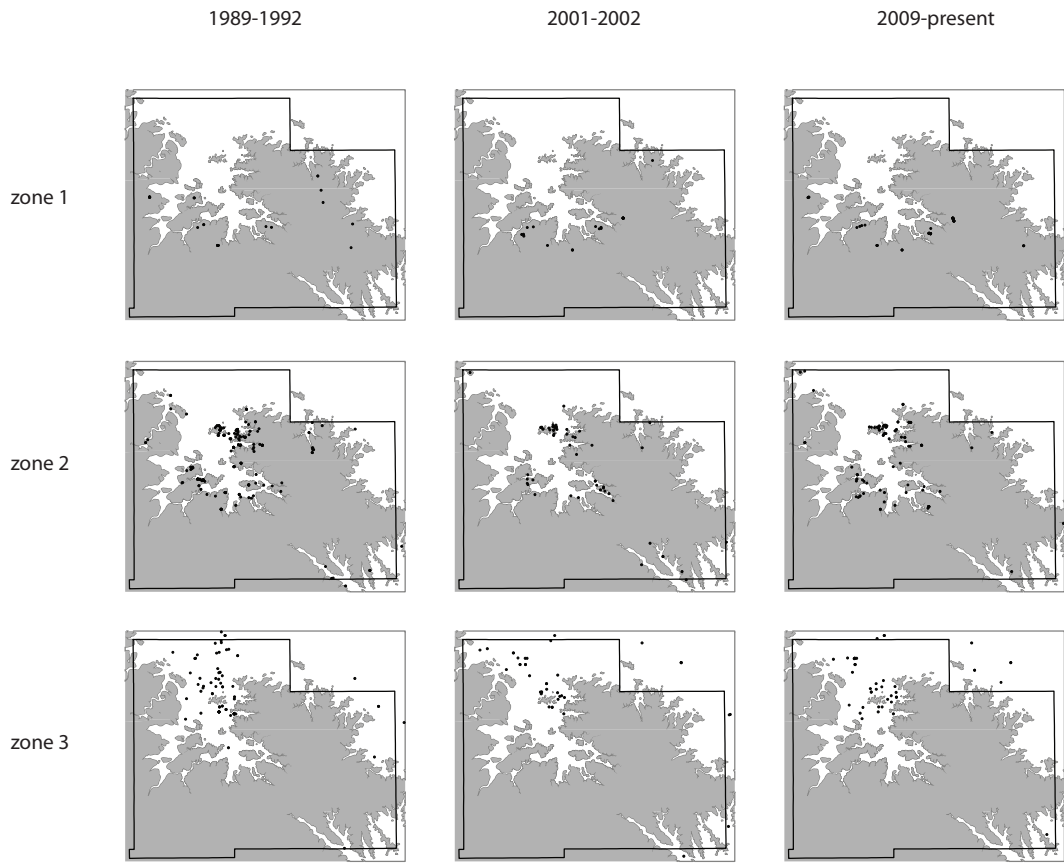


Figure 22

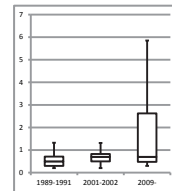


Chloride concentrations over time - Jordan Sandstone



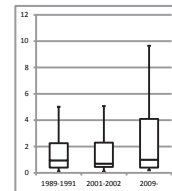
	1989-1991	2001-2002	2009-
count	26	20	40
min	0.2	0.2	0.3
max	4.2	56	5.7
median	0.5	0.7	0.7
mean	1	4	2
upper quartile	0.7095	0.825	2.625
lower quartile	0.3	0.5	0.475
std dev	0.8	12.4	1.6

Kruskal-Wallis two-sided test
alpha = 0.05
medians statistically different
p-value = 0.02



	1989-1991	2001-2002	2009-
count	164	55	88
min	0.1	0.1	0.2
max	62.6	27.7	50.6
median	0.9495	0.7	1
mean	3	3	4
upper quartile	2.25	2.3	4.1
lower quartile	0.4	0.45	0.4
std dev	7.5	6.5	7.3

Kruskal-Wallis two-sided test
alpha = 0.05
medians not statistically different
p-value = 0.55



	1989-1991	2001-2002	2009-
count	49	40	43
min	0.2	0.2	0.3
max	11.3	153	151.5
median	0.6	0.9	2.1
mean	2	10	9
upper quartile	2.4	3.2	5.25
lower quartile	0.4	0.575	0.45
std dev	2.5	26.2	25.1

Kruskal-Wallis two-sided test
alpha = 0.05
medians not statistically different
p-value = 0.08

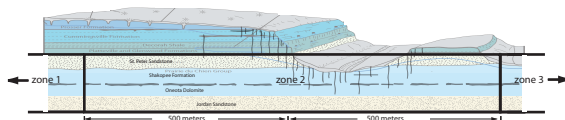
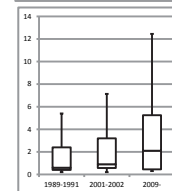


Figure 23

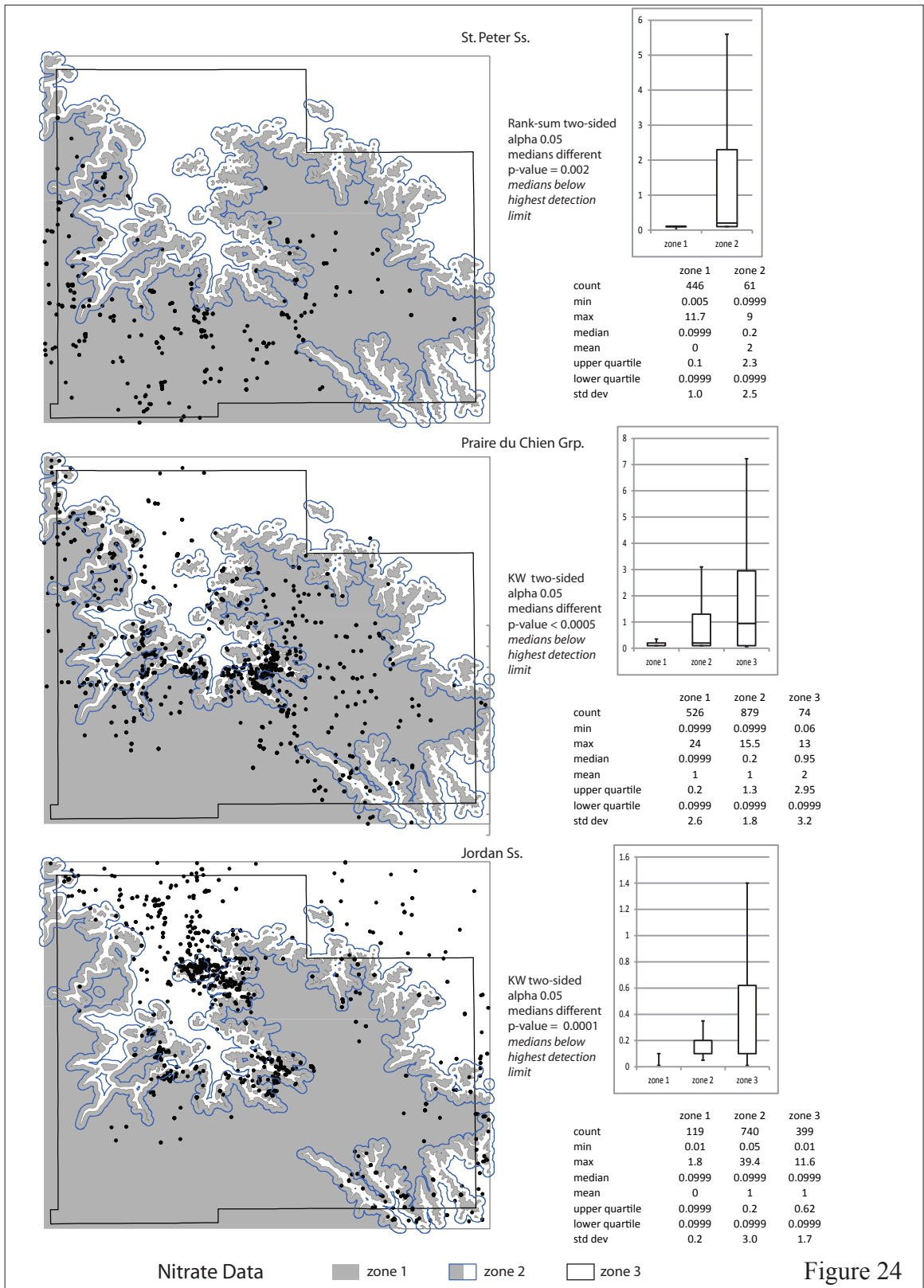
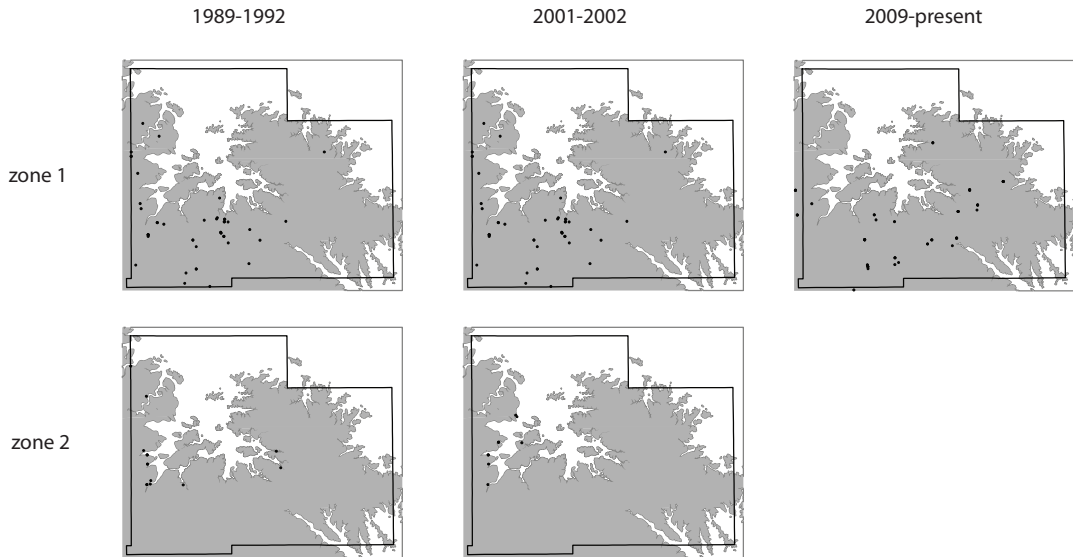


Figure 24

Nitrate concentrations over time - St. Peter Sandstone



	1989-1991	2001-2002	2009-
count	45	39	56
min	0.0999	0.0999	0.0999
max	6.7	5.9	0.9
median	0.2	0.0999	0.0999
mean	0.34	0.54	0.16
upper quartile	0.2	0.0999	0.0999
lower quartile	0.2	0.0999	0.0999
std dev	1.0	1.3	0.2

Kruskal-Wallis two-sided test
 alpha = 0.05
 medians statistically different
 p-value < 0.005
all median values below highest detection limit

n/a

	1989-1991	2001-2002
count	14	9
min	0.0999	0.0999
max	7	2.3
median	0.2	0.3
mean	0.8	0.7
upper quartile	0.2	0.6
lower quartile	0.2	0.0999
std dev	1.8	0.9

Rank-sum two-sided test
 alpha = 0.05
 medians not statistically different
 p-value = 0.75

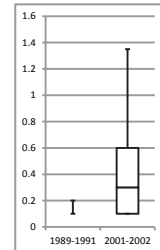
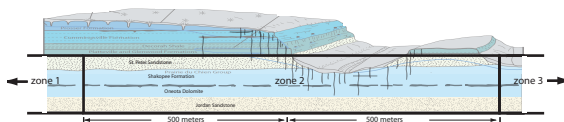
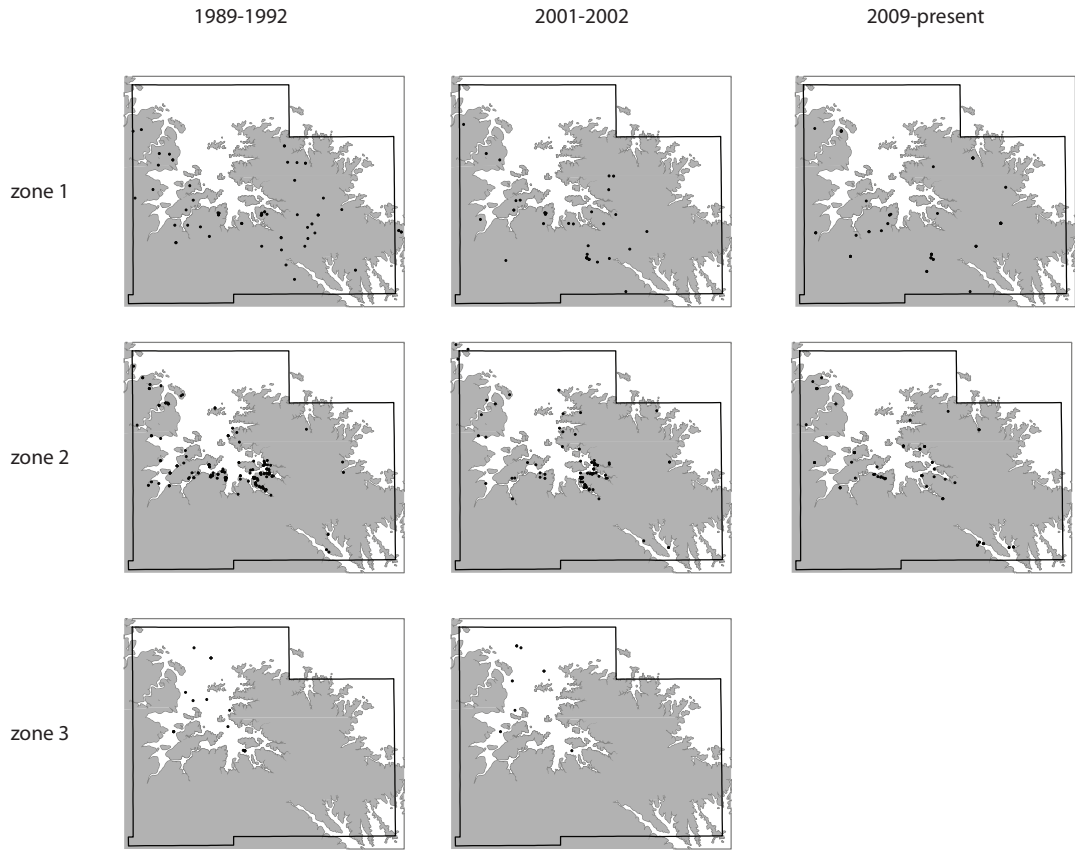


Figure 25



Nitrate concentrations over time - Prairie du Chien Group



	1989-1991	2001-2002	2009-	
count	60	37	47	
min	0.0999	0.0999	0.0999	Kruskal-Wallis two-sided test alpha = 0.05 medians statistically different p-value < 0.005 <i>all median values below highest detection limit</i>
max	24	2.3	0.1	
median	0.2	0.0999	0.0999	
mean	2	0	0	
upper quartile	0.375	0.0999	0.0999	
lower quartile	0.2	0.0999	0.0999	
std dev	5.1	0.4	0.0	

n/a

	1989-1991	2001-2002	2009-	
count	149	81	78	
min	0.0999	0.0999	0.0999	Kruskal-Wallis two-sided test alpha = 0.05 medians statistically different p-value = 0.001 <i>all median values below highest detection limit</i>
max	14.1	12.5	7.9	
median	0.2	0.0999	0.0999	
mean	1	1	1	
upper quartile	1.4	1	1.475	
lower quartile	0.2	0.0999	0.0999	
std dev	1.9	2.2	1.5	

n/a

	1989-1991	2001-2002	2009-	
count	17	9	3	
min	0.0999	0.0999	2.5	Rank-sum two-sided test alpha = 0.05 medians not statistically different p-value = 0.31
max	11.1	6.4	5	
median	0.2	1.9	3	
mean	1	2	4	
upper quartile	0.9	2.5	4	
lower quartile	0.2	0.0999	2.75	
std dev	2.6	2.5	1.3	

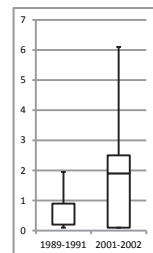
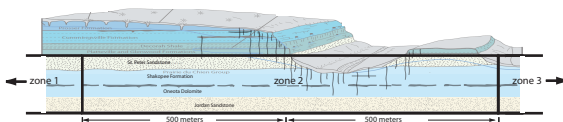


Figure 26



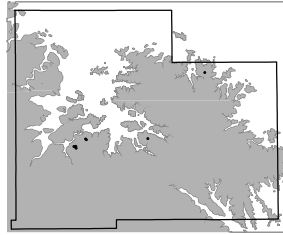
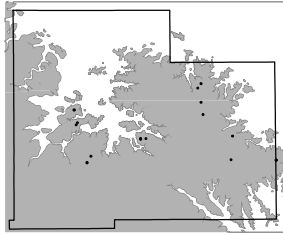
Nitrate concentrations over time - Jordan Sandstone

1989-1992

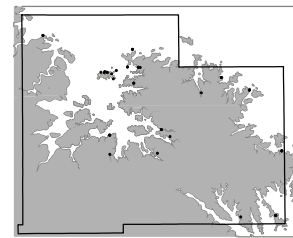
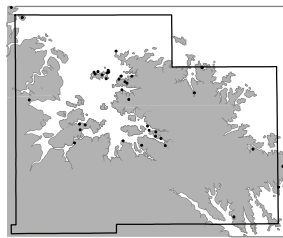
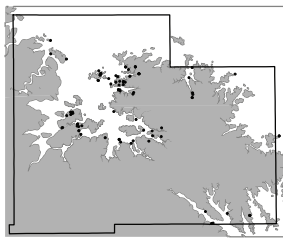
2001-2002

2009-present

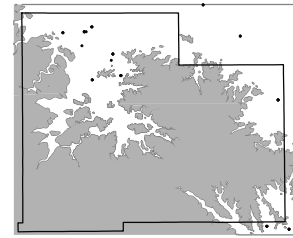
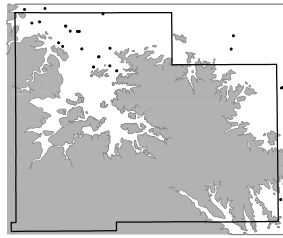
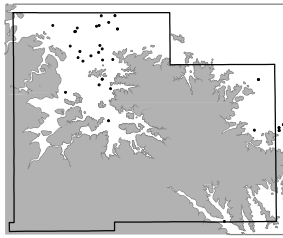
zone 1



zone 2



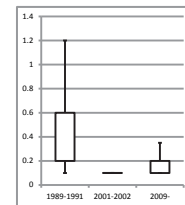
zone 3



	1989-1991	2001-2002	2009-	
count	18	7	7	
min	0.01	0.0999	0.0999	Kruskal-Wallis two-sided test alpha = 0.05 medians statistically different p-value = 0.14 all median values below highest detection limit
max	1	0.0999	0.0999	
median	0.2	0.0999	0.0999	
mean	0	0	0	
upper quartile	0.2	0.0999	0.0999	
lower quartile	0.099925	0.0999	0.0999	
std dev	0.3	0.0	0.0	

n/a

	1989-1991	2001-2002	2009-	
count	89	38	43	
min	0.0999	0.0999	0.0999	Kruskal-Wallis two-sided test alpha = 0.05 medians statistically different p-value < 0.005 all median values below highest detection limit
max	32.8	13.3	16.8	
median	0.2	0.0999	0.0999	
mean	2	1	1	
upper quartile	0.6	0.1	0.2	
lower quartile	0.2	0.0999	0.0999	
std dev	4.6	2.9	2.7	



	1989-1991	2001-2002	2009-	
count	37	24	35	
min	0.0999	0.0999	0.0999	Kruskal-Wallis two-sided test alpha = 0.05 medians statistically different p-value < 0.005 all median values below highest detection limit
max	9.2	10.9	6	
median	0.2	0.0999	0.0999	
mean	2	2	1	
upper quartile	2.8	1.135	0.0999	
lower quartile	0.2	0.0999	0.0999	
std dev	2.6	2.9	1.4	

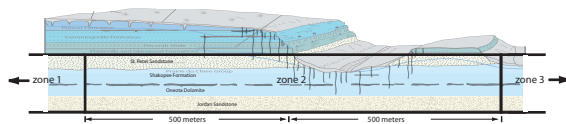
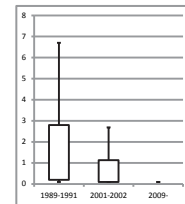


Figure 27

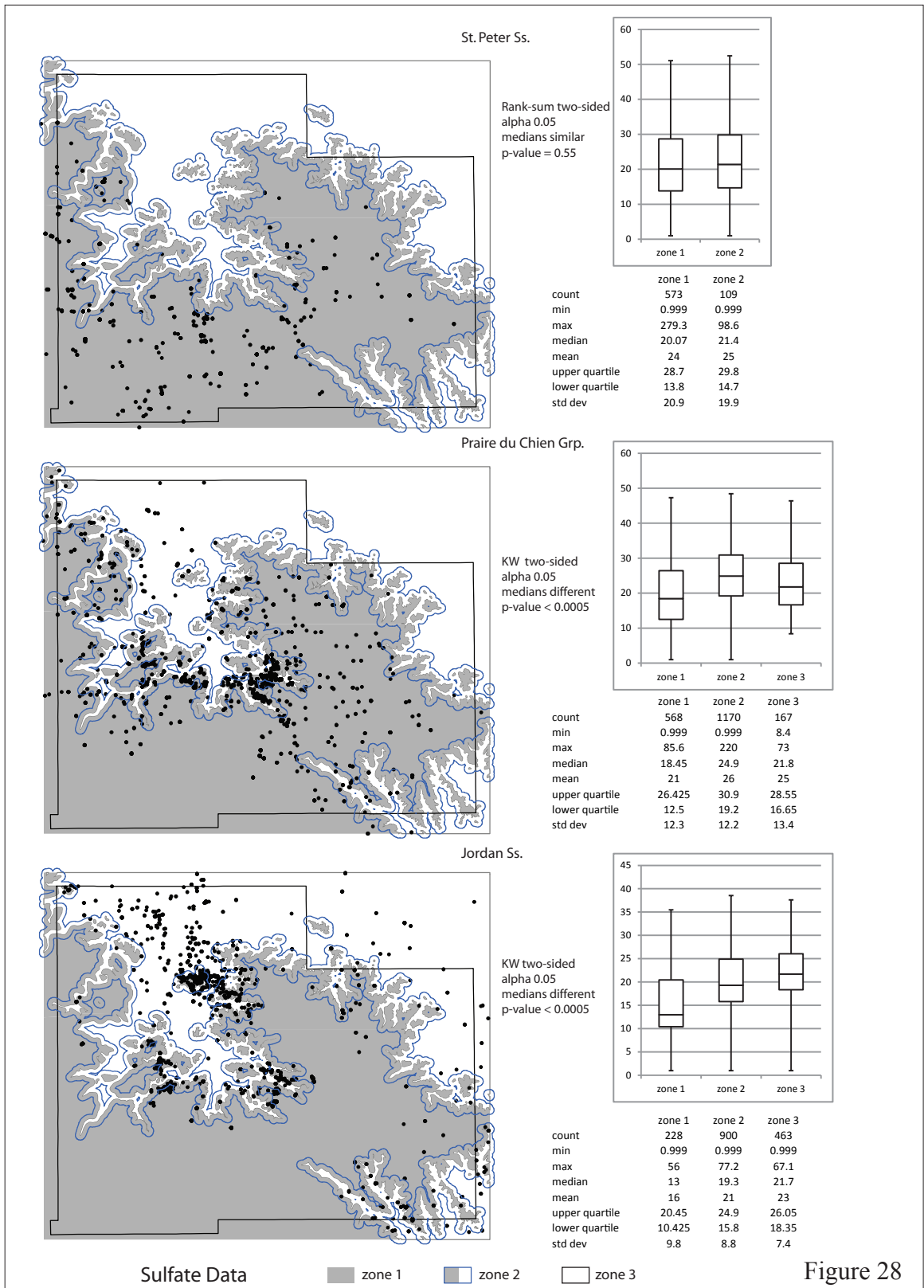
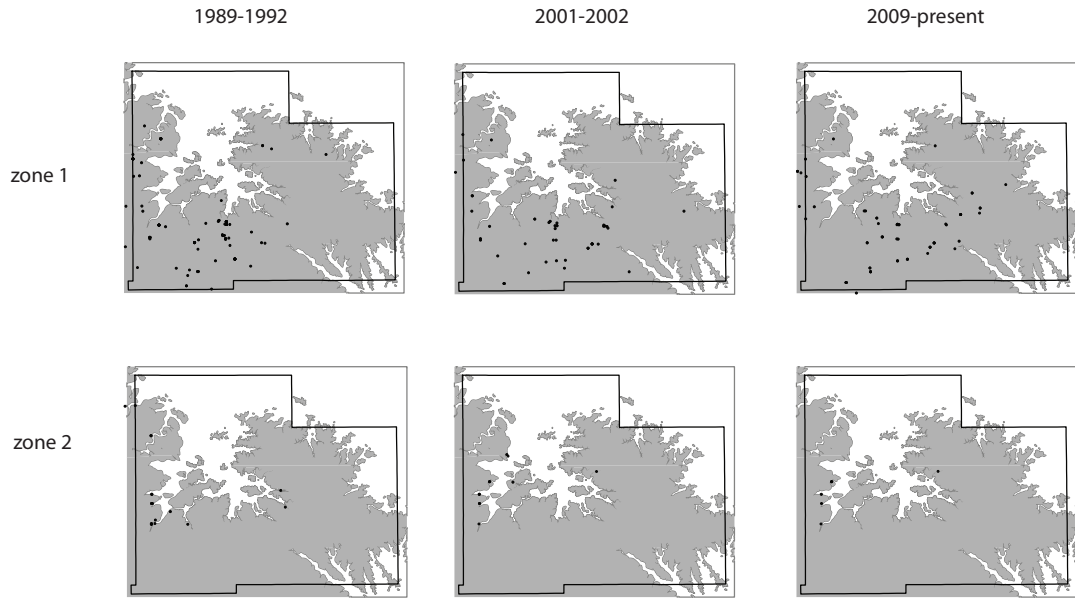


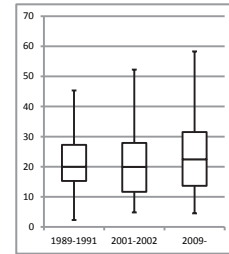
Figure 28

Sulfate concentrations over time - St. Peter Sandstone



	1989-1991	2001-2002	2009-
count	130	54	70
min	2.3	4.8	4.5
max	279.3	52	180
median	19.9967	19.95	22.45
mean	24.56	20.51	30.41
upper quartile	27.275	27.9	31.5
lower quartile	15.25	11.675	13.65
std dev	25.8	11.3	28.8

Kruskal-Wallis two-sided test
alpha = 0.05
medians not statistically different
p-value = 0.2



	1989-1991	2001-2002	2009-
count	44	16	9
min	1	0.999	5.1
max	72.3	35.6	49.9
median	20.2	19.3	21.6
mean	21	21	24
upper quartile	29.075	29.6	29.8
lower quartile	12.75	17.25	20.3
std dev	14.7	10.2	13.1

Kruskal-Wallis two-sided test
alpha = 0.05
medians not statistically different
p-value = 0.7

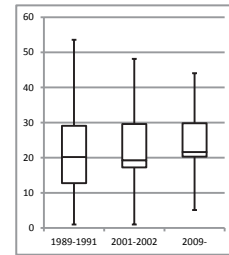
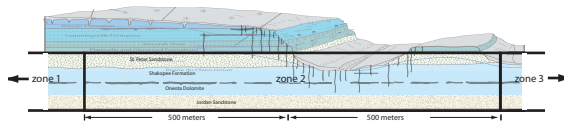


Figure 29



Sulfate concentrations over time - Prairie du Chien Group

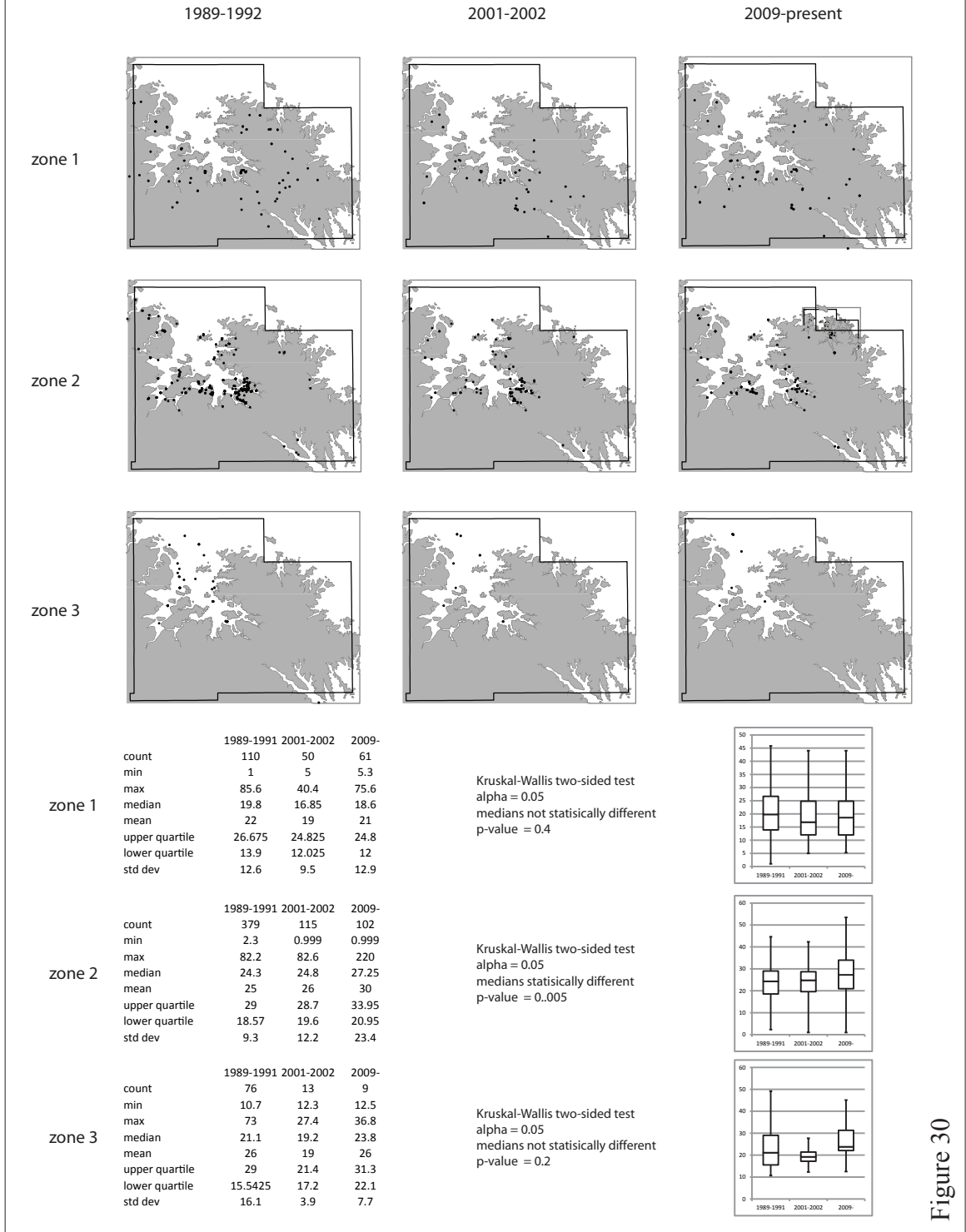
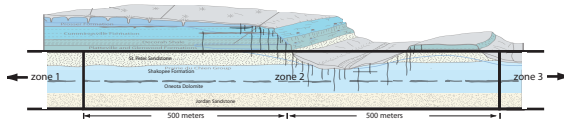


Figure 30



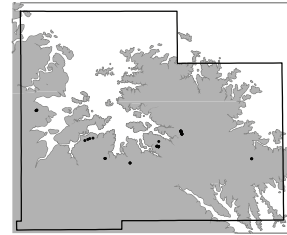
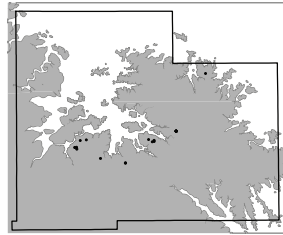
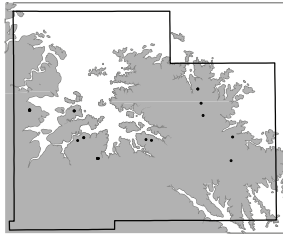
Sulfate concentrations over time - Jordan Sandstone

1989-1992

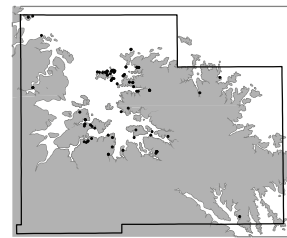
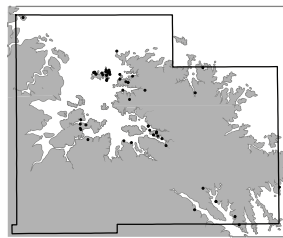
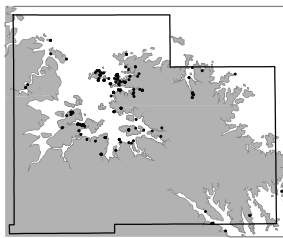
2001-2002

2009-present

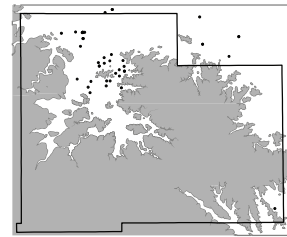
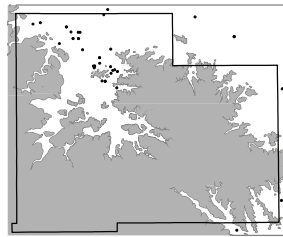
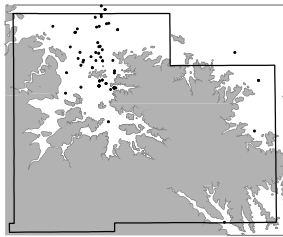
zone 1



zone 2

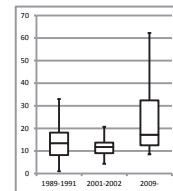


zone 3



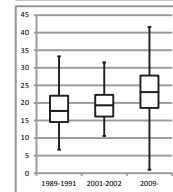
	1989-1991	2001-2002	2009-
count	28	20	41
min	1	4.3	8.5
max	24.1	23.9	48.6
median	13.45	11.75	17.2
mean	14	12	22
upper quartile	18.1	13.7	32.4
lower quartile	8.175	9.025	12.5
std dev	6.4	4.7	11.8

Kruskal-Wallis two-sided test
alpha = 0.05
medians statistically different
p-value = 0.001



	1989-1991	2001-2002	2009-
count	212	58	95
min	6.7	10.6	0.999
max	66.5	42.6	53.1
median	17.75	19.35	23.1
mean	20	20	24
upper quartile	22.05	22.3	27.8
lower quartile	14.575	16.125	18.6
std dev	9.0	6.2	9.7

Kruskal-Wallis two-sided test
alpha = 0.05
medians statistically different
p-value < 0.0005



	1989-1991	2001-2002	2009-
count	72	42	45
min	11.4	11.9	11.1
max	57	44.5	49.9
median	21.735	21.1	22.9
mean	22	23	25
upper quartile	24.025	26.1	29.2
lower quartile	18.175	17.95	20
std dev	6.4	7.1	7.6

Kruskal-Wallis two-sided test
alpha = 0.05
medians not statistically different
p-value = 0.06

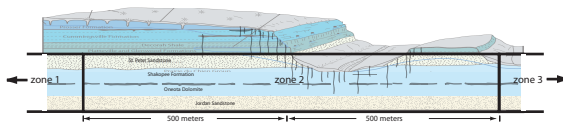
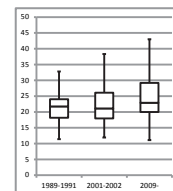


Figure 31

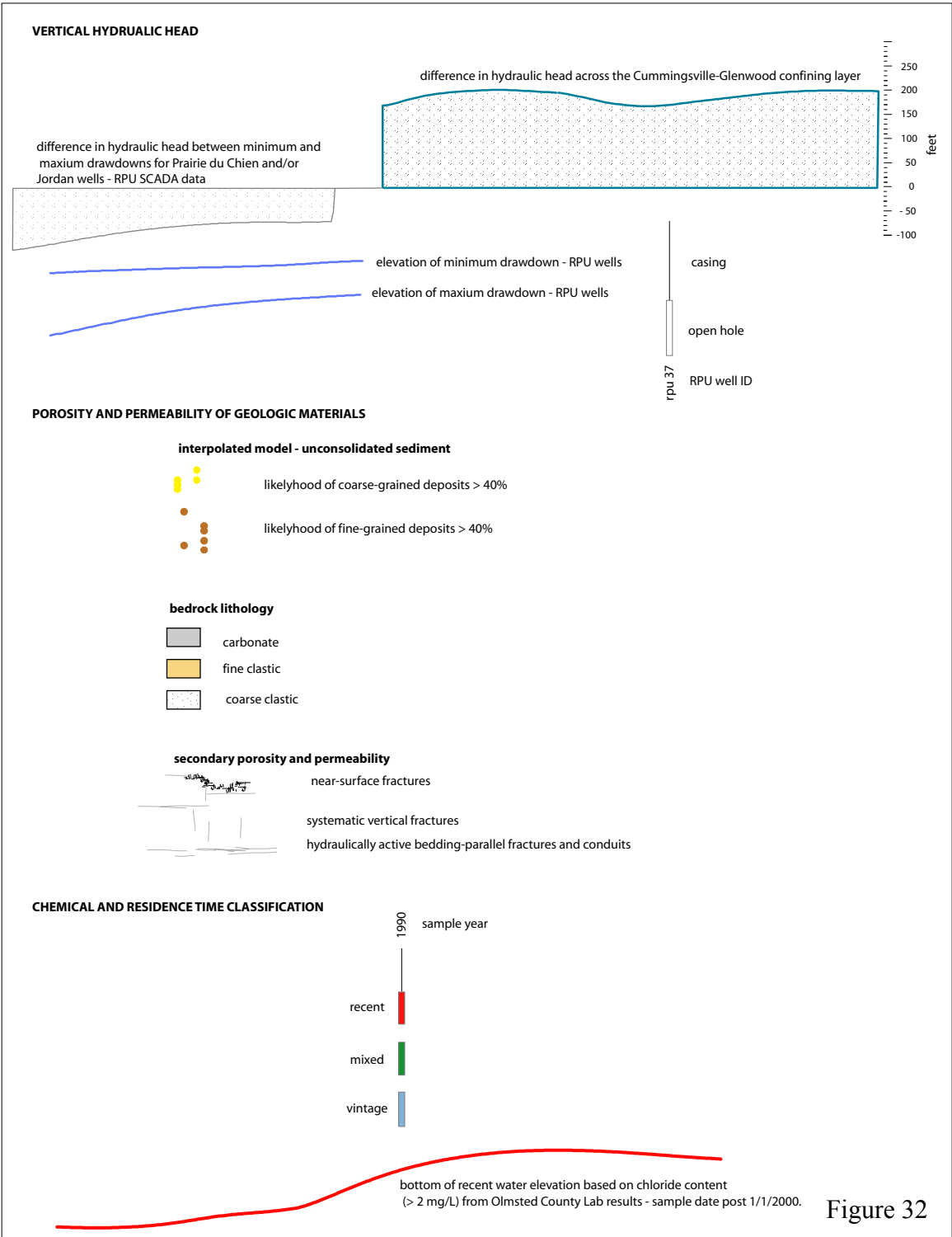


Figure 32

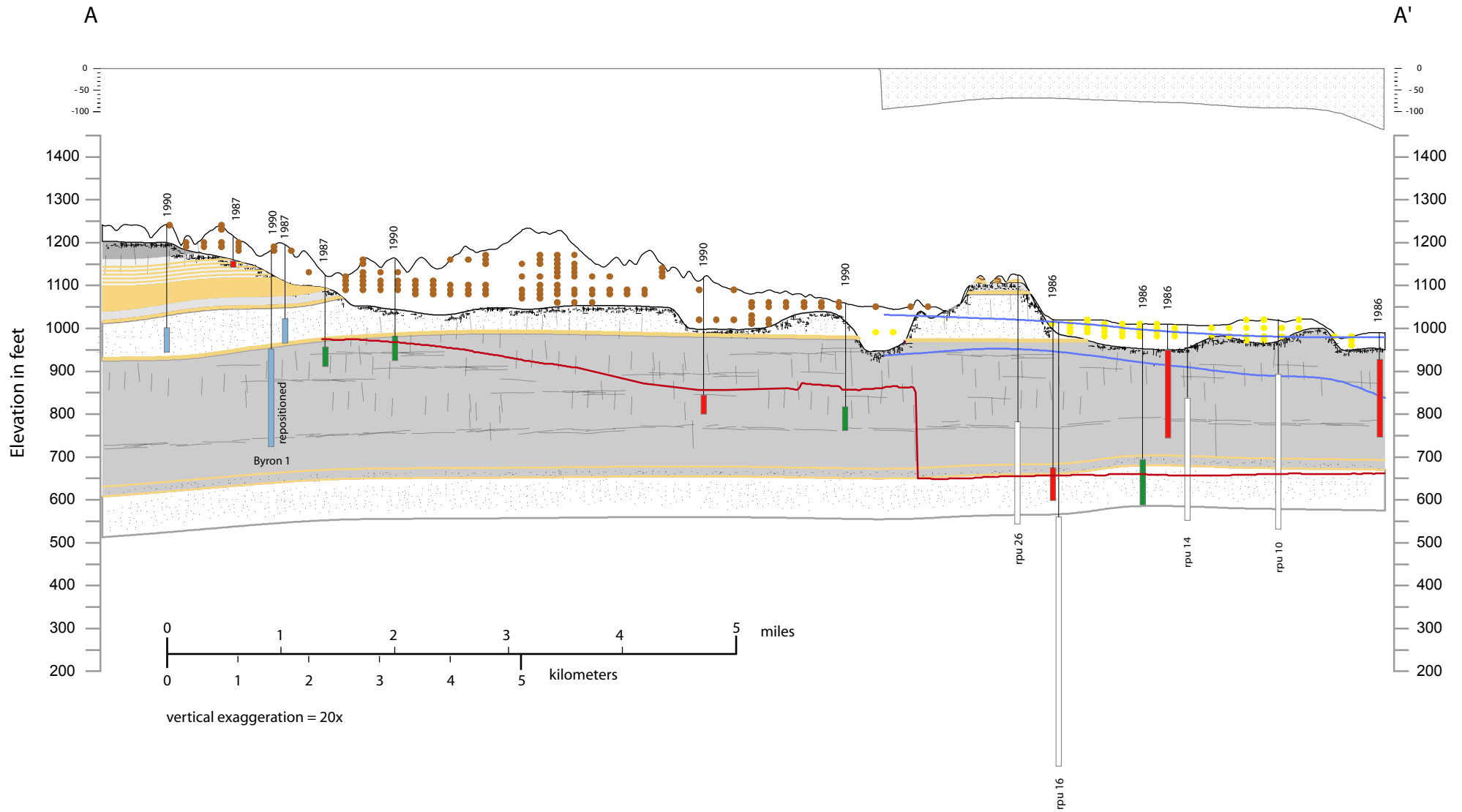


Figure 33

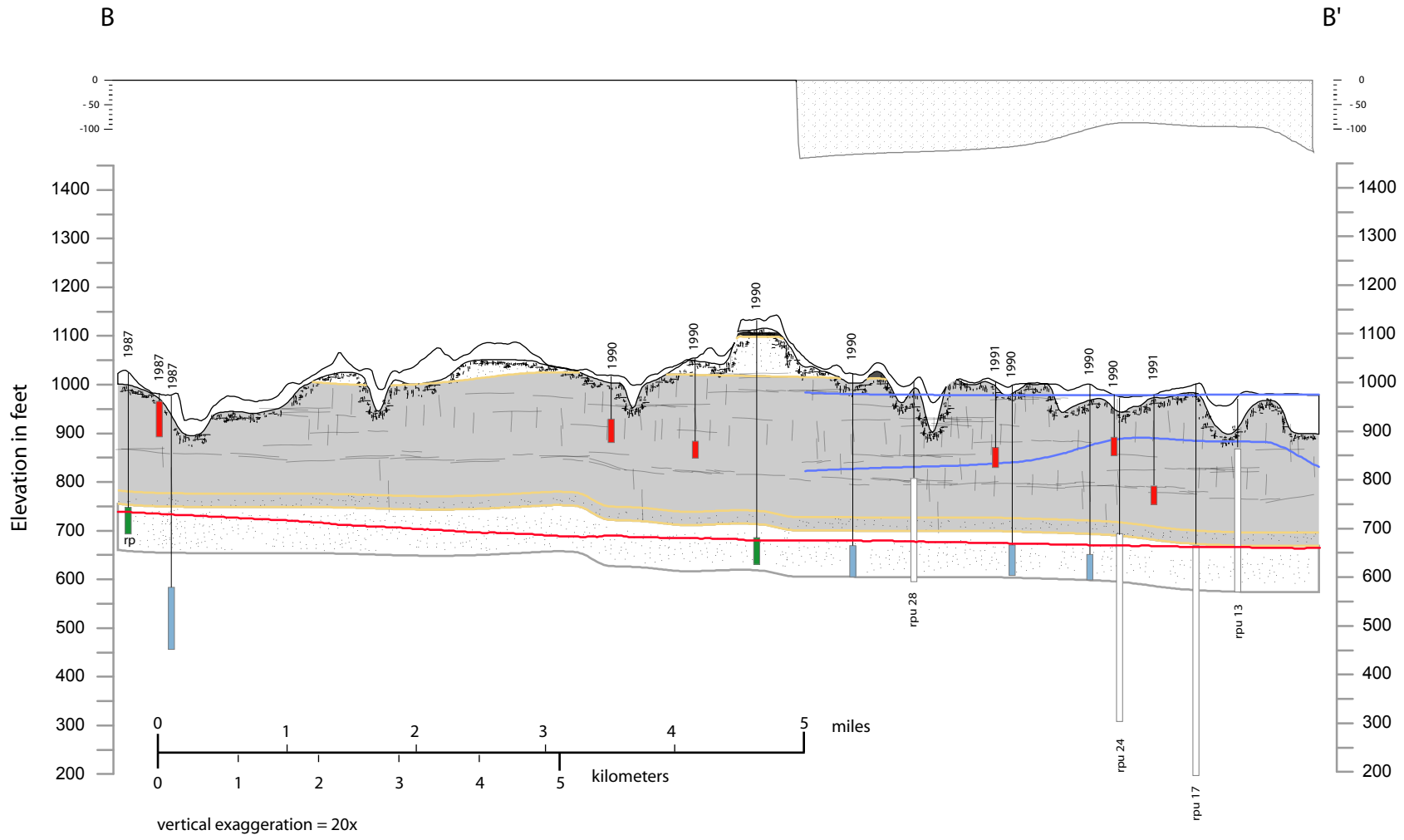


Figure 34

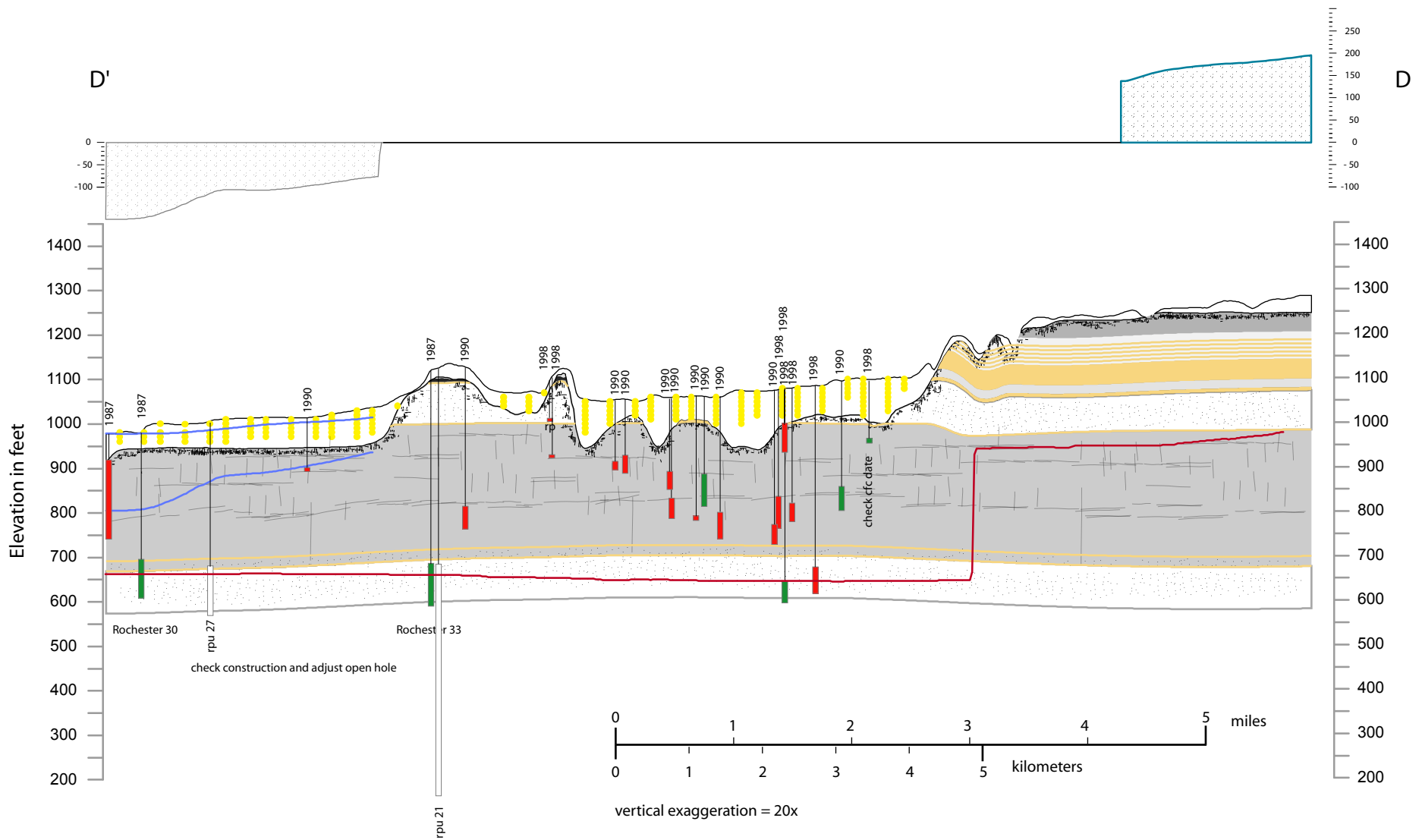


Figure 36

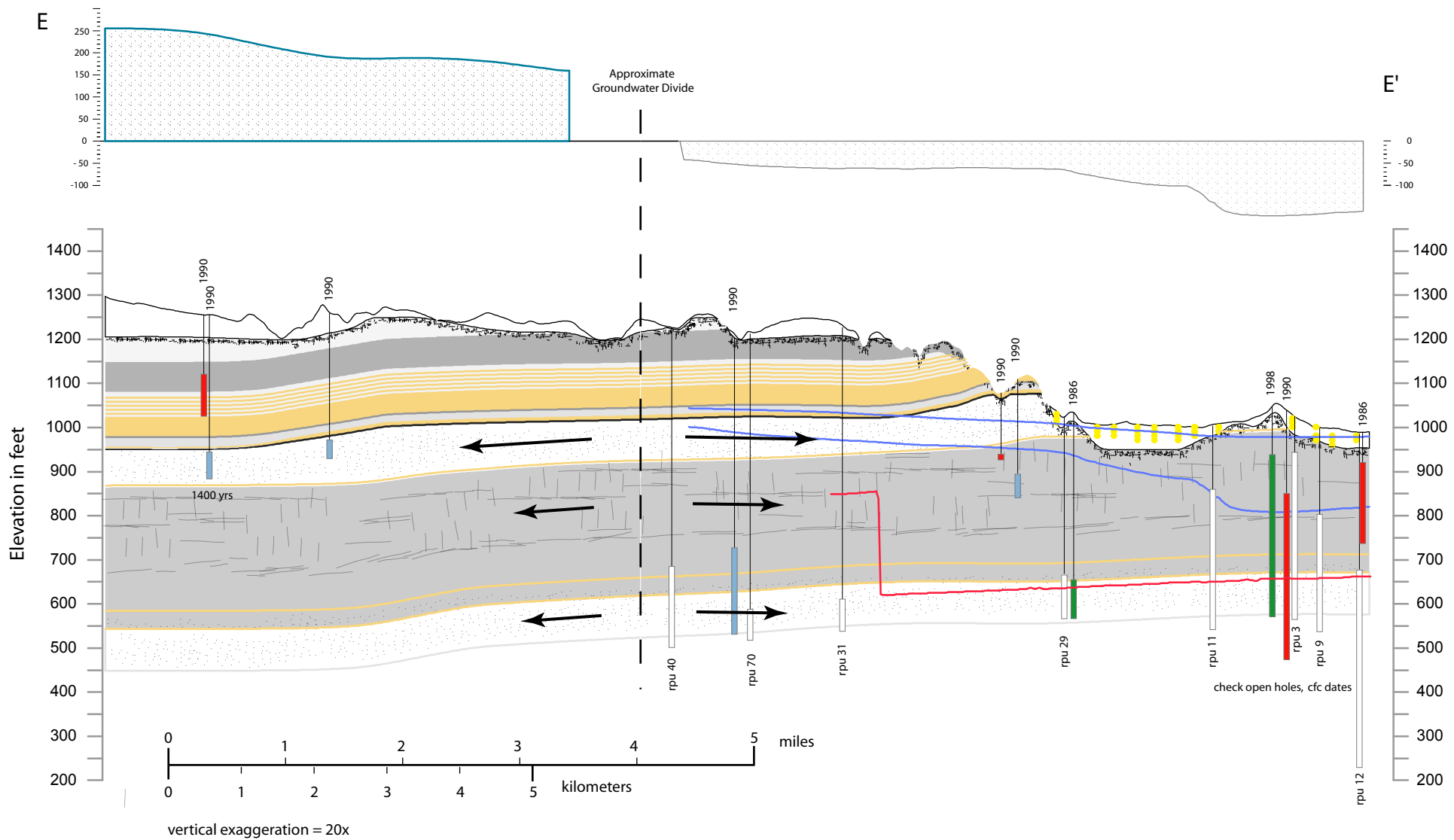
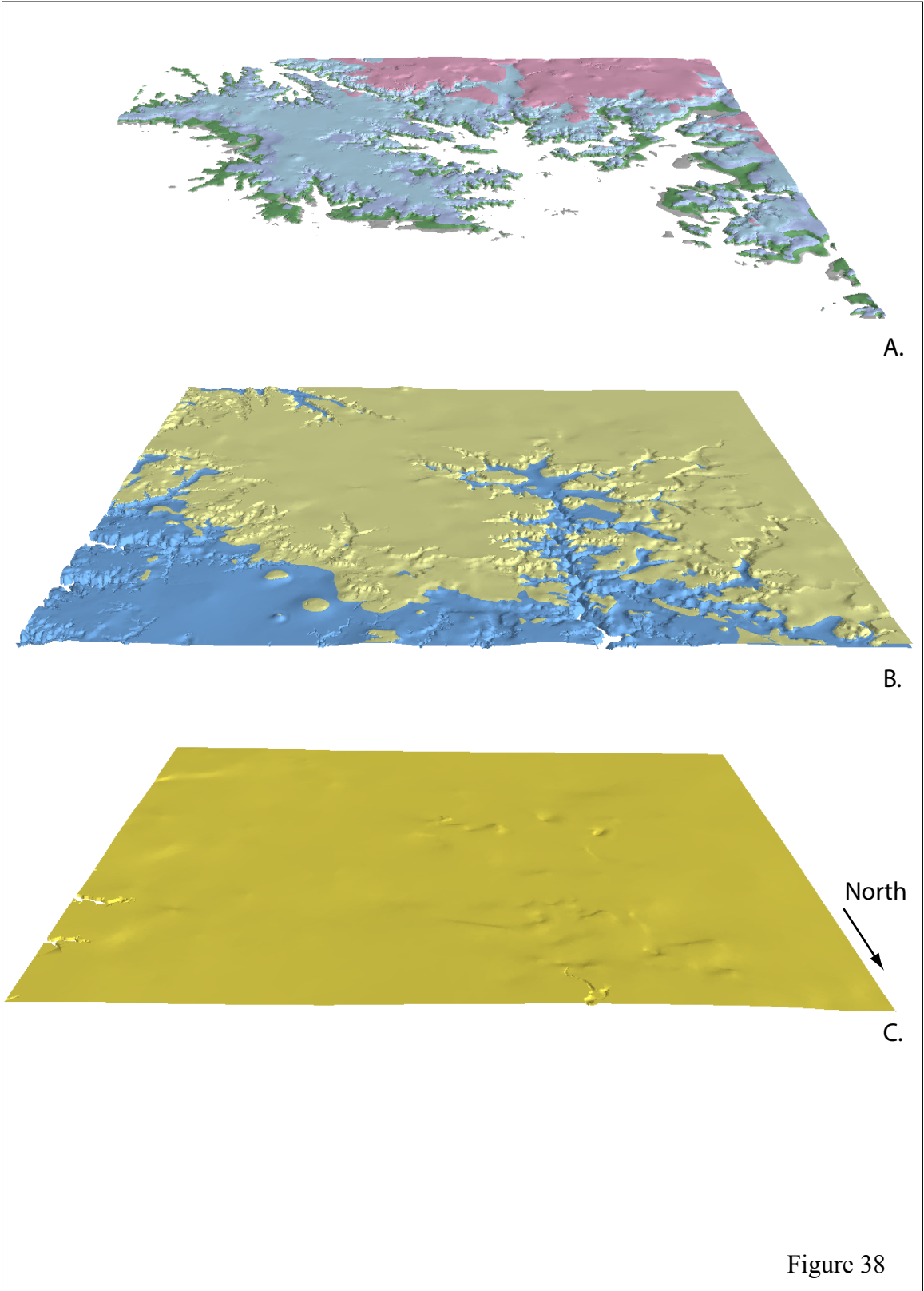
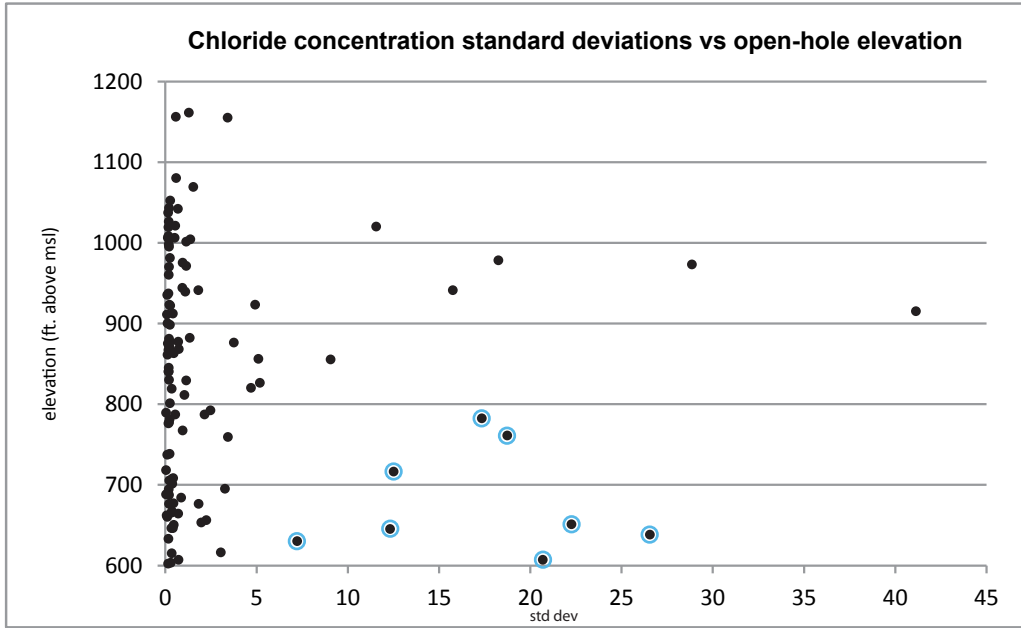


Figure 37





- ◆ standard deviation of chloride concentrations for wells sampled more than 4 times since 1999
- wells with open hole elevations below 800 and standard deviations greater than 5

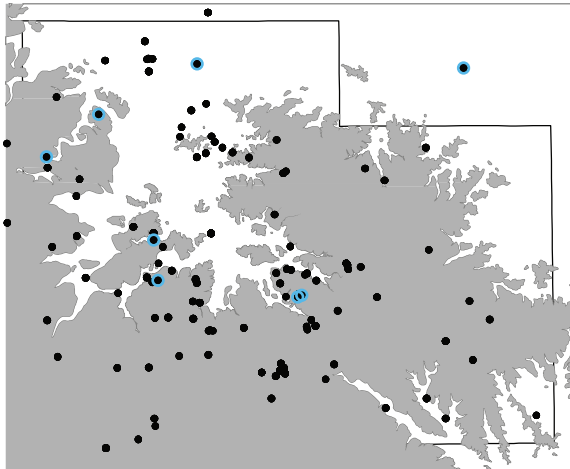
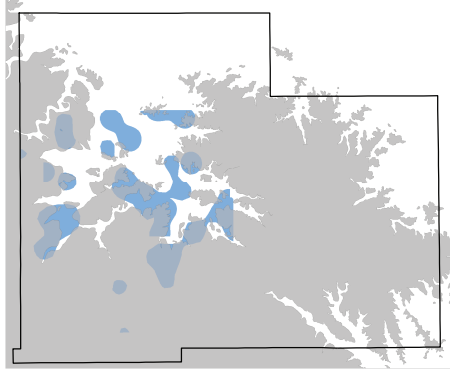


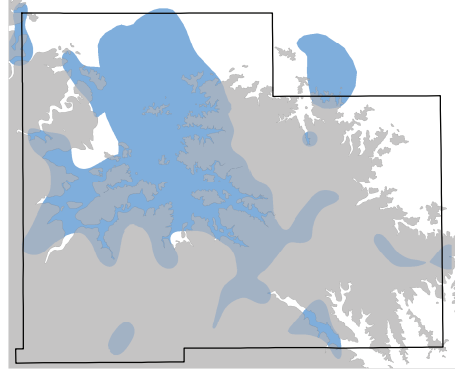
Figure 39

A.



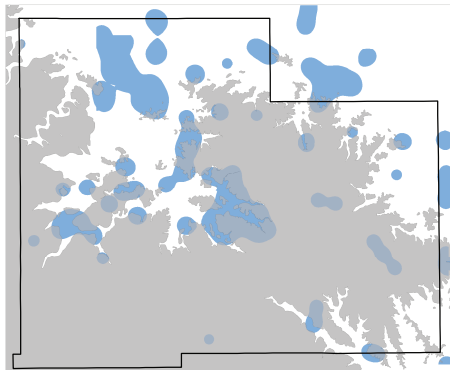
calcium to magnesium ratio greater than 2.2

B.



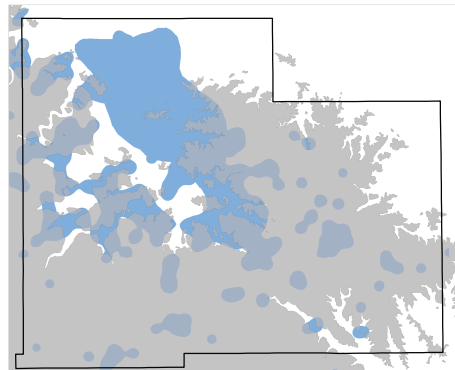
chloride concentration greater than 2 mg/L

C.



nitrate as nitrogen concentration greater than 2 mg/L

D.



sulfate concentration greater than 22 mg/L

Figure 40

References cited

- Almendinger, J.E. and Mitton, G.B., 1995, Hydrology and relation of selected water-quality constituents to selected physical factors in Dakota County, Minnesota, 1990-91: United States Geological Survey Water-Resources Investigations Report 94-4207, 26 p.
- Alexander, E.C., Jr., Runkel, A.C., Tipping, R.G., and Green, J.A., 2013, Deep time origins of sinkhole collapse failures in sewage lagoons in southeast Minnesota: 13th Sinkhole Conference, National Cave and Karst Research Institute, Symposium 2, p. 285-292.
- Anderson, J.R., Runkel, A.C., Tipping, R.G., Barr, K., Alexander, E.C., Jr., 2011, Hydrostratigraphy of a fractured urban aquitard: Geological Society of America Field Guides 24, pp457-475.
- Crawford, K. 2012, Sampling of CWP-2011 and 2012, Draft 8/16/2012: Terry Lee, written communication, on-file at Minnesota Geological Survey, 39 p.
- Crawford, K., 2013, Whole rock chemistry for selected Paleozoic rocks. Spreadsheet "kimm_crawford_rockchemistry_Dolomite-1.xls": Terry Lee, written communication, on-file at Minnesota Geological Survey.
- Dakota County, 2006, Dakota County Ambient Groundwater Quality Study, 1999-2003 Report, 108p.
<http://www.co.dakota.mn.us/Environment/WaterQuality/WellsDrinkingWater/Documents/AmbientGroundwaterStudy.pdf> (accessed May 9, 2014)
- Delin, G.N., and Woodward, D.G., 1984, Hydrogeologic setting and the potentiometric surfaces of regional aquifers in the Hollandale Embayment, southeastern Minnesota: United States Geological Survey Water-Supply Paper 2219, 56 p.
- Delin, G.N., 1991, Hydrogeology and simulation of ground-water flow in the Rochester area, southeastern Minnesota, 1987-88: United States Geological Survey Water-Resources Investigation Report 90-4081, 108 p.
- Delin, G.N., and Almendinger, J.E., 1993, Delineation of recharge areas for selected wells in the St. Peter-Prairie du Chien-Jordan aquifer, Rochester, Minnesota: United States Geological Survey Water-Supply Paper 2397, 39 p.
- Helsel, D.R. and Hirsch, R.M., 2002, Statistical methods in water resources: chapter A3 in United States Geological Survey, Book 4, Hydrologic Analysis and Interpretation, <http://pubs.usgs.gov/twri/twri4a3/> (accessed 4/30/2012).
- Hobbs, H. 1988, Surficial Geology. Plate 3 of N.H. Balaban, editor, Geologic Atlas of Olmsted County: Minnesota Geological Survey County Atlas C-3.

- Lehmann, C.M.B. and Gay, D.A., 2011 Monitoring long-term trends of acidic wet deposition in US precipitation, results from the National Atmospheric Deposition Program: Power Plant Chem. 2011, 13 (7), 378–385.
- Lindgren, R. J., 2001, Ground-water recharge and flowpaths near the edge of the Decorah-Platteville-Glenwood confining unit, Rochester, Minnesota: United States Geological Survey Water-Resources Investigation Report 00-4215, 46 p.
- Maki, G., 1989, Nitrate, flow and temperature data collected from 251 springs in Olmsted County as part of the Olmsted County Geologic Atlas: Terry Lee - OCER, written communication. on file at the Minnesota Geological Survey.
- Meyer, J.R., Parker, B.L., and Cherry, J.A., 2008, Detailed hydraulic head profiles as essential data for defining hydrogeologic units in layered fractured sedimentary rock: Environmental Geology, v. 56, p. 27-44.
- Meyer, J.R., Parker, B.L., and Cherry, J.A., 2014, Characteristics of high resolution hydraulic head profiles and vertical gradients in fractured sedimentary rocks: Journal of Hydrology, v 517, p. 493-507.
- Minnesota Department of Natural Resources, 2011, AVSWUDS.ZIP, Water appropriation installation locations, reported pumping data for 1988-2010: file created August 5, 2011. Water Appropriations Permit Program http://www.dnr.state.mn.us/waters/watermgmt_section/appropriations/wateruse.html (accessed August 10, 2011)
- Minnesota Department of Natural Resources, 2014, Ground water level data: http://www.dnr.state.mn.us/waters/groundwater_section/obwell/waterleveldata.html (accessed May 9, 2014)
- Minnesota Pollution Control Agency, 1999, Baseline Water Quality of Minnesota's Principal Aquifers - Region 5, Southeast Minnesota: Minnesota Pollution Control Agency, Environmental Outcomes Division, Environmental Monitoring and Analysis Section, Ground Water and Toxics Monitoring Unit. 91 p. <http://www.pca.state.mn.us/index.php/view-document.html?gid=6295>, (accessed December 26, 2013)
- Minnesota Pollution Control Agency, 2013, Environmental Data Access: <http://www.pca.state.mn.us/index.php/data/groundwater-data.html> (accessed March 6, 2013)
- Mossler, J.H., 2008, Paleozoic stratigraphic nomenclature for Minnesota: Minnesota Geological Survey Report of Investigations 65, 84 p.
- Mossler, J.H., and Hobbs, H.C., 1995, Depth to Bedrock and Bedrock Topography, pl. 4 of Mossler, J.H., project manager, Geologic atlas of Fillmore County, Minnesota: Minnesota Geological Survey County Atlas Series C-8, Part A, scale 1:100,000.

- Mubarak, K.E., 2003, Utilizing GIS to estimate the quantity and distribution of nitrate-nitrogen and chloride in Olmsted County groundwater: unpublished M.S. thesis, St. Mary's University <http://www.gis.smumn.edu/GradProjects/MubarakK.pdf> (accessed 6/7/2012).
- Nemetz, D.A., 1993, The geochemical evolution of ground water along flowpaths in the Prairie du Chien-Jordan aquifer of southeastern Minnesota: Unpublished M.S. Thesis, University of Minnesota, 182p.
- Olmsted County Environmental Resources, 2012, Mississippi River – watershed water quality data compilation and trend analysis report. Final Report 2012: prepared for the Whitewater Watershed Joint Powers Board, 182 p.
<http://www.co.olmsted.mn.us/environmentalresources/waterresourcemanagement/Documents/FullMissWinReport.pdf> (accessed 4/12/2013)
- Olmsted County Environmental Resources, 2014, Clean Water Partnership groundwater sampling program: Terry Lee, written communication.
- Olsen, B.M., 1976, Stratigraphic occurrence of argillaceous beds in the St. Peter Sandstone, Twin City Basin, Minnesota: Minneapolis, University of Minnesota, M.S. thesis, 86 p
- Rochester-Olmsted Planning Department, 2012, Olmsted County Water Management Plan – 2013-2023. 188 p.
<http://www.co.olmsted.mn.us/environmentalresources/waterresourcemanagement/Documents/Water%20Plan%202013%20Cover%20Acronyms.pdf> (accessed 12/26/2013)
- RPU, 2013, Observation well and Muncipal well depth to water data: Todd Osweiler, Rochester Public Utilities, written communication.
- Runkel, A.C., 1996, Geologic investigations applicable to groundwater management, Rochester Metropolitan Area, Minnesota: Minnesota Geological Survey, Open File Report OFR-96-01, 30 p. <http://conservancy.umn.edu/handle/122068> (accessed 6/30/2013).
- Runkel, A.C., Steenburg, J.R., Tipping, R.G., and Retzler, A.J., 2013, Geologic controls on groundwater and surface water flow in southeastern Minnesota and its impact on nitrate concentrations in streams: Contract deliverable summarizing work conducted by the Minnesota Geological Survey for the Minnesota Pollution Control Agency, contract number B50858 (PRJ number PRJ07522), entitled “Geologic Controls on Nitrate in Southeast Minnesota Streams”. 154 p.
- Runkel, A.C.; Tipping, R.G.; Alexander, E.C. Jr.; Green, J.A.; Mossler, J.H.; Alexander, S.C., 2003, Hydrogeology of the Paleozoic bedrock in southeastern Minnesota: Minnesota Geological Survey Report of Investigations, RI-61, 113 plus 2 plates.
<http://conservancy.umn.edu/handle/58813> (accessed 6/30/2013)

- Runkel, A.C., Tipping, R.G., Alexander, E.C., Jr., and Alexander, S.C., 2006, Hydrostratigraphic characterization of intergranular and secondary porosity in part of the Cambrian sandstone aquifer systems of the cratonic interior of North America: Improving predictability of hydrogeologic properties: *Sedimentary Geology*, v. 184, p. 281-304.
- Runkel, A.C., Mossler, J.H., and Tipping, R.G., 2007, The Lake Elmo Downhole Logging Project: Hydrostratigraphic Characterization of Fractured Bedrock at a Perfluorochemical Contamination Site: Minnesota Geological Survey Open-File Report 07-5, 55p.
- Smith, S.E., and Nemetz, D.A., 1996, Water quality along selected flowpaths in the Prairie du Chien Jordan aquifer, southeastern Minnesota: United States Geological Survey Water-Resources Investigations Report 95-4115, 76p.
- Tipping, R.G., 1994, Southeastern Minnesota regional ground water monitoring study: a report to the Southeast Minnesota Water Resources Board: Minnesota Geological Survey Open File Report 94-1, 117 p. with appendices. <http://conservancy.umn.edu/handle/122062> (accessed 4/15/2013).
- Tipping, R.G., Runkel, A.C., Alexander, E.C., Jr., Alexander, S.C., and Green, J.A., 2006, Evidence for hydraulic heterogeneity and anisotropy in the mostly carbonate Prairie du Chien Group, southeastern Minnesota, USA: *Sedimentary Geology*, v.184, p.305-330 .
- Tipping, R.G. and Runkel, A.C., 2008, Geologic investigations to support ground-water management II, Rochester metropolitan area, Minnesota: Project summary report to Rochester Public Utilities: Minnesota Geological Survey Open-File Report 08-6. ftp://mgssun6.mngs.umn.edu/pub6/ofr08_06/ (accessed 6/7/2012).
- Tipping, R.G., 2012, Characterizing groundwater flow in the Twin Cities metropolitan area, Minnesota a chemical and hydrostratigraphic approach: Ph.D. dissertation, University of Minnesota, 186 p. with appendices. <http://conservancy.umn.edu/handle/132004> (accessed 4/7/2013)
- United States Geological Survey, 2013, National Water Inventory System: <http://waterdata.usgs.gov/nwis> (accessed April 4, 2013).
- Wall, D.B., and Regan, C.P., 1994, Water quality and sensitivity of the Prairie du Chien-Jordan Aquifer in western Winona County, Minnesota: Unpublished report of the Minnesota Pollution Control Agency, Division of Water Quality, St Paul, MN, 65 p.
- Walsh, J., 1993, Pesticides and their breakdown products in Minnesota groundwater: Minnesota Department of Health, prepared for the Legislative Commission on Minnesota Resources, July, 1993. 83 p.

Wilson, R. and Crawford, K., 2006, A chloride budget for Olmsted County: abstract in Minnesota Water 2006 Final Program and Book of Abstracts, University of Minnesota http://wrc.umn.edu/prod/groups/cfans/@pub/@cfans/@wrc/documents/asset/cfans_asset_113658.pdf (accessed 6/7/2012).

Woodward, D., 1986, Hydrogeologic framework and properties of regional aquifers in the Hollandale Embayment, southeastern Minnesota: United States Geological Survey HA -677.

Worthington, S.R.H., 2003, A comprehensive strategy for understanding flow in carbonate aquifers: / Speleogenesis and Evolution of Karst Aquifers 1 (1), www.speleogenesis.net , 8 pages, re-published from: Palmer, A.N., Palmer, M.V., and Sasowsky, I.D. (eds.), Karst Modeling: Special Publication 5, The Karst Waters Institute, Charles Town, West Virginia (USA), 30-37.

Appendix: (GIS data included in supplementary files)

Feature Class Name: CHEMISTRY_DATA_ALL (one record per sample event)

Field Name	Description	Lookup Table
relateid	CWI unique identifier	
unique_no	Minnesota unique well number	
wellname	well name. Info from CWI if available	
alt_id	alternate identifier, e.g. field sample number	
mpca_EDA_id	MPCA Environmental Data Access Identifier	
agency	agency	xAGENCY
program_id	agency program associated with sample event	xPROGRAM_ID
Dataset	concatenation of agency and program_id fields	xDATASET
sample_date	date of sample collection as text in format yyyyymmdd where equivalent sample_date2 available	
sample_date2	date of sample collection as date/time field	
cond	specific conductance of sample reported as microsiemens per centimeter - may or may not be corrected for temperature.	
temp_c	temperature in degrees Celsius, assumed to be at time of sampling unless noted otherwise in remarks	
pH	Negative log of hydrogen concentration	
ORP	Eh: oxidation-reduction potential referenced to standard hydrogen electrode, in millivolts	
DO	dissolved oxygen concentration in milligrams per liter	
Ca	calcium concentration in milligrams per liter	
Mg	magnesium concentration in milligrams per liter	
Na	sodium concentration in milligrams per liter	
K	potassium concentration in milligrams per liter	
Fe	iron concentration in milligrams per liter	
Mn	manganese concentration in milligrams per liter	
Sr	strontium concentration in milligrams per liter	
Ba	barium concentration in milligrams per liter	
P	phosphorous concentration in milligrams per liter	
Al	aluminum concentration in milligrams per liter	
Si	silicon concentration in milligrams per liter as SIO2 - assumed	

Alk_CaCO3	total alkalinity of the solution reported as calcium carbonate in milligrams per liter	
Cl	chloride concentration in milligrams per liter	
SO4	sulfate concentration in milligrams per liter	
Br	bromide concentration in milligrams per liter	
F	fluoride concentration in milligrams per liter	
NO3_N	nitrate concentration in milligrams per liter reported as nitrogen	
NO2_N	nitrite concentration in milligrams per liter reported as nitrogen	
NO3_NO2_asN	Nitrate plus nitrite concentration in milligrams per liter reported as nitrogen	
PO4_P	phosphate concentration in milligrams per liter reported as phosphorus	
TOTAL_CATIONS	total cations in milli-equivalents per liter	
TOTAL_ANIONS	total anions in milli-equivalents per liter	
PERCENT_ERR	charge balance percent error	
TDS	total dissolved solids in milligrams per liter	
TDC_MC	Total dissolve solids method code, "EV" indicates residue on evaporation	
deuterium	deuterium isotope (per mil)	
oxygen_18	oxygen 18 isotope (per mil)	
H3_det		
tritium	tritium concentration in tritium units (TU)	
H3_err	tritium error (precision)	
C14_PMC	carbon-14 reported as percent modern carbon	
C14_PMC_unc	reported one sigma counting error	
C13	carbon-13 (per mil)	
SF6	sulfur hexafluoride concentration in femtograms per kilogram	
CFC	Chlorofluorocarbon	
Years_modifier	modifier, less than (<) or greater than (>)	
Years	Model estimated age in years	
Years_unc	Model estimated age uncertainty in years	
age_Model	Name of model used to estimate age (C14; H3/He; SF6; CFC; other)	
age_class	age class:V = vintage, M = mixed, R = recent	<i>xAGE_CLASS</i>
age_class_no	numeric version of age_class for query purposes: 1 = V, 2=M, 3=R	
age_basis	basis for age class	<i>xAGE_BASIS</i>
file_src	name of source file(s)	
agency_prg	unique agency-program ID: concatenation of agency and program_id fields	

relate_date	sample event comparison field
duplicate	duplicate from same sample date, 1 = yes
remarks	comments on data in row
report_ref	report reference, if available
redox_cat	Redox category as assigned by Jurgens and others (2009) based on DO, NO ₃ _N, Mn, Fe and SO ₄ concentrations
redox_process	Redox process as assigned by Jurgens and others (2009) based on DO, NO ₃ _N, Mn, Fe and SO ₄ concentrations
sr_ca_mg_ratio	strontium to calcium plus magnesium molar ratio
cl_br_ratio	chloride to bromide ratio, mg/L
ca_mg_ratio	Calcium to magnesium molar ratio
flg_goodchargebalance	data flag - good charge balance
flg_fieldparameters	data flag – 1 indicates field parameters/physical characteristics (cond, temp, pH, DO)
flg_stable_radio_isotope	data flag - 1 indicates stable and radiogenic isotopes
flg_nutrients	data flag - 1 indicates nutrient data (phosphorous, nitrogen compounds)
flg_other	data flag - 1 indicates major cations and anions, physical characteristics - no or poor charge balance
flg_age	data flag - 1 indicates age determination
flg_redox_condition	data flag - 1 indicates redox condition assigned
flg_swuds	data flag - 1 indicates unique number matched DNR SWUD
checked	Data individually checked relative to surrounding wells and hydrogeologic setting
comments	Comments on checked wells
HCO ₃	
aHCO ₃	
aCa	
aMg	
aNa	
aCO ₃	
aSO ₄	
SI_calcite	
SI_dolomite	
SI_quartz	

SI_anydrite
 meqCa
 meqMg
 meqNa
 meqHCO3
 meqCl
 meqSO4
 thard
 file_src name of source file(s)
 file_src2

Feature Class Name: CWI_WELLS, County Well Index (CWI) summary table records for wells in CHEMISTRY_DATA_ALL with Minnesota unique well numbers. Feature class is linked to CHEMISTRY_DATA_ALL by field "relateid"

Field Name	Description	Lookup Table
RELATEID	CWI unique identifier	
COUNTY_C	Two digit county code	xCOUNTY_C
UNIQUE_NO	Minnesota Unique Well Number	
WELLNAME	Well name. Information from CWI if available	
TOWNSHIP	Public Land Survey, Township number	
RANGE	Public Land Survey, Range number	
RANGE_DIR	Public Land Survey, Range direction	
SECTION_	Public Land Survey, Section number	
SUBSECTION	Subsection codes - ABCD system from largest subsection to smallest	
MGSQUAD_C	USGS 7.5 minute quadrangle map code	xMGSQUAD_C
ELEVATION	Elevation in feet above sea level. Information from CWI if available	
ELEV_MC	Elevation method code. Information from CWI if available	xELEV_MC
STATUS_C	Well status. Information from CWI if available	xSTATUS
USE_C	Use code. Information from CWI if available	xUSE_C
LOC_MC	Location method code. Information from CWI if available	xLOC_MC
LOC_SRC	Location source code. Information from CWI if available	xLOC_SRC
DATA_SRC	Data source code. Information from CWI if available	
DEPTH_DRLL	Depth drilled (in feet). Information from CWI if available	
DEPTH_COMP	Depth completed (in feet). Information from CWI if available	
DATE_DRLL	Date drilled (reported as YYYYMMDD). Information from CWI if available	

CASE_DIAM	Minimum casing diameter (in inches). Information from CWI if available	
CASE_DEPTH	Casing depth (in feet). Information from CWI if available	
GROUT	Well grouted? (Y,N, U). Information from CWI if available	
	Distance to nearest known pollution source (in feet). Information from CWI if available.	
POLLUT_DST	Information from CWI if available	
POLLUT_DIR	Direction to nearest known pollution source. Information from CWI if available	
POLLUT_TYP	Type of nearest known pollution source. Information from CWI if available	<i>xPOLLUT_TYP</i>
STRAT_DATE	Date of stratigraphic interpretation. Information from CWI if available	
STRAT_UPD	Date of stratigraphic interpretation update. Information from CWI if available	
STRAT_SRC	Source of stratigraphic interpretation. Information from CWI if available	
STRAT_GEOL	Interpreting geologist. Information from CWI if available	<i>xSTRAT_GEOL</i>
STRAT_MC	Method of stratigraphic interpretation. Information from CWI if available	<i>xSTRAT_MC</i>
DEPTH2BDRK	Depth to bedrock, in feet. Information from CWI if available	
FIRST_BDRK	Upper-most bedrock. Information from CWI if available	<i>xSTR_CODE</i>
	Lowest most stratigraphic unit encountered while drilling. Information from CWI if available.	<i>xSTR_CODE</i>
LAST_STRAT		<i>xSTR_CODE</i>
OHTOPUNIT	Open hole top unit. Information from CWI if available	<i>xSTR_CODE</i>
OHBOTUNIT	Open hole bottom unit. Information from CWI if available	<i>xSTR_CODE</i>
AQUIFER	Aquifer code. Information from CWI if available	<i>xSTR_CODE</i>
CUTTINGS	Cuttings available?	
CORE	Core available?	
BHGEOPHYS	Borehole geophysics available?	
SWL	Static water levels available?	
INPUT_SRC	Input source	
ENTRY_DATE	Date log was entered into CWI	
UPDT_DATE	CWI update date	
GEOC_TYPE	Geographic coordinate type	
GCM_CODE	Geographic coordinate method code	<i>xGCM_CODE</i>
GEOC_SRC	Geographic coordinate source	
GEOC_PRG	Geographic coordinate program	
UTME	Universal Transverse Mercator easting, UTM zone 15 extended, NAD83	
UTMN	Universal Transverse Mercator northing UTM zone 15 extended, NAD83	
GEOC_ENTRY	Geographic coordinate entry source	
GEOC_DATE	Geographic coordinate entry date	

GEOCUPD_EN	Geographic coordinate update source
GEOCUPD_DA	Geographic coordinate update date
RCVD_DATE	Date received
WELL_LABEL	Well label to be used for mapping purposes (typically unique well number)
SWLCOUNT	Number of static water level measurements from this well
SWLDATE	static water level date
SWLAVGMEAS	Average static water level measurement
SWLAVGELEV	Average static water elevation (ELEVATION - SWLAVGMEAS)

Feature Class Name: sgpg_se (regional surficial geologic map, compiled at 1:100,000 scale)

Field Name	Description	Lookup Table
map_label	abbreviation representing map unit suitable for labeling features on map	
description	text expansion of map_label/unit_code	
unit_code	mapped unit	
lithology	primary lithology	
text_mod	texture modifier	
thickness	relative thickness	
carbonate	carbonate content	
environmen	depositional environment	
dep_type	depositional type	
age	approximate age	
erosion	erosional environment	
interp	interpreted geologic setting	
K_class	numeric categorical variable indicating hydraulic conductivity class based on texture	xK_CLASS
K_class_desc	text expansion of K_class category	
Kmax_ftday	maximum estimated hydraulic conductivity in feet per day for specified K_class	
Kmin_ftday	minimum estimated hydraulic conductivity in feet per day for specified K_class	

Feature Class Name: bgpg_se (regional bedrock geologic map, compiled at 1:100,000 scale)

Field Name	Description	Lookup Table
map_label	label symbology for printed map	
description	name of geologic unit	
unit_code	geologic unit code	xSTR_CODE

Regional - rasters

Name	Description	layer file
rpu_1981	Raster represents the elevation of 1981 horizontal and vertical distribution of recent waters in RPU wells below an elevation of 870 feet. Raster created from contours of open hole top (casing bottom) elevation for wells with chloride concentrations greater than 2 mg/L	rpu_1981.lyr
rpu_2011	Raster represents the elevation of 2011 horizontal and vertical distribution of recent waters in RPU wells below an elevation of 870 feet. Raster created from contours of open hole top (casing bottom) elevation for wells with chloride concentrations greater than 2 mg/L	rpu_2011.lyr
camg_p99_cjdn	Raster represents the lowest-most elevation of recent waters within the Jordan Sandstone, based post_1999 calcium to magnesium molar ratios (sampled since 1/1/2000). Raster created by using ordinary kriging to interpolate top-of-open-hole elevations for wells with ratios greater than 2.2. Surface extent limited by assigning no data values in areas where data is sparse.	
camg_p99_ospc	Raster represents the lowest-most elevation of recent waters within the St. Peter Sandstone and Prairie du Chien Group, based post_1999 calcium to magnesium molar ratios (sampled since 1/1/2000). Raster created by using ordinary kriging to interpolate top-of-open-hole elevations for wells with ratios greater than 2.2. Surface extent limited by assigning no data values in areas where data is sparse.	
camg_p99_comb	Raster represents the combined lowest-most elevation of recent waters within the St. Peter Sandstone and Prairie du Chien Group and Jordan Sandstone, based post_1999 calcium to magnesium molar ratios (sampled since 1/1/2000). Raster created by combining 'camg_p99_cjdn' with 'camg_p99_ospc', replacing the latter with Jordan values where Jordan raster is present.	
cl_p99_cjdn	Raster represents the lowest-most elevation of recent waters within the Jordan Sandstone, based post_1999 chloride concentrations (sampled since 1/1/2000). Raster created by using ordinary kriging to interpolate top-of-open-hole elevations for wells with concentrations greater than 2 mg/L. Surface extent limited by assigning no data values in areas where data is sparse.	
cl_p99_ospc	Raster represents the lowest-most elevation of recent waters within the St. Peter Sandstone and Prairie du Chien Group, based post_1999 chloride concentrations (sampled since 1/1/2000). Raster created by using ordinary kriging to interpolate top-of-open-hole elevations for wells with concentrations greater than 2 mg/L. Surface extent limited by assigning no data values in areas where data is sparse.	
cl_p99_comb	Raster represents the combined lowest-most elevation of recent waters within the St. Peter Sandstone and Prairie du Chien Group and Jordan Sandstone, based post_1999 chloride concentrations (sampled since 1/1/2000). Raster created by combining 'cl_p99_cjdn' with 'cl_p99_ospc', replacing the latter with Jordan values where Jordan raster is present.	
no3_p99_cjdn	Raster represents the lowest-most elevation of recent waters within the Jordan Sandstone, based post_1999 nitrate as nitrogen concentrations (sampled since 1/1/2000). Raster created by using ordinary kriging to interpolate top-of-open-hole elevations for wells with concentrations greater than 2 mg/L. Surface extent limited by assigning no data values in areas where data is sparse.	

Name	Description	layer file
no3_p99_ospc	Raster represents the lowest-most elevation of recent waters within the St. Peter Sandstone and Prairie du Chien Group, based post_1999 nitrate as nitrogen concentrations (sampled since 1/1/2000). Raster created by using ordinary kriging to interpolate top-of-open-hole elevations for wells with concentrations greater than 2 mg/L. Surface extent limited by assigning no data values in areas where data is sparse.	
no3_p99_comb	Raster represents the combined lowest-most elevation of recent waters within the St. Peter Sandstone and Prairie du Chien Group and Jordan Sandstone, based post_1999 choride concentrations (sampled since 1/1/2000). Raster created by combining 'no3_p99_cjdn' with 'no3_p99_ospc', replacing the latter with Jordan values where Jordan raster is present.	
so4_p99_cjdn	Raster represents the lowest-most elevation of recent waters within the Jordan Sandstone, based post_1999 sulfate concencatations (sampled since 1/1/2000). Raster created by using ordinary kriging to interpolate top-of-open-hole elevations for wells with concentrations greater than 2 mg/L. Surface extent limited by assigning no data values in areas where data is sparse.	
so4_p99_ospc	Raster represents the lowest-most elevation of recent waters within the St. Peter Sandstone and Prairie du Chien Group, based post_1999 sulfate concentrations (sampled since 1/1/2000). Raster created by using ordinary kriging to interpolate top-of-open-hole elevations for wells with concentrations greater than 2 mg/L. Surface extent limited by assigning no data values in areas where data is sparse.	
so4_p99_comb	Raster represents the combined lowest-most elevation of recent waters within the St. Peter Sandstone and Prairie du Chien Group and Jordan Sandstone, based post_1999 choride concentrations (sampled since 1/1/2000). Raster created by combining 'no3_p99_cjdn' with 'no3_p99_ospc', replacing the latter with Jordan values where Jordan raster is present.	
so4_p1999	Raster represents the lowest-most elevation of recent waters based post_1999 sulfate results (sampled since 1/1/2000). Raster creatd by using ordinary kriging to interpolate top-of-open-hole elevations for wells with greater than 22 mg/L sulfate. Surface extent limited by assigning no data values in areas where prediction error was greater than 65. Interpolated data is a generalized surface, and does not capture all top-of-open hole recent water elevations shown on cross sections.	
btgd	Raster represents the elevation above mean sea level, in feet, for the top of bedrock. Raster created from 1:100,000 scale bedrock topography contour maps. In places where resultant raster cells had elevations greater than the USGS National Elevation Dataset (NED) 1 arc-second resolution (approx 30m cell size), cell value was replaced with the NED cell value. Data is current to the publication date of each 1:100,000 scale contour map; no additional corrections were made based on well data available since that time. Due to its source and compilation scale, this dataset is not suitable for site specific investigations.	
d2br	Depth to bedrock raster where cell value represents the depth from the land surface to the bedrock surface. Raster was created by subtracting bedrock topography raster (btgd_se, this project) from the National Elevation Dataset (NED), 1 arc-second resolution (approx 30m cell size), Data is current to the publication date of each 1:100,000 scale bedrock topography contour map; no additional corrections were made based on well data available since that time. Due to its source and compilation scale, this dataset is not suitable for site specific investigations.	d2br_gt_50 feet.lyr

Regional - polygons
Name

Description

Name	Description	layer file
bpgg_se	Bedrock geologic map, regional, 1: 100,000 scale	bpgg_se.lyr
sgpg_se	Surficial geologic map, regional, 1:100,000 scale	sgpg_se_till.lyr
papg	study area boundary	
papg_odcr_500mbuffer	study area divided into zones based on 500 meter buffer around the edge of the Decorah Formation	papg_odcr_500mbuffer.lyr

Regional - polylines. Contained as feature classes in ESRI personal geodatabase "mgs_hydrochem_rochester.mdb"

Name	Description
cross_section_locations	locations of cross sections A-A' through E-E' referred to in report

Regional - points. Contained as feature classes in ESRI personal geodatabase "mgs_hydrochem_rochester.mdb"

Name	Description	layer file
chemistry_data_all	groundwater chemical data collected as part of this investigation. Data loaded into GIS format from original datasets not in this format; fields standardized to conform to a single table. Data tied to a unique identifier - Minnesota unique well number used where possible. One row for each sample event	
cwi_wells	State water well database - County Well Index (CWI) data for wells linked to chemistry_data_all (this investigation) by unique well number/relatedid.	
unconsolidated_model_coarsegrained_sediment	3D collection of regularly spaced grid points showing where likelihood of coarse-grained sediment occurrence is greater than 40 percent	layers\unconsolidate_model_fine-grained_sediment.lyr
Unconsolidated_model_fine_grained_sediment	3D collection of regularly spaced grid points showing where likelihood of fine-grained sediment occurrence is greater than 40 percent	layers\unconsolidate_model_coarse-grained_sediment.lyr

Multipatches

Name	Description	layer file
mp_cecr30_top	Elevation of Eau Claire Formation top. Multipatch format for display in ArcGIS - ArcScene	layers\mp_cecr30_top.lyr
mp_cjdn30_top	Elevation of Jordan Sandstone top. Multipatch format for display in ArcGIS - ArcScene	layers\mp_cjdn30_top.lyr
mp_cstl30_top	Elevation of St. Lawrence formation top. Multipatch format for display in ArcGIS - ArcScene	layers\mp_cstl30_top.lyr
mp_ctcg30_top	Elevation of Tunnel City Group (formally Franconia Formation) top. Multipatch format for display in ArcGIS - ArcScene	layers\mp_ctcg30_top.lyr
mp_cwoc30_top	Elevation of Wonewoc Sandstone (Formally Iron-ton-Galesville) top. Multipatch format for display in ArcGIS - ArcScene	layers\mp_cwoc30_top.lyr
mp_ned30	Elevation of the land surface - data from USGS National Elevation 30 meter dataset. Multipatch format for display in ArcGIS - ArcScene	layers\mp_ned30.lyr
mp_odcr30_top	Elevation of Decorah Shale top. Multipatch format for display in ArcGIS - ArcScene	layers\mp_odcr30_top.lyr
mp_ogcm30_top	Elevation of Cummingsville Formation top. Multipatch format for display in ArcGIS - ArcScene	layers\mp_ogcm30_top.lyr
mp_ogpr30_top	Elevation of Galena Group - Prosser Formation top. Multipatch format for display in ArcGIS - ArcScene	layers\mp_ogpr30_top.lyr
mp_ogsv30_top	Elevation of Galena Group - Stewartville Formation top. Multipatch format for display in ArcGIS - ArcScene	layers\mp_ogsv30_top.lyr
mp_ogwd30_top	Elevation of Glenwood Shale top. Multipatch format for display in ArcGIS - ArcScene	layers\mp_ogwd30_top.lyr
mp_opdc30_top	Elevation of Prairie du Chien Group top. Multipatch format for display in ArcGIS - ArcScene	layers\mp_opdc30_top.lyr
mp_opvl30_top	Elevation of Platteville Formation top. Multipatch format for display in ArcGIS - ArcScene	layers\mp_opvl30_top.lyr

Name	Description	layer file
mp_ostp30_top	Elevation of St. Peter Sandstone top. Multipatch format for display in ArcGIS - ArcScene	layers\mp_ostp30_top.lyr